UNIVERSITÀ
DEGLI STUDI
DI PADOVA

Sede Amministrativa: Università degli Studi di Padova

Dipartimento di Ingegneria Industriale

CORSO DI DOTTORATO DI RICERCA IN INGEGNERIA INDUSTRIALE
CURRICOLO: INGEGNERIA ENERGETICA
CICLO XXXI

EXPERIMENTAL AND THEORETICAL ENERGY AND COMFORT ANALYSES ON RADIANT SYSTEMS

Coordinatore: Prof. Paolo Colombo
Supervisore: Prof. Michele De Carli

Dottoranda: Giulia Alessio

ABSTRACT

When dealing with emission systems, energy and comfort aspects should be considered simultaneously since the terminal units directly affect the indoor thermal environment. The present work focuses on radiant systems and presents both experimental and theoretical energy and comfort analyses.

Simulations taking into account the dynamic behaviour of the building structures and the transient operation of water in the embedded pipes were carried out to analyse the seasonal emission efficiency of radiant systems in buildings with different levels of insulation and thermal mass and, with constant and variable supply water temperature. Their energy performance when supplied by a water to water heat pump and overheating risk were also investigated. A better performance of the radiant systems was found with a better quality of the envelope, the climatic control was confirmed to ensure a lower overall energy consumption and overheating effects were found to be not especially due to radiant system but happening in any case also with ideal convective systems.

In the second activity field measurements in a building were carried out to compare the performance of a wet floor radiant system with a reduced thickness of the screed with the performance of a traditional floor radiant system. First air and surface temperature data along with water temperature and thermal power recorded by the energy meters were analyzed. Then simulations under the same boundary conditions were performed, in continuous and intermittent operation and limited and unlimited available thermal power. No significant difference was found in the thermal energy need neither comparing the two systems, nor comparing continuous and intermittent operation.

As regards comfort, two activities involving test rooms are presented. Thermal global and local sensations were assessed by means of questionnaires during experimental investigations in a test room. The surface temperatures of the upper and lower parts of the room were progressively increased and decreased, while inlet air temperature was kept constant. Air stratification and vertical radiant asymmetry were analysed in the two kinds of tests, along with air velocity. No relevant asymmetry problem resulting in opposite sensations on head and feet at the same time was found in the analysis of the answers, while other factors played a significant role. For more comprehensive analyses on well-being of people, perception of the indoor environment and productivity, a novel test room equipped with radiant systems on all the surfaces and fresh air with controlled flow rate, supply temperature and relative humidity has been designed. The design and partial realisation are presented in the thesis as well as some hints on future research activity.

TABLE OF CONTENTS

1 INTRODUCTION

About 40% of the energy end-use in European Union is due to the building sector (28% to residential buildings and 12% to commercial ones), which has a high improvement potential and thus plays an essential role in the reduction of CO_2 emissions to control the impact on the environment. Energy savings and high energy performance in buildings should be achieved keeping in mind that people spend most of their time in indoor environments and therefore the main task of buildings should be to provide a comfortable, healthy and productive environment for their occupants. Energy and comfort aspects should be considered simultaneously especially when dealing with emission systems, since they directly affect the indoor thermal environment. Among emission systems, the use of water-based radiant systems for heating and cooling purposes have been steadily increasing because of their energy saving potential, possibility of coupling with natural heat sources and sinks, space saving, integration with building design, quiet operation, no cleaning requirements, improved indoor air quality, high thermal comfort level thanks to reduced risk of draught, reduced vertical air temperature differences and uniform temperature distribution in indoor spaces.

Even though radiant systems are used and studied for several years, there are questions frequently asked by designers and practitioners which are still open and under discussion.

Some questions are related to the thermal inertia of the systems and to the control strategies. In particular, in new and retrofitted buildings, where the envelope presents high levels of insulation, it is argued if it is better to have low or high inertia radiant systems for controlling the indoor operative temperature and avoid overheating, especially in mid seasons when outdoor temperature is mild and solar radiation is high. Moreover, it is asked if the newly-developed types of wet floor radiant systems with a reduced thickness of the screed which are recently spreading in the market perform better than the traditional ones, if they can be efficiently used in intermittent operation and if they allow better or lower comfort conditions for the occupants.

Another important open question is related to radiant temperature asymmetry with heating ceilings, which are used especially in commercial buildings. Practitioners usually do not calculate radiant asymmetry, since they prefer to deal with a limit on the maximum allowed surface temperature. Moreover, the studies of Fanger which still today represent the basis of the radiant asymmetry limits were performed on a limited number of test subjects and some criticisms were moved by some authors in literature. Thus, each producer currently declares different allowed temperature values.

The objectives of the present thesis in relation to the aforementioned questions are:

- the evaluation of the influence of the thermal mass and insulation level of the building on the efficiency of the radiant system (during heating operation) and on the possibility that temperature overheating occurs;
- the evaluation of the performance of a new kind of floor radiant system with a reduced thickness of the screed in comparison with a traditional system;
- the investigation on how vertical radiant asymmetry along with air stratification affect global and local thermal comfort;
- the design of a new test room for the study of people well-being under radiant heating ceilings and for indoor environmental quality analysis.

To deal with the objectives of the thesis, theoretical, numerical and experimental analyses were carried out. As regards experimental analyses, both field measurements and laboratory tests were performed.

After this introductory chapter, Chapter 2 provides a literature overview on radiant systems, from origins to construction technologies, currently applications, coupling with renewable energy sources, comfort aspects and existing standards.
Chapter 3 presents a simulation-based analysis on the emission efficiency of typical current radiant systems in heating conditions in buildings with different types of structures (masonry, light and timber walls) and different insulation levels.
In chapter 4 numerical simulations and field measurements analyses on a traditional radiant floor heating system and a radiant floor system with a reduced thickness of the screed are presented.
Chapter 5 presents the experimental investigations on thermal comfort performed in a test room with vertical radiant asymmetry and air stratification.
In chapter 6 a new test room equipped with radiant systems and fresh air with controlled flow rate, supply temperature and relative humidity is shown, from the very first design to the building up.
Chapter 7 gives the overall conclusions of the thesis and identifies topics for future possible investigations.

2 LOW TEMPERATURE HEATING AND HIGH TEMPERATURE COOLING RADIANT SYSTEMS

Abstract

This chapter provides a literature overview on low temperature heating and high temperature cooling radiant systems. The origins and the concept are presented, and the different classifications are shown. Current applications and coupling with renewable energy sources are then debated, with some hints on exergy aspects as well as thermal comfort. Finally, the most important building codes and standards related to the application of radiant systems are briefly illustrated.

2.1 INTRODUCTION

Due to a strong economic growth and rising standards of living, the problems related to energy use, indoor air quality, draught and noise highlight the need of new solutions for heating and cooling of building. Currently, many existing buildings are equipped with out-of-date conditioning systems, possibly inefficiently scheduled, which contributes to the 40% energy consumption attributed to the residential and office buildings [1, 2]. The main goal of engineers and designers is reducing energy demand in the building sector, either replacing existing systems with more efficient heating and cooling systems or installing energy saving plants in the new buildings.

Low-temperature heating and high-temperature cooling systems (i.e. systems that can heat or cool buildings with a small temperature difference between the supply fluid and indoor air) are a potential solution for these problems [3]. Radiant heating and cooling systems (RHC) have been increasingly used due to their well-known advantages, such as improved thermal comfort, quiet operation, space saving and so on. Moreover, they reduce energy consumption providing adequate thermal comfort at lower air temperature for heating and at higher air temperature for cooling [4].

2.2 ORIGINS OF RADIANT SYSTEMS

Through archaeology and historical research, it was found that the origin of radiant systems traces back during the Roman civilization. Roman hypocaust was warmed by hot combustion gases passing through cavity walls and floors and escaping from holes in the roof. Bansal [5] reviewed the Roman concept of radiant heating and defined the basic parameters to determine the thermal performance of a hypocaust. Modern applications have been suggested supported by case studies, such as the combination with solar chimneys and solar air collectors.

Literature showed that Asia developed this technology even earlier. Looking into the northern areas of China, including northern Manchuria region and northern Korea, early forms of radiant heating were known as *kang*, *dikang* and *ondol* [6]. The *kang* has been used more frequently in ancient Northern China, which was a raised heated living and sleeping surface but originally meant “to dry”. The *dikang* was mostly used in the north east Manchuria region, constructed with a fireplace and chimneys (depending on the fuel burned). The origin of this system can be dated between 5300 and 4800 B.C., where in Shenyang archeologists fund evidences of “baked earth”. The choice between *kang* and *dikang* is due to a cultural difference in preferring to sit on the floor or furniture.

Koreans developed an underfloor heating system called *ondol (or gudeul)*, consisting on a fire source and a series of flues, that warm flat stones placed above. At the beginning the fire furnace was inside the house and was used for heating, resulting in an overheating of the rooms (700-1100 A.D.). Further developments (1000-1200 A.D.) planned to move outside the furnace and design the radiant heating system using the net area available, as is still popular in North Korea.
Hydronic systems using hot water flowing has spread in China from 2000, even if it is still cost efficient to couple traditional *kangs* with biomass, trying to improve the low energy efficiency. Hot water radiant floor heating has become popular also in Korea in 1975 to improve thermal comfort, maintenance, energy efficiency and to prevent gas hazard.

2.3 CONCEPT OF RHC SYSTEMS

Radiant systems are terminal units in which the heat exchange within the conditioned space is covered by radiant heat transfer for more than 50% [7] [8]. Water-based radiant panels include each kind of system built with water pipes embedded in plaster, concrete or other kinds of material and characterized by a large surface of heat transfer toward the room. This kind of terminal units can be prefabricated (dry systems) or built in place (wet systems).
RHC systems have been widely applied in office and residential buildings due to their energy saving potential and enhanced thermal comfort [7]. Experimental measurements and subjective surveys verified that radiant heating systems provide quiet operation and less air movement, which results in lower draught risk and reduced vertical temperature gradient [9]. CFD studies combined with boundary data from experiments confirmed that the use of cooling ceiling allows low vertical gradient and thermal comfort is obtained, according to the PMV scale [10].
Exploiting the high heat exchange between the human body and the radiant surfaces, the supplied water temperature is close to room temperature, using lower temperatures for heating and higher temperatures for cooling. In radiant systems air temperature is lower than mean radiant temperature in winter and higher in summer.
There are many classifications of the RHC systems. The most common refers to the position of the pipes in the building, dividing them into embedded surface systems, thermally activated building systems and radiant panels system [4].
Depending on the building structure where they are installed, RHC systems can be divided into the following types [4]: floor systems, ceiling systems, wall systems and active thermal slab systems.
Pipes are usually embedded in the building structures or separated by an air gap, as in the case of hung ceiling systems.
Radiant systems have a somehow adaptive self-regulation: although a rise in the room temperature cannot be immediately stopped because of the relatively high thermal inertia, this effect is counterbalanced by a related reduction of the temperature difference and consequently of the heat exchange. Nonetheless, in order to work in a proper way, a good control system is required both in winter and summer [11]. Moreover, in cooling operating conditions, surface condensation must be avoided and a dehumidification system controlled by the relative humidity and air temperature is necessary. The proper design of high thermal mass radiant systems is effective to exploit energy storage in structural floors and slabs and daily peak loads, shifting them to the night-time [12].
Low temperature radiant systems allow uniform temperatures in the room and low air velocities. Since the water temperature is not very different from room temperature, it is possible to use renewable energy (e.g. ground heat exchangers [13]), condensing boilers or heat pumps in winter, chiller at higher values of COP in summer with respect to convective systems.

The heat exchange coefficient is the most important parameter which affects the amount of heat transferred within the room volume. The total heat transfer is composed of radiant and convective heat transfer, hence the thermal capacity of the RHC system should be determined by defining the radiant and convective coefficients [4, 7].
ISO 11855 [14] provides the following equations:

- heating floor and cooling ceiling: $q_u = 8.92\,(t_o - t_{s,m})^{1.1}$;
- heating and cooling wall: $q_u = 8\,(|t_o - t_{s,m}|)$;
- heating ceiling: $q_u = 6\,(|t_o - t_{s,m}|)$;
- cooling floor: $q_u = 7\,(|t_o - t_{s,m}|)$

where t_o is the operative temperature and $t_{s,m}$ the average surface temperature.
While the radiant heat exchange coefficient can be considered constant and approximately equal to 5.5 W/m^{2}K for a temperature range between 15 °C and 35 °C, the convective heat transfer coefficient may change between 0.3 and 6.5 W/m^{2}K, depending on the surface position and temperature [15].
The maximum heating and cooling capacity of a radiant surface depends on the maximum (for heating) and minimum (for cooling) allowable surface temperature. Considering an indoor temperature of 20 °C in winter and a maximum surface temperature of 29 °C, floor heating gives about 100 W/m^2. For ceiling, the surface temperature is not limited for reasons of contact with people, but for the resulting radiant temperature asymmetry; considering the maximum surface temperature in the range 29-35 °C, the heating capacity is between 55 and 90 W/m^2. The minimum surface temperature during cooling operation depends on air humidity; with a minimum value of 20 °C and an indoor temperature of 26 °C, the sensible cooling capacity is about 40 W/m^2 for floor systems and about 60 W/m^2 for ceiling systems. The sensible cooling capacity for the floor may increase up to 100 W/m^2 if there is direct sun radiation on its surface.

2.4 CLASSIFICATION OF RHC SYSTEMS

2.4.1 According to ISO 11855

Radiant systems are currently categorized following the standard ISO 11855:2015 [14] and guidebooks [16] as a function of their structure and geometry. The most common refers to the position of the pipes in the building, dividing them into embedded surface systems (ESS), thermally activated building systems and radiant panels system [7]. Moreover, depending on the position of the embedded pipes, ESS are sub-classified as Type A, Type B, Type C, Type D and Type G, as shown in Figure 2.1.

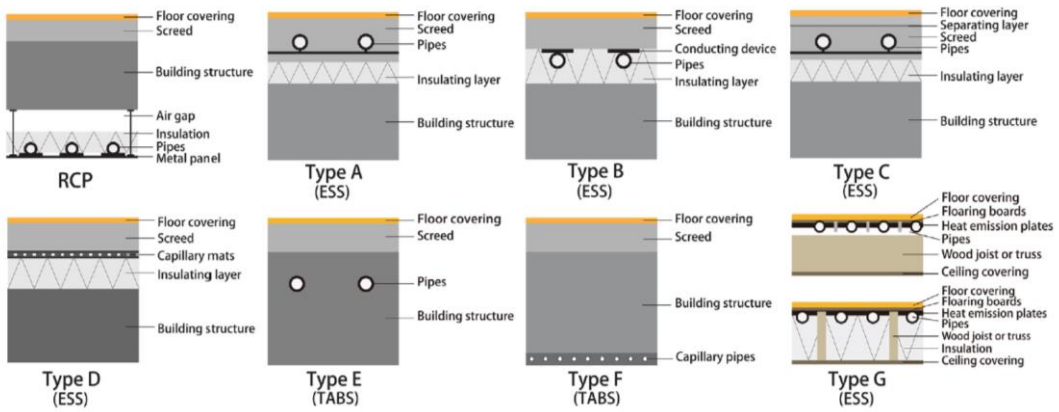

Figure 2.1 - Schematic drawings of radiant systems [17]

Type A is the system with pipes embedded in the screed. In Type B the pipes are embedded outside of the screed, in the thermal insulation layer. In Type C the pipes are embedded in a levelling layer above which a second screed layer is placed. Type D presents a thin layer which contains capillary mats above the insulation. In Type G the pipes are placed below the floor of a wooden construction. Type E is a TABS system with pipes embedded in massive concrete slab, while Type F is a TABS system with capillary pipes embedded in a thin layer that can be thermally connected to a massive slab.

2.4.2 According to response time

Ning et al. [17] developed a novel classification scheme for design and control of radiant system based on a new definition of thermal response time (τ_{95}) which provides a more consistent metric of long-term thermal response for the full range of radiant system types. The response time τ_{95} is defined as "the time it takes for the surface temperature of a radiant system to reach 95% of the difference between its final and initial values when a step change in control of the system is applied as input.". Calculating τ_{95} for radiant systems with different combinations of geometric and thermal parameters, the research shows that for Type E of TABS concrete type and thickness as well as pipe spacing have a significant impact. Indeed, pipe diameter, room operative temperature, supply water temperature and water flow regime have a negligible impact. The following classification scheme is proposed: fast response systems (τ_{95} < 10 min, like RCP), medium response systems (1 h < τ_{95} < 9 h, like Type A, B, D, G) and slow response systems (9 h < τ_{95} < 19 h, like Type E and Type F). Following this classification scheme, the dynamic thermal performance of radiant systems is more clearly defined.

2.4.3 According to installation position

Depending on the building structure where they are installed, RHC systems can be divided into the following types [4]: floor systems, ceiling systems, wall systems and active thermal slab systems.

Floor radiant systems

Heating floor systems represent a consolidated technology and nowadays also solutions in cooling mode are widely applied.
The pipe distribution can be with coil shape or, more common especially in residential buildings, with spiral shape. In the case of coil shape, the supply is generally close to the external surfaces [18]. In the past the adoption of variable pipe distance was common, decreasing the distance near the external surfaces in order to reach a higher surface temperature, but nowadays the quality of the building envelopes ensures good comfort conditions also with constant pipe spacing.
Radiant floor systems can be "wet" or "dry". In the first the pipes are embedded in a wet screed layer, with a standard thickness of about 60 mm; recently also systems with a lower thickness of the screed have been developed by producers and started spreading in the market. Dry floor systems were developed for renovations or projects where height is limited or additional weight on the slab should be limited. In these systems the pipes are placed inside the insulation layer and an aluminum plate diffusers are used to achieve a uniform distribution of temperature. Above the pipes a thin steel board can be used to replace the screed for weight distribution or a gypsum-fiber board about 10 mm height. There are also floor dry systems in which the pipes are not placed in the insulation layer, but directly inside the gypsum-fibre board.
Pipes can be in steel, copper or plastic material: cross-linked polyethylene, polybutylene and polypropylene pipes are nowadays the most commonly used for their flexibility, lightness, ease of

installation and low cost. Some floor systems are made by extruded plastic material which forms micro channels. In this case the heat exchange surface is very wide, which allows very low temperature differences.
Different floor coverings can be adopted above radiant floor systems, such as ceramic tiles, parquet, marble, linoleum, resin etc. Slab thickness (in case of wet systems), pipe spacing and flooring have all a strong influence on the temperature level at which the water must be supplied in order to guarantee the desired surface temperature.
Control strategies have to be applied, because the time delay due to the floor thermal capacity highly influences the thermal behaviour of the panel. Due to the significant thermal storage effect, the use of this type of heating system is recommended only in buildings with continuous or well-defined occupancy during the day or where the building conditioning works over all the 24 hours of the day. The control strategies can act both on the flow rate modulation and on the supply temperature control, taking into account the limitation imposed by the water temperature difference between supply and return, limited at 5-10 °C due to reasons of panel surface temperature uniformity.

Wall radiant systems

This type of radiant systems has a limitation due to the possibility of using furniture. For this reason it is common to install wall radiant systems only in some spaces in combination with floor and ceiling systems, in order to get higher values of heating and cooling capacity (e.g. in bathrooms).
The installation can be under plaster, behind linings (wood, carpet) or, in the case of prefabricated panels, on the profiles of dry wall structures. In the first case a wire net must be placed on the bricks to hang the pipes. Behind linings radiant systems are installed on existing walls, by interposing insulating material, and the lining is directly applied over the pipes. In the case of dry walls, the radiant panels are generally made of plasterboard with embedded pipes coupled with an insulation board on the back; the panels are generally connected in series creating groups which are connected to a manifold.

Ceiling radiant systems

Radiant ceilings have the main advantage, with respect to other radiant systems, of being not influenced by the interposition of obstacles toward the occupied area of the room (e.g. furniture).
Radiant ceilings show very good performance in cooling mode; as a consequence, they are typically applied in office buildings, hospitals and commercial buildings. Their main characteristic of is a very low thermal inertia. Moreover, ceiling panels can be used for acoustic control when sound-proofing materials are placed on their back side.
The control strategy is the same of radiant floors but taking into account the lower thermal inertia of the system and the generally higher operating temperatures in heating conditions.
The most common types of radiant ceiling are:

- embedded pipe radiant ceilings;
- radiant ceilings installed after ceiling construction;
- light radiant metal panels.

Embedded pipe radiant ceilings systems are installed during the building construction hanging on the reinforcements. These systems have a high thermal inertia. Active thermal slab systems pertain to this category.
In the case of radiant ceilings installed after ceiling construction the ceiling is already built and has some hangers in order to fix the pipes, which are usually made by steel or copper. The ceiling is

composed by different layers: insulation, hangers, pipes, wire net, plaster. Moreover, superposition of metal planes over the pipes is possible, in order to improve the performance of the radiant ceiling. In the last years the use of small pipes embedded in plasterboard panels coupled with insulation have been spreading.
Light radiant metal panels present high conductivity and the related mass and thermal capacity is very small compared with other radiant systems [19] [20]. They can work both in heating and in cooling conditions with good performances. The space required is limited between 5 cm to 7 cm in thickness.

Active thermal slab

In this solution pipes are embedded in the centre or close to the centre of the slab (or wall), in order to act directly on the thermal mass of buildings [16]. This technique is used in multi-storey buildings, since the thermal exchange occurs both upwards and downwards. Due to the high thermal mass the control of the system cannot be fast, and thus the temperature in the room shows fluctuations during the day.
In the heating season, the slabs where the pipes are embedded adsorb thermal energy from the warm water and release it after a time lag into the room. During the cooling season, the slab is cooled down by the water running in the pipes and accumulates heat due to peak loads in the room. The accumulated thermal energy is removed by the fluid after a time lag, when thermal loads are lower. The main difference between the other radiant systems and thermo-active system is the possible asynchrony of the operation of the conditioning plant and thermal loads.
The main advantages are the following:

- the thermal load is distributed in a longer period, which leads to lower peak loads, thus allowing to use conditioning plants of reduced sizes;
- the possibility to use two radiant surfaces leads to more uniform conditions in the conditioned space;
- the building dimensions are reduced with respect to buildings with suspended ceilings;
- it is possible to use conditioning plants suitable for temperatures close to the room, i.e. heat pumps, condensation boilers, solar collectors, ground heat exchangers;
- for cooling purposes, the night overventilation can be used as well;
- low installation costs and low operation costs are possible;

On the other hand, the use of thermo-active systems should be evaluated considering these aspects:

- active thermal slabs can be used only in multi-storey buildings with a central plant;
- attention must be paid in the case of raised floors, while the ceiling surfaces must be free from obstacles (no suspending ceilings can be used);
- the design is very critical and adequate solar radiation shading and good thermal insulation of the envelope are needed.

2.5 CURRENT APPLICATION OF RHC SYSTEMS

The long-term planning perspective is to develop towards a sustainable society [21, 22]. Consequently, both new and renovated buildings should be planned to use or be suited to use sustainable energy sources for heating and cooling; this is possible only developing systems that use a relatively moderate temperature level. The lower the temperature level for heating and the higher for cooling, the better the efficiency of the system can be [23].

RHC systems have been widely applied in office and residential buildings mainly due to the improved thermal comfort [7] and the reduced energy consumption. Moreover, experimental measurements and subjective surveys verified that they ensure quiet operation, space saving, less air movement, which results in less draught risk, and reduced vertical temperature gradient [9]. Comparing radiant systems with traditional heating systems RHC can provide the same thermal comfort because of the exploitation of the radiant heat exchange between the human body and the radiant surfaces, using lower temperatures for heating and higher temperatures for cooling [4]. Since the energy consumption is directly influenced by the temperature of the source [24], the optimization of the supplied temperatures can enhance the energy efficiency of the system.

Bojić et al. [25] compared four different types of radiant systems coupled with natural gas boiler. Results showed that the floor/ceiling radiant heating system has the best performances: lowest energy and exergy consumption, CO_2 emissions and operation costs. However, it confirmed that heat losses (e.g. to the ground) should be considered carefully for some of the radiant heating types (e.g. floor heating in slab-on-grade).

In another research, Bojić [26] compared radiators, the most typical old-designed heating system, without additional thermal insulation of external walls of the building with a low-temperature radiant panel system in a residential building with additional thermal insulation of external walls. This combination reduces primary energy consumption of 39%. Another interesting result has been obtained, showing that the effect of the applied thermal insulation is a reduction of primary energy consumption by 22% for the radiative panels, and by 15% for radiators.

Radiant systems can be generally compared to all-air systems, which perform similarly considering building energy simulations and laboratory experiences, as showed by Olesen, Mustakallio et al. [27, 28, 29] but also developing human testing as confirmed by Schellen [30, 31].

A side-by-side field comparison based on occupant survey responses was developed by Sastry et al. [32] between an all-air system and TABS with dedicated outdoor air system. Occupants showed increased satisfaction with thermal comfort for the radiant system.

Karmann et al. [33] stated that even if there is suggestive evidence of the better or equal thermal comfort provided by radiant systems with respect to all-air systems, further studies are needed to confirm this statement. In fact, literature showed that both systems are able to provide acceptable thermal comfort, depending on several factors, including operation and control.

2.6 COUPLING RHC SYSTEMS WITH RENEWABLE ENERGY SOURCES

The raising living standards and the increasing world population lead to an increase in energy use and pollutant emissions due to heating and cooling systems of buildings up to 30-50% of the global energy consumption [34].

The research and the application of renewable energy sources (RES) are the best alternative to tackle these issues, being equally distributed and reducing dependence on fossil fuels. Since the introduction of the Bruntland Report in 1987 [21], the concept of “sustainable development” guided the research towards the implementation of innovative technologies and their application coupled with renewables.

Besides the installation of photovoltaic, solar and combined PV/T panels to produce electricity and hot water [35], geothermal energy is the most studied application since it can be exploited for electricity generation, direct heating and indirect heating and cooling. Ground source heat pumps (GSHP) take advantage of the fact that the ground temperature is almost constant and close to the

building desired temperature during the whole year [36], leading to high coefficient of performance (COP).
The supply water temperature of radiant heating and cooling systems (25-40 °C during heating season, 16-20 °C during cooling season) is close to the room temperature, enhancing the interest in coupling them with low temperature RES.
Serbachievici et al. [37] demonstrated that the use of heat pumps is more efficient compared to conventional heating solutions for new or renovated buildings: rather than replacing fossil fuel energy use, it provides significant energy savings thanks to high COP values. For a radiant wall heating system coupled with a GSHP under real outdoor conditions, energy savings in continuous operation can be between 20% and 40% depending on the set-point temperature [38].
De Carli et al. [39] used TRNSYS to simulate the use of heat pumps to supply heating and cooling systems and verify a reduction of primary energy consumption up to 60% with respect to traditional systems. Additional implementations coupling GSHP with PV cells lead to a reduction of 80% compared to traditional systems.
Table 2.1 shows some examples of studies performed coupling different types of radiant heating systems with renewable energy sources, showing the amount of energy saved and the percentage of energy covered by renewables. The use of radiant heating/cooling as indoor heat emission/removal system allows the ground source to be used, and thanks to the matching temperature levels it enables higher performance of heat pumps both in heating and cooling mode and possibly gives the option of using free cooling, using the ground source without the heat pump.

Table 2.1 - Some studies on RHC systems coupled with RES.

Reference	Study type	System	Energy saved / RES contribution
Kazanci et al. [40]	Field experiment	PV/T panels enable the house to perform as a plus-energy house	Solar fraction of 63% in Madrid, 31% in Copenhagen
Bojić et al. [41]	EnergyPlus simulations	GSHP and PV combined with floor and ceiling radiant heating	Final energy decreased by 87% and primary energy decreased by 40%
De Carli et al. [39]	TRNSYS EED simulations	District heating and cooling coupled with closed loop GSHP	Primary energy decreased by 50-60%
		District heating and cooling coupled with closed loop GSHP and PV array	Primary energy decreased by 70-80%

Lizana et al. [42] showed a reduction of the energy consumption close to 30% compared to non-renewable sources applying thermal energy storage in different situations (e.g. free-cooling ventilation systems, solar energy storage solutions, demand-side management strategies towards zero energy buildings).
Energy efficiency can be enhanced storing the thermal energy provided by RES in the building structure to overcome their intermittency, as well as the thermal mass can be activated in climates with big diurnal temperature variations to store thermal energy for heating and cooling purposes [43]. Ongoing research activities are investigating TABS and phase change materials (PCM) to incorporate them into new and challenging renovated buildings. As showed by Pavlov et al. [44], building storage capacity can be increased through the temporary storage of high or low-temperature energy of PCM, controlling the temperature and reducing temperature fluctuations.

In conclusion, literature showed that radiant systems can be efficiently coupled with RES thanks to the good match with temperature levels, reducing energy consumption and enhancing the overall efficiency of the system.

2.7 EXERGY AND RHC SYSTEMS

The thermodynamic concept of exergy assigns a qualitative value to an amount of energy. The second law of thermodynamics makes it possible to compare the output of a technical process with the theoretical maximum output from a thermodynamic point of view. Different types of energy exist: thermal, electrical, mechanical workload etc. Energy which is entirely convertible into other types of energy, such as electricity and mechanical workload, is high-valued energy. Energy which is very limitedly convertible, such as heat close to room air temperature, is low-valued energy.
Hence, the quality and quantity of energy used in a building can be described by the concept of exergy, which is the maximum useful work convertible into different types of energy. RHC systems are considered low exergy heating and cooling systems, being able to exploit energy close to the room temperature which has limited convertibility potential. Kazanci et al. [45] calculated the exergy consumption of different heating system: the exergy consumption of radiators increases with increasing average water temperature, whereas radiant floor heating systems have the lowest consumption.
Starting with the improvement of the energy efficiency of separate options, nowadays an integral approach is becoming of increasing importance. The improvement of the energy efficiency of supply and conversion systems is mostly based on the energy balance of the systems. In principle, no distinction is made between the different forms of energy, for example heat or electricity. This means that the efficiency is based on the quantitative comparison of energy flows with no distinction to qualitative aspects. Taking into account the qualitative aspects of energy leads to the introduction of the exergy concept in the comparison of systems, which is the key idea of some recent works [46]. Low exergy heating and cooling systems use low valued energy sources. Low temperature heating and high temperature cooling systems are an integrated configuration. The different parts of the configuration are the source, the distribution systems outside the building and the system within the building. The heating and cooling system is a part of the building system.
The literature review [47] showed that low-temperature heating systems have many advantages over high-temperature systems in terms of comfort, health and safety:

- thermal comfort increases thanks to higher radiant heat transfer, lower temperature gradients, more comfortable floor temperature, lower draught and air turbulence;
- indoor air quality is positively influenced: less dust mites, better perceived air quality thanks to lower air temperatures, and less sick building symptoms;
- safety is improved: lower risk for hand burning and for physical injury when falling.

In most cases, the disadvantages found (e.g. warming up time, radiant asymmetry near windows) only apply in case of improper design.

2.8 THERMAL COMFORT AND RHC SYSTEMS

The aim of any conditioning system in building is to provide a healthy and comfortable indoor environment for occupants, enhancing their performance and possibly with the minimum energy consumptions and greenhouse gas emissions. The basis of the thermal comfort theory is the correlation between the human thermoregulation and some climatic parameters.

The evaluation of the thermal environment refers to the personal perception, as can be gathered from the definition: thermal comfort is the condition of mind which expresses satisfaction with the thermal environment. In order to provide acceptable thermal conditions according to the general regulation about PMV and PPD [48], both air temperature and mean radiant temperature have to be taken into account. Their combined influence is evaluated as the operative temperature, eventually approximated to the simple average when the difference between the mean radiant temperature and the air temperature is smaller than 4°C and air velocity is low.
These considerations explain one of the most important advantages of using RHC systems, since the same level of operative temperature can be achieved using lower air temperature while heating and a higher air temperature when cooling. This results in a lower ventilation heat loss for buildings with high ventilation rates, causing higher energy consumption. On the contrary, for new well-insulated buildings this effect is minor because of the smaller temperature difference [16].
Acceptable thermal comfort depends on the constant heat transfer between the human body and the surroundings. The metabolic rate, which represents the heat released from the body per unit skin area, assumes different values depending on the activity and is expressed in met (1 met = 58.2 W/m^2).
The mathematical formulation derived by Fanger in 1972 is based on human body perception and defines the main index to predict thermal sensation in controlled indoor environments. Predicted mean vote (PMV) is expressed as a seven-point scale: -3 (cold), -2 (cool), -1 (slightly cool), 0 (neutral), +1 (slightly warm), +2 (warm), +3 (hot).
Further correlations have been developed by Fanger who introduced the predicted percentage of dissatisfied persons (PPD), stating that it cannot be physiologically lower than 5% (Figure 2.2). The thermal environment is usually considered acceptable if the PPD is lower than 10%.
More details about the calculation of PPD and PMV are included in the standard ISO 7730 [48].

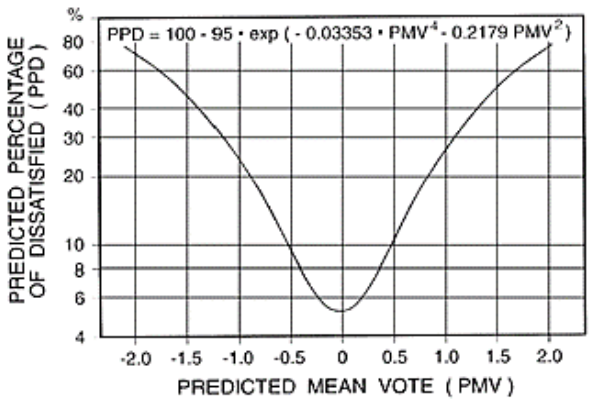

Figure 2.2 - Relation between PMV and PPD (ISO 7730).

The optimal operative temperature, which corresponds to a PMV equal to 0 (neutral thermal sensation), can be expressed as a function of the metabolic rate and of the clothing unit, which expresses the clothing thermal resistance (1 clo = 0.155 m^{2}K/W). Adaptive thermal comfort theory expresses the natural tendency of occupants to adapt to changing conditions in the environment for example by acting on their clothing and activity.
In order to maintain a constant inner temperature for the human body around 37°C, it exchanges heat with the surroundings through the skin by respiration, evaporation through sweating,

conduction, convection and irradiation. Personal clothing should be considered, since its thermal insulation can affect the heat transfer.
The thermoregulation system must consider other variables that can be summarized with the following mathematical formulation:

$$S = M \pm W \pm R \pm C \pm K - Esk - RES$$

where:

- S is the variation of the internal heat of the human body (positive if the body temperature is increasing, negative if the body temperature is decreasing, equal to zero if there is thermal equilibrium and therefore potential comfort);
- M is the metabolic rate, which is function of the activity;
- W is the external mechanical work, positive if done by the human body;
- R is the radiant heat exchanged between the body and the surroundings, positive or negative depending on the air temperature;
- C is the convective heat exchanged, positive or negative depending on the air temperature and on the clothing;
- K is the conductive heat exchanged. It can be considered negligible for people standing, whereas conduction is significant for sitting people;
- Esk is the heat transferred through skin evaporation;
- RES is the heat exchanged through respiration, associated to the enthalpy variation of the air breathed.

The heat exchanged by mean of thermal radiation between the radiant system, the environment and the human body can influence the mean radiant temperature in rooms, which is one of the key parameters of thermal comfort. Mean radiant temperature is defined as the uniform temperature of an imaginary enclosure in which radiant heat transfer from the human body equals the radiant heat transfer in the actual non-uniform enclosure.
The improvement of the thermal environment is a consequence of the modification of the air temperature by convection and surfaces temperature by radiation. Hence, RHC systems are the only heating/cooling system able to influence occupants' thermal comfort by means of an indirect action (heat transfer with walls and air) and by means of a direct action (heat transfer with occupants) [49].
The combination of air temperature and mean radiant temperature is operative temperature, which is the index representing the thermal sensation felt by occupants due to sensible heat transfer, which is the most relevant part of the human body heat balance since the latent heat transfer can be neglected as a first approximation. Operative temperature should thus be used for any evaluation of radiant system influence on the built environment. Radiant heating system can ensure, if compared to an all-air system, the same operative temperature with a lower air temperature, generating energy savings due to the reduced values of ventilation heat losses.
National and international standards define different levels of thermal comfort depending on: type of building, type of occupants, type of climate and national differences.
The design of heating, cooling and ventilation systems in buildings is defined based on either the necessities due to the end use of the building or to the personal choice of the category that should be achieved (ISO 7730 [48] and EN 15251 [50]). Mandatory requirements are established for the lower category of indoor thermal quality in buildings; depending on the requests of the customer, higher levels of comfort can be achieved, referring to higher categories. It is useful to remember that comfort level and energy consumption are strictly connected.

Although global thermal comfort is acceptable, occupants may experience local thermal discomfort sensations due to cold air draught, vertical air temperature differences or radiant asymmetries which can be natural or provoked by mechanical system (e.g. a cold downdraught generated by a cold window or an air jet).
ISO 7730 [48] and ANSI/ASHRAE 55 [51] list all the limitations to avoid possible local thermal discomfort. The main limitation regarding radiant systems concerns the radiant floor temperature which must be always within the range between 19°C and 29°C (eventually raising up to 35°C within an area of one meter around external walls).
Radiant ceilings and walls surface temperatures are restricted indirectly by radiant asymmetry limitations. At the same time radiant systems may provide excellent performance in reducing existing radiant asymmetries, because of the direct radiant heat exchange with all the surfaces in the room.

2.9 EXISTING BUILDING CODES AND STANDARDS ON RHC SYSTEMS

An important contribution to the development of RHC system can derive from the implementation of suitable codes and standards.

UNI EN 1264. Water based surface embedded heating and cooling systems [52].
The standard consists of 5 parts:

- Part 1: Definitions and symbols (2011)
- Part 2: Underfloor heating: methods for determining the heat output through calculation methods and tests (2013)
- Part 3: Sizing (2009)
- Part 4: Installation (2009)
- Part 5: Heating and cooling surfaces integrated into floors, ceilings and walls - Determination of thermal power (2009).

The standard published in 2009 is a completion of the previous version presented in 1999 and 2003. It represents the main reference for embedded radiant systems. The contents of Part 5 concern the design, installation, laboratory tests and calculation methodology for the system efficiency. The final part has been added later in order to consider all the installation possibilities. While the measurement procedure is generally valid for each type of RHC system, the hypothesis made for the calculations have not been verified, being a significant limitation for this standard.

UNI EN ISO 11855. Design, dimensioning, installation and control of embedded radiant heating and cooling systems [14].
The first five parts were published in 2012-2013:

- Part 1: Definition, symbols, comfort criteria
- Part 2: Determination of the design thermal and cooling capacity
- Part 3: Design and sizing
- Part 4: Sizing and calculation of thermal performance and cooling capacity of mass thermal activation systems - Thermo Active Building Systems (TABS)
- Part 5: Installation

Part 6, concerning control, is currently under revision.
The standard does not include guidelines for testing systems and cannot be applied to ceiling heating/cooling panels. The calculation methods for determining the characteristic curve are two: simplified method (similar to the provisions of *UNI EN 1264*) and FEM or FDM simulations.

UNI EN ISO 18566. Building environment design - Design, test methods and control of hydronic radiant heating and cooling panel systems [53].
The standard, concerning hanging panels, consists of 5 parts:

- Part 1: Definitions, symbols, technical specifications and requirements
- Part 2: Determination of the thermal capacity and cooling of the ceiling panels
- Part 3: Design of ceiling panels
- Part 4: Adjustment and operation of the ceiling heating and cooling panels
- Part 5: Technical Report.

Guidelines for testing activities are given in standard *UNI EN 14037:2016* [54] and *UNI EN 14240:2005* [55]. They provide strategies for test methods and applications of radiant ceilings and other plant technologies.
The Italian standard *UNI 11300-2:2014* [56] defines emission, regulation and distribution efficiencies that have to be considered for the evaluation of the average seasonal efficiency of the heating system. The corresponding European standard is *EN 15316-2* [57], which uses a different methodology by giving temperature differences instead of plant efficiencies.
Indoor environmental parameters for building system design and energy performance calculation are defined using the standard *UNI EN 15251:2008* [50], whose title is “Indoor environmental input parameters for design and assessment of energy performance of buildings addressing indoor air quality, thermal environment, lighting and acoustics”. This standard is applicable mainly in non-industrial buildings, such as single-family houses, apartment blocks, offices, educational buildings, hospitals, hotels, restaurants and similar, since criteria for indoor environment are set by human occupancy.

3 THEORETICAL ANALYSIS OF THE EFFICIENCY OF RADIANT SYSTEMS IN DIFFERENT KINDS OF BUILDINGS IN HEATING CONDITIONS

Abstract

Thermal inertia of buildings influences the energy and comfort performance of their heating and/or cooling systems. Numerical simulations on a room with three insulation levels and different structures (masonry, light and timber walls) combined with three types of radiant systems (traditional wet floor, dry floor and ceiling) are presented in this chapter. Both constant supply temperature and variable temperature according to outdoor temperature have been simulated. The results looked at the embedded and control efficiency, the energy performance in case of coupling with a water-to-water heat pump and the long-term possible overheating analysis. The efficiency found in dynamic conditions is higher than the efficiency calculated in steady-state conditions, working at variable temperature leads to lower consumptions, overheating effects are not especially due to the radiant system and there is no evidence that dry floor systems perform better than wet screed systems.

3.1 INTRODUCTION

Radiant systems are being used for heating and cooling purposes for a long time time [58, 59]. Radiant ceilings are increasingly used, especially for commercial applications, but the most common type of radiant system is still the radiant floor.

The sizing of radiant systems has been debated in the past and standardized methods are today available [14]. Even though the systems are used and studied since several years, there are questions which are frequently asked by designers and practitioners which are still open and under discussion. The questions are related to the thermal inertia of the systems and which control strategies should be better in buildings during the heating period. In particular in new and retrofitted buildings, where the envelope presents high levels of insulation, it is argued if it is better to have low or high inertia radiant systems for controlling the indoor operative temperature and avoid overheating especially in mid seasons when outdoor temperature is mild and solar radiation is high. There are, hence, mainly two aspects to take simultaneously into account: the building envelope and the radiant systems.

Looking at building envelope, the thermal inertia of the building structure has been under debate for a long time. One of the first works looking at the different models to be used in the calculation of thermal behaviour of structures is the one of Bojic and Loveday [60], where several simplified methods were already criticized while dynamic simulations were predicted as most suitable methods. More recently thermal inertia of buildings structures has been debated, mainly in cooling conditions, e.g. [61, 62]. Looking at results dealing with heating purposes, several papers have been published in the last years. Aste et al. [63] examined external wall systems with the same U-value but different dynamic properties in order to evaluate the associated achievable energy savings. They found that the difference in the heating demand with a low inertia wall compared to a high inertia one may reach

about 10%. A similar saving has been evaluated by Stazia et al. [64], who found a difference in heating conditions of about 15% among the different solutions of retrofit in both continuous and intermittent operation by combining both thermal insulation and thermal mass techniques in Mediterranean climates. These percentages seem to be the maximum difference which can be found in literature when dealing with heating demand in well-insulated buildings. As an example in [65] a parametric simulation study has been performed based on different climatic conditions and with different heaviness of the structures in Mediterranean climates. Regarding heating demand there was no sensible difference in the same location with massive or light structures. This is also in agreement with the most extensive and recent review on the thermal inertia of buildings [66]. The reported impact of thermal inertia on energy demand found in this work is relatively small. For residential buildings the energy savings reported are often in the order of magnitude of a few percent, which is far less pronounced than the impact of other energy saving measures such as increasing thermal insulation of the building envelope.

As for the radiant systems, in the past the works have been carried out especially under steady-state conditions. The most important steady-state parameters which describe the performance of radiant systems are heating/cooling capacity and thermal resistance [14, 16, 67]; however, steady-state analysis is not sufficient to describe the performance of radiant systems involving an important amount of thermal mass, like embedded surface systems and thermo-active building systems (TABS). Since the 1990s dynamic simulations have been carried out especially for the TABS which is a type of radiant system based on the thermal inertia of the structural slab [68]. For less massive radiant systems some works have been recently published looking at their behaviour in dynamic conditions, but the analyses mainly looked at the radiant system, without taking into account the room.

In particular, the influence of geometrical and construction parameters on the thermal performance of floor heating systems has been widely investigated, focusing mainly on wet systems, in which the pipes are embedded in a concrete layer. The pipe material, diameter and spacing, along with the thickness and material of the covering layer were studied, finding that the pipe material has negligible effect on the amount of useful heat [69], while the conductivity and thickness of the finishing layer have a high influence [69, 70]. In the case of wood flooring, also the installation method (floating or adhesive covering) was investigated [71]. While the pipe spacing and the mean value of the water temperature have large impacts on the surface temperature and heat transfer of the radiant floor, the thickness of the screed was found to have almost no influence [72].

Dry floor systems have been investigated less than wet systems. Experimental and numerical analysis of a lightweight system with aluminum foil covering a non-profiled insulation board were carried out by Zhang et al. [73], while the dynamic performance of a dry system with pipes laid in a profiled insulation board was investigated by Zhao et al. [74]. Qiu and Li [75] compared wet and dry floor systems based on numerical simulations, finding higher mean values, but lower uniformity, of the surface temperature of the dry system. Thomas et al. [76] developed a numerical model for the study of the steady-state and dynamic operation of a new light floor heating construction made of wood planks and aluminum diffuser, focusing also in this case only on the thermal behaviour of the emitter itself and stressing the importance of developing a model including also the building to fully investigate the performance of the radiant system and perform an energy comparison with traditional heating floor systems and other emission devices.

The present work hence looks at the overall balance of a room taking into account the thermal inertia of the radiant system as well as the water inside the pipes, as better described in detail hereafter. Usually for solving this problem dynamic simulations have to be run in order to properly take into

account the dynamic behaviour of building structures, as well as transient operation of water in the embedded pipes. The heat conduction through the radiant systems can be modelled in different ways. The most widely used methods are the simplified RC-model [77] and the response factors technique [78]. Both models have been demonstrated to be accurate against measurements.

3.2 METHOD

The simulation of the dynamic behaviour of the considered radiant systems in different kinds of buildings was carried out with the model DIGITHON [78]. This numerical model performs the detailed simulation of the dynamic behaviour of water-based surface heating and cooling systems.
In the model DIGITHON, each surface of the room is divided into elements named tiles (Figure 3.1); an overall heat balance is carried out for each element, considering the following thermal nodes:

- the air of the room, considered as a single uniform volume;
- the surface (inner and outer sides) of each tile of the walls, the floor and the ceiling;
- the water inside each pipe segment;
- the surfaces of each pipe segment.

The results of the model are the inner side temperature and the heat flow of each surface element, the air temperature and the return water temperature of the radiant system.

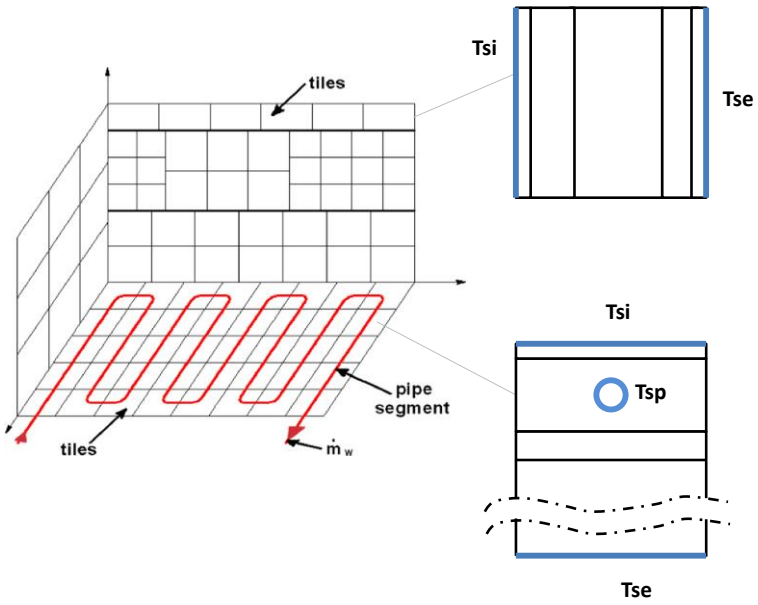

Figure 3.1 - Example of discretization of a room equipped with a radiant system embedded in the floor [78] with the relevant surfaces where the heat balance is solved for structures with or without embedded pipes.

As shown in [79], there is no difference in the overall balance when considering solar radiation in detail or when it is assumed to be uniformly distributed. Hence the solar radiation in the present work is considered as uniformly diffused.
As regards the air temperature in the room, in rooms with conventional dimensions (less than 3 m height), air temperature can be assumed to be uniform both in heating [80] and in cooling conditions [81] for radiant systems as well as in a wide range of situations that have been confirmed by other studies [82].

As for convective heat transfer coefficients, a recent review [83] shows that the most reliable analyses are those based on measurements in real size test rooms. In particular, as shown in [78], constant values can be considered for the convective heat exchange coefficients. For this purpose convective heat exchange coefficients are assumed constant in the calculations.
As regards the water convection heat transfer coefficients inside the pipes, correlations of literature are used [84].
To solve the dynamic heat transfer problem in DIGITHON, the “response factor” technique is used [85, 86]. In the present work the heat transfer response factors were calculated by using the commercial software HEAT2 [87], which is based on the Finite Difference Method (FDM). Three simulations have to be performed to describe the thermal conduction in a building structure with embedded pipes. In each simulation a triangular impulse of temperature is given on the inner surface, on the outer surface or on the internal surface of the pipes, and the resulting heat flows on the three surfaces are recorded. After normalization, for a generic trend of temperature on the inner surface of the building structure, on the outer surface of the building structure and on the internal surface of the pipe, the response factor can be used, by superposing of effects, to calculate the specific heat fluxes on the three considered surfaces. More details about this method, included an example showing its accuracy, can be found in [79].
In the present work the FDM was also used to find the average value of the water temperature in the pipes of the radiant floor system which gives, in steady state conditions, a useful heat flux towards the heated room equal to the thermal losses in design conditions for heat transmission through the building structures, for infiltration and ventilation [88].

3.3 CASE STUDY

3.3.1 Building geometry and structures

Simulations were carried out in a room with a floor area of 100 m^2 (Figure 3.2). The windows are East and West oriented and their total surface is equal to 12.5 m^2. The other two walls are adjacent to flats at the same temperature of the simulated one, as well as the ceiling and the floor. The case study represents a flat in an intermediate floor of a multi-storey building. No internal walls were considered, therefore the entire space was simulated as a single room. The point P, situated in the middle of the room at 1.10 m height from the floor, was considered for the evaluation of the operative temperature.

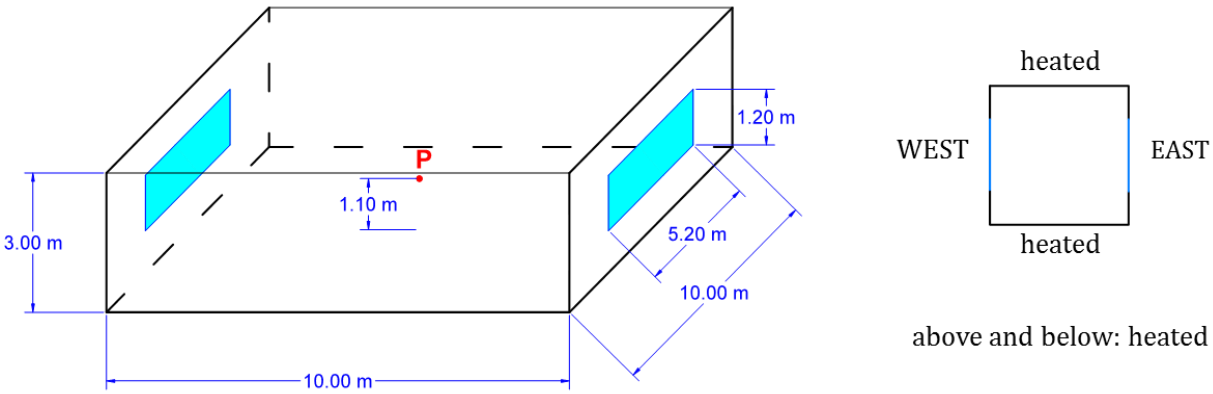

Figure 3.2 - The simulated room considered as case study.

Eight types of building structures were considered (Table 3.1): one type of stock building with a U-value of the walls equal to 1.3 $W\,m^{-2}K^{-1}$, three types of insulated buildings with a U-value of about 0.5 $W\,m^{-2}K^{-1}$ and four types of well-insulated buildings with a U-value going from 0.15 to 0.20 $W\,m^{-2}K^{-1}$. The stratigraphies of the structures of each type of building, along with the thermal properties of each layer, are listed in the APPENDIX. Two kinds of windows were considered in this work, one for the buildings which are not insulated and a more performant one for all the other cases. The U-value of the window, the g-factor of the glass and the ratio between frame area and the entire window area are listed in
Table 3.2.

Table 3.1 - Codification of the 8 types of buildings simulated.

Codification	Type of building
N	Non-insulated building
I-M	Insulated building - insulation in the middle of the wall
I-E	Insulated building - insulation on the external surface
I-I	Insulated building - insulation on the internal surface
WI-E	Well-insulated building - insulation on the external surface
WI-I	Well-insulated building - insulation on the internal surface
WI-X	Well-insulated building - cross laminated timber building
WI-L	Well-insulated building - light structure building

Table 3.2 - Properties of the windows.

Type of building	U_w [$Wm^{-2}K^{-1}$]	g [-]	A_f/A_w [-]
N	3.0	0.755	0.15
I, WI	1.5	0.600	0.15

3.3.2 Radiant systems: kinds and circuits

The eight kinds of building structures described above have been combined with the three kinds of radiant systems described in Figure 3.3 and Table 3.3. The stratigraphies of the radiant systems and the thermal properties of each layer can be found in the APPENDIX.
For each kind of building the number of circuits of the radiant system was defined. The goal was to keep the pressure drop under 1 m w.c. The entire floor surface was considered to be thermally active, against the 70% of the ceiling surface. The ceiling system was designed with 12 circuits, the floor system with dry screed with 8 circuits and the floor system wet screed with 6 circuits. Only the floor systems in the building without insulation present a different number of circuits: 12 for the dry screed and 8 for the wet screed, due to the high design heat load. The geometries of the different circuits are presented in Figure 3.4.

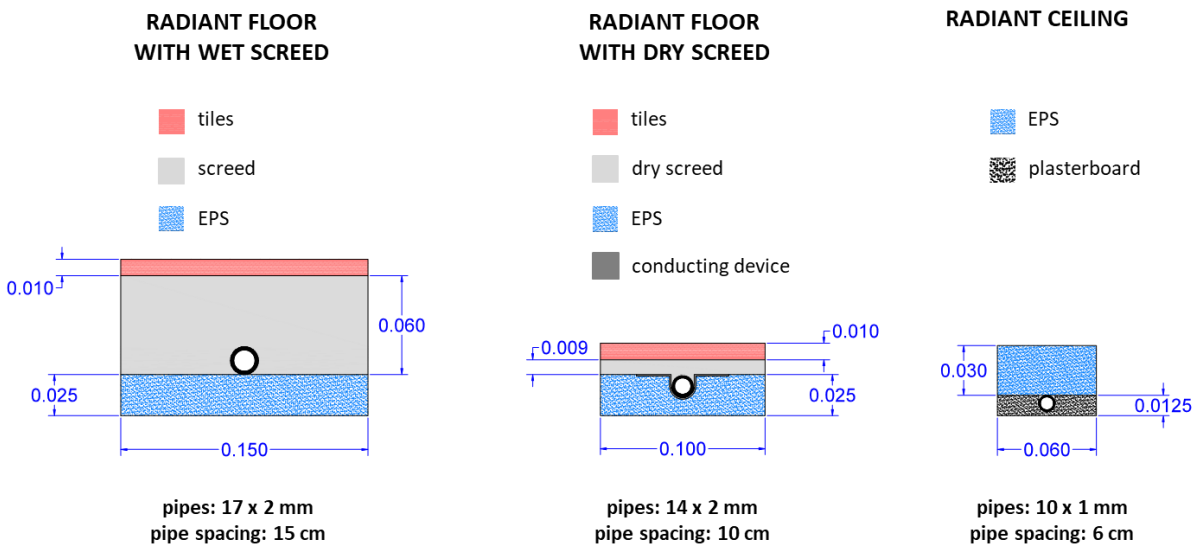

Figure 3.3 - Description of the radiant systems considered in this work.

Table 3.3 - Codification of the 3 types of radiant systems.

Codification	Type of radiant system
FW	Radiant floor with wet screed
FD	Radiant floor with dry screed and aluminum plate diffuser
C	Radiant ceiling with plasterboard coupled with insulation panels

3.3.3 Supply water temperature control modality

Two operation modes were considered for the circuits of the radiant systems. First the simulations were done with a constant supply water temperature, regardless of external air temperature. Then a climatic control modality was implemented: the supply water temperature was set equal to the design value for an external air temperature up to -5°C (which is the design outdoor temperature for the considered climate) and a linear interpolation was done considering the value of 22.5°C for an external temperature of 20°C.

Table 3.4 - Design heat load and design values of the supply water temperature.

Type of building	Design heat load [kW]	Water temperature [°C] for each type of radiant system		
		FW	FD	C
N	3.77	29.8	28.6	35.7
I-M	2.39	27.1	26.4	30.8
I-E	2.29	26.9	26.2	30.5
I-I	2.28	26.9	26.2	30.5
WI-E	1.97	26.3	25.7	29.4
WI-I	1.98	26.3	25.7	29.4
WI-X	1.90	26.1	25.6	29.0
WI-L	1.94	26.2	25.6	29.2

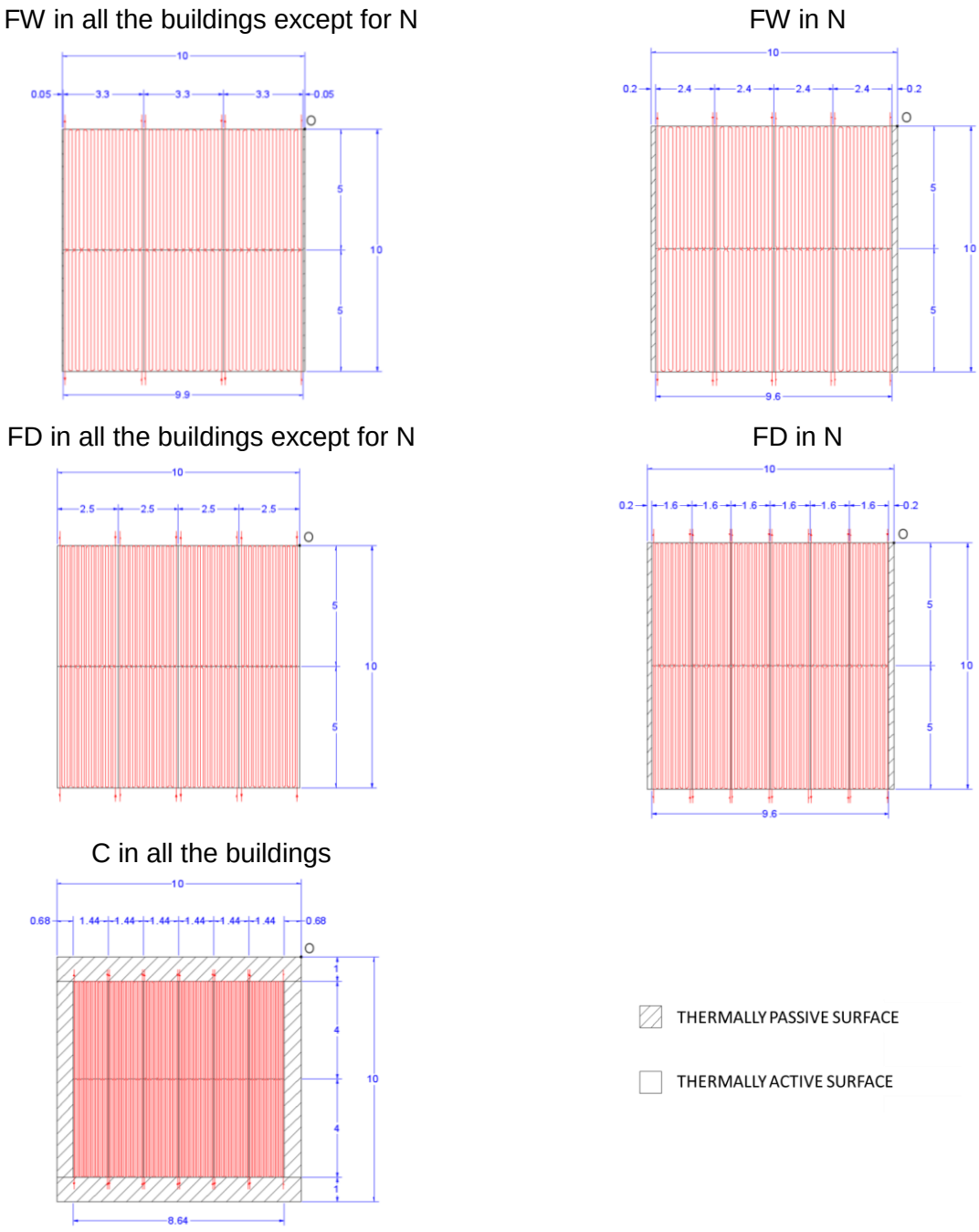

Figure 3.4 - Description of the circuits of the radiant systems implemented in DIGITHON.

The mean value of the water temperature circulating in the radiant system was obtained by means of HEAT2. As already explained, the desired temperature is that value which gives a heat flux towards the considered room equal to the specific design heating load. The design supply water temperature was set 2.5°C higher than that mean value (Table 3.4).
An example of the different values of the mean water temperature required by the different kinds of radiant systems to heat the same building can be seen in Figure 3.5. It is useful to specify that, for the calculation of the specific heating load, the entire floor surface was considered to be thermally

active, against the 70% of the ceiling surface (according to the water loops of Figure 3.4). For the heat loss calculation as well as FDM calculations in design conditions, a temperature of 20 °C was set both in the heated room and in the rear room.

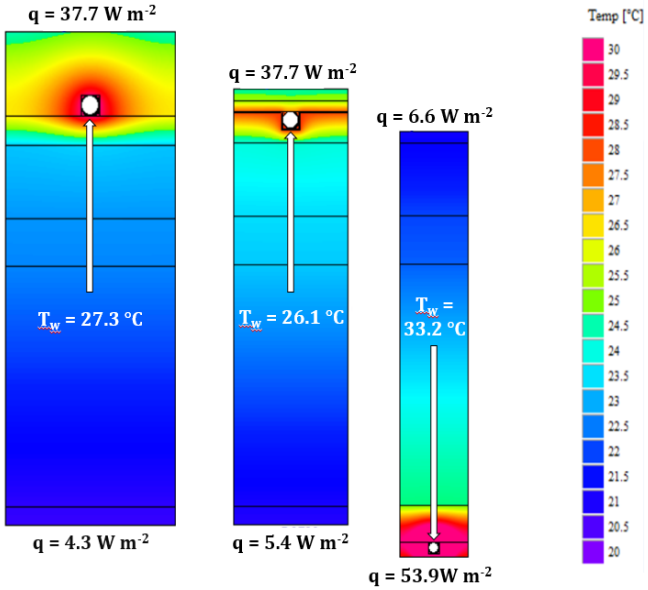

Figure 3.5 - Example of calculation of the mean value of the water temperature required to fulfil the design heating load of the not insulated building (3770 W) with the 3 different types of radiant systems. Average temperatures of the active surfaces are 23.4 °C in the floor heating cases and 28.3 °C in the case of radiant ceiling.

3.3.4 Simulations performed

In order to evaluate the energy and comfort performance, three simulations were performed with DIGITHON for each combination of building structures and radiant systems:

- an ideal convective simulation with air temperature set to 20.0 °C;
- two radiant simulations with a reduced value of air temperature setting, so that the mean value of the operative temperature in the point P (in the middle of the room at 1.1 m height, as shown in Figure 3.2) in the period from December to February is the same of the ideal convective simulation.

The radiant simulations were two because of the 2 examined control modalities of the supply water temperature (fixed and variable according to outdoor ambient temperature). The air temperature setting and the resulting average operative temperature in the different types of buildings are shown in Table 3.5.

Table 3.5 - Mean value of operative temperature and air temperature of the radiant simulations.

Building	T_o [°C]	T_{air} [°C]	
		FW, FD	C
N	19.4	19.3	18.8
I-M, I-E, I-I	19.8	19.7	19.4
WI-E, WI-I	20.0	19.8	19.6
WI-X, WI-L	20.0	19.7	19.6

For the comfort analysis other 8 ideal convective simulations were done, one for each kind of building, removing the layers of the radiant system. In this way a comfort comparison was done between a building heated by a radiant system and the same building heated by an ideal convective system.
The external heat transfer coefficient of the external walls was set to 25 $W\,m^{-2}\,K^{-1}$ and the solar absorption coefficient was set to 0.6.
The heat transfer coefficient used for the different heated surfaces were assumed constant according to [78]. Considering the part of the heat transfer coefficient due to infrared radiation equal to 5.5 $W\,m^{-2}\,K^{-1}$ [89] [90], the resulting convective coefficients are listed in Table 3.6. As found in a previous work [78], the choice of constant values for convective heat transfer coefficients instead of variable values implies negligible changes in the overall thermal balance calculated by DIGITHON.
Other parameters were defined for all the simulations: air change rate and internal gains (Table 3.7).

Table 3.6 - Convective heat transfer coefficient of each surface of the room.

Surface	α_c [$W\,m^{-2}\,K^{-1}$]
Radiant floor	5.5
Radiant ceiling	1.0
Non-active surfaces	2.5

Table 3.7 - Other parameters of the simulations.

Parameter	Set value
Air change rate	0.3 Vol/h = 90 m^3/h (infiltrations + ventilation)
Internal gains	374 W, 70% convective and 30% radiant

The simulations were performed on an hourly basis, with the climatic data *De Giorgio* [91] of the city of Venice. In particular, the following hourly mean data were considered: air temperature, direct solar radiation and diffuse solar radiation, while the effect of wind on the infiltrations was not taken into account. The official heating period defined by law for Venice has been considered, i.e. from mid-October to mid-April.

3.4 RESULTS

The software DIGITHON provides, in the case of ideal convective system, the thermal power needed in the time step to get the required air temperature. This means that the air temperature is kept constant and heating is needed only if the air temperature could go below 20 °C as calculated by the thermal balance. If the thermal balance leads to air temperatures greater than 20 °C the air temperature is calculated as a result of the thermal balance. The surface temperatures are provided as results and hence the mean radiant temperature and the operative temperature can be calculated.
The heating system was considered to work constantly 24 h, i.e. no overnight set-back was assumed. The seasonal energy required by the ideal convective heating system has been named Q_{id}.
When the radiant system is simulated, the inputs are the supply water temperature and the mass flow rate in each circuit, and the thermal balance gives as output the return temperature of the water;

in this way the energy delivered/absorbed by the water in the time step can be evaluated, as well as the surface temperature. As already mentioned, the control system was supposed to be on-off with a set-point of 20 °C and a dead band of ±0.5 °C. This means that if the temperature of the room in the time step is lower than 19.5 °C, the water circulates in the pipes of the radiant system with a defined supply temperature which could be fixed or variable as a function of external temperature. If the air temperature reaches 20.5 °C, the water stops circulating and the temperature fluctuates depending on the thermal balance of the room without any active system working in that time step. As regards the circuits in the room, either all of them work or none of them operates, i.e. no zone control was set since the room was considered as an open space. From the hydronic point of view no other assumptions was considered, such as a tank or a limited power supplied by the generator, except for the water volume of the circuits in the room and related thermal capacity. The seasonal energy required by the water embedded heating system has been named Q_w. The on-off control between 19.5 °C and 20.5 °C was chosen based on a survey provided to companies producing radiant systems in Italy. All producers declared that on-off regulation is the standard control strategy in flats and that PI or PID control is only installed in single family houses due to the high cost of this technology.

3.4.1 Radiant systems efficiency

The hourly values of the energy provided as results of the simulations performed by DIGITHON allow the evaluation of the efficiency of the radiant system. Considering the seasonal energy Q_{id} of an ideal convective system and the seasonal energy provided to the radiant system Q_w, the efficiency of the radiant system can be defined as:

$$\eta_{em+ctr} = \frac{Q_{id}}{Q_w} = \eta_{em} \cdot \eta_{ctr} \qquad (3.1)$$

This is a joint embedded and control efficiency since it takes into account the losses of the radiant system behind the pipes as well as the effects of the control system. In Figure 3.6 the results obtained for the combination of 8 building structures, 3 radiant systems and 2 supply water temperature control modalities are represented. These efficiency values are calculated along the whole heating season and hence they include not only the heat losses in the room behind the radiant system and the way the water circulation is controlled, but also the thermal inertia of the building structures as well as the influence of solar and internal gains. Since it is a combination of all these factors, it is not possible to split among control efficiency and embedded efficiency.
In the same figure, the steady-state embedded efficiency calculated through HEAT2 is represented. These efficiency values take into account only the geometry and the thermal properties of the building structure where the radiant system is placed and proper boundary conditions. Considering the useful thermal power q_u towards the heated space and the thermal losses q_l towards the adjacent space, the emission efficiency in steady-state conditions of the radiant system can be calculated as:

$$\eta_{em,H2} = \frac{q_u}{q_u + q_l} \qquad (3.2)$$

The following boundary conditions were fixed: room temperatures equal to 20°C, convective heat transfer coefficient on the surfaces according to Table 3.6, adding the radiant heat transfer coefficient on the surfaces equal to 5.5 W m^{-2} K^{-1}, water temperature according to the specific design heat load for each case (Table 3.4).

In order to maintain the same comfort conditions (i.e. same operative temperature), the radiant simulations were repeated reducing the air temperature set-point compared to the convective ideal simulation. As already mentioned, the set-point was chosen in such a way that the resulting mean value of the operative temperature in the point P in the period from December to February was the same of the mean value of the ideal convective simulations with set-point of the air equal to 20 °C. This way an iterative process was carried out for each single case in order to reach the same operative temperature. The period from December to February was chosen to evaluate the mean value of the operative temperature, because during mild months the average temperature is quite high in insulated buildings, the heating system works rarely and it is difficult to compare the different kind of buildings under the same operating conditions. The heating energy need in the period December-February is, depending on the insulation level, from 75% to 90% of the heating energy need of the entire season.

The embedded and control efficiency values for the radiant systems have been calculated via Equation 3.1. The results are shown for the period December-February (Figure 3.6) and for the whole season (Figure 3.7). As a matter of fact, the first value shows the results under the same indoor conditions (operative temperature), the second one gives an idea on the embedded and control efficiency over the whole season. In Figure 3.6 and Figure 3.7 also the embedded values which can be calculated in steady state conditions by using Equation 3.2 with results of FDM are represented.

As can be seen, the red line of the climatic control is on average slightly above the blue line of the constant supply temperature control modality. In well-insulated timber and light buildings the efficiency is almost the same (98-99%) regardless the type of radiant system used. These buildings present 2% higher efficiency compared to masonry structures; with these last structures there is no difference among radiant systems in climatic control strategy, while with constant temperature the wet floor performs slightly better. The results of well-insulated buildings of the period December-February (Figure 3.6) are very similar to the ones related to the whole season (Figure 3.7), since the energy evaluated in this period takes into account 90% of the heating demand of the whole season. In non-insulated buildings and in insulated buildings usually the dry floor radiant system performs slightly worse than both the wet floor and the ceiling system (about 2%). In these cases when considering the whole season instead of the period December-February there is a 2% difference in the embedded and control efficiency.

The interesting aspect is that the embedded and control efficiency calculated via dynamic simulations (Equation 3.1) is higher than the embedded efficiency calculated via FDM in steady-state conditions (Equation 3.2). In light well-insulated structures the embedded and control efficiency of dynamic simulations is 1.5% better than the embedded efficiency estimated via FDM (1% if considering the period December-February, 2% if the whole season). In masonry well-insulated buildings the embedded and control efficiency of dynamic simulations is 3.5% better than the embedded efficiency estimated via FDM with constant supply temperature (3% if considering the period December-February, 4% if the whole season), while dynamic simulations provide 4.5% better embedded and control efficiency than the embedded efficiency estimated via FDM in the case of climatic control (4% if considering the period December-February, 5% if the whole season). In insulated buildings the difference is almost 4% regardless to the water supply temperature, while for non-insulated buildings the difference is 6%.

It is useful to highlight that the efficiency calculated via FDM is evaluated with constant indoor temperature and in steady-state conditions, as usually done by producers of radiant systems and practitioners and, therefore, depends only on the difference between water temperature and room

temperature and on the thermal conductivity of the materials of the various layers, but not on their thermal capacity. In dynamic conditions the situation is completely different, both for the water inside the pipes and for the boundary conditions. For most of the time the heat load required by the room is lower than the design heat load, and hence warm water is not continuously flowing in the pipes of the radiant system. The changing indoor conditions and the consequent on-off operation of the radiant system lead to a complex mechanism of absorption and release of heat in the different layers of the floor and the percentage losses are lower than in steady-state conditions.

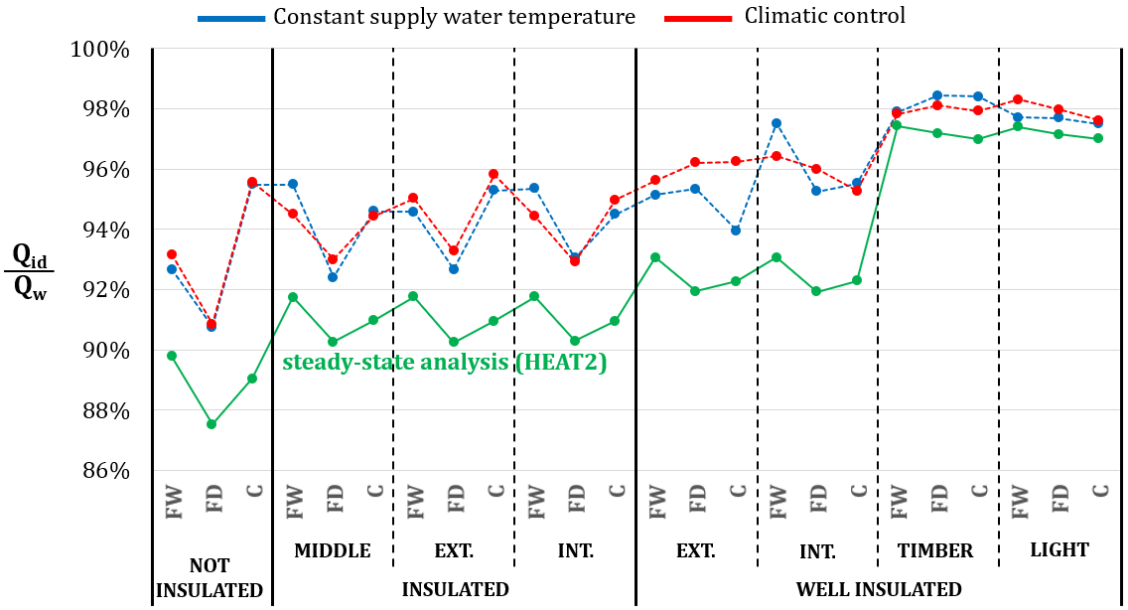

Figure 3.6 - Efficiency of the radiant systems limited to the period from December to February (blue and red), obtained considering the same operative temperature of the ideal convective simulations, and efficiency calculated by FDM in steady-state conditions (green).

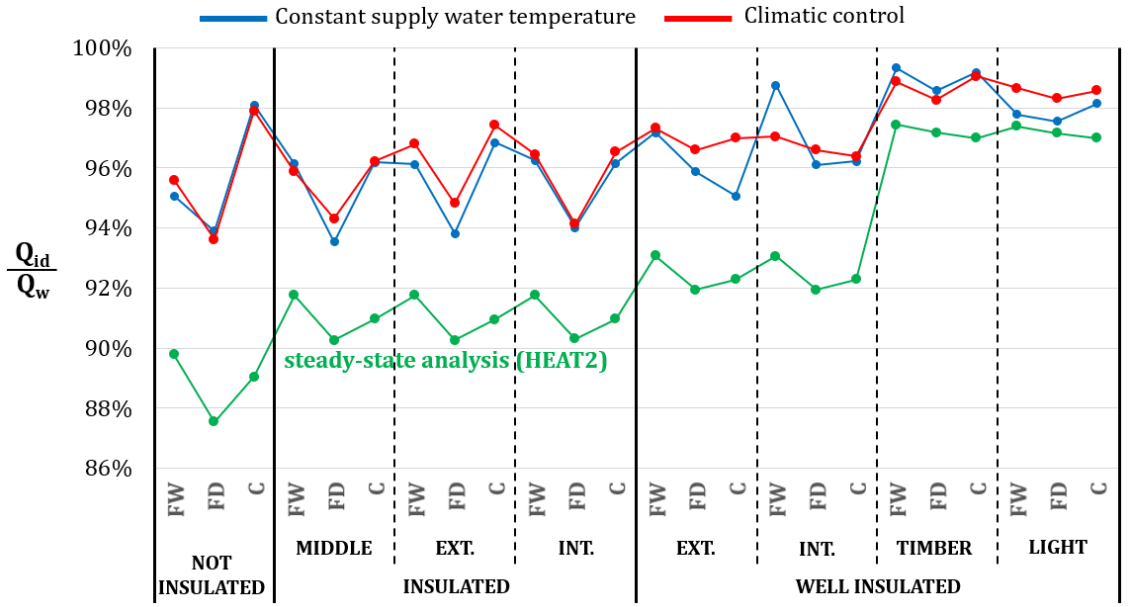

Figure 3.7 - Efficiency of the radiant systems over the whole heating season (blue and red) and efficiency in steady-state conditions (green).

As regards the efficiency values which can be found in the standards, the old version of EN ISO 15316-2-2007 [92] recommends to use an embedded and control efficiency value which is equal to 90% for the wet floor and ceiling systems (η_{ctr} = 0.95, η_{emb} = 0.94) considered in this study and 91.3% for the dry floor system (η_{ctr} = 0.95, η_{emb} = 0.955). In the old version of the standard o difference in the efficiency values is considered to take into account the different insulation level and thermal inertia of the building.
In the last version of the standard EN ISO 15316-2-2017 [93], the calculation method to evaluate the energy required by a heating or cooling system is only based on internal temperature variations, while the calculation method based on efficiency values was removed. Besides efficiency values, also the internal temperature variation was therefore calculated from the results of the simulations for the period from December to February.

Table 3.8 - Temperature variation values calculated from the results of the dynamic simulations with DIGITHON and values according to EN ISO 15316-2 (2017).

Type of building	Type of radiant system	Temperature variation $\Delta T_{i,emb} + \Delta T_{i,ctr}$ [°C]		
		Simulations		EN ISO 15316-2
		Constant supply water temperature	Climatic control	
N	FW	1.1	1.1	1.9
	FD	1.5	1.4	2.2
	C	0.7	0.7	2.2
I-M	FW	0.7	0.9	1.9
	FD	1.2	1.1	2.2
	C	0.8	0.9	2.2
I-E	FW	0.8	0.8	1.9
	FD	1.2	1.1	2.2
	C	0.7	0.6	2.2
I-I	FW	0.7	0.9	1.9
	FD	1.1	1.1	2.2
	C	0.9	0.8	2.2
WI-E	FW	0.8	0.7	1.9
	FD	0.7	0.6	2.2
	C	1.0	0.6	2.2
WI-I	FW	0.4	0.6	1.9
	FD	0.7	0.6	2.2
	C	0.7	0.7	2.2
WI-X	FW	0.3	0.3	1.9
	FD	0.2	0.3	2.2
	C	0.2	0.3	2.2
WI-L	FW	0.4	0.3	1.9
	FD	0.4	0.3	2.2
	C	0.4	0.4	2.2

As can be seen in Table 3.8,the current standard overestimates the losses of the radiant systems: in the non-insulated case the difference is about 0.7 °C for the radiant floor and 1.5 °C for the ceiling. In insulated buildings the difference is 1.1 °C in insulated buildings and 1.4 °C for the radiant ceiling. In well-insulated masonry buildings the difference with the temperature variation of the existing standard is 1.2 ÷ 1.5 °C for the radiant floor and 1.2 °C for the radiant ceiling. In well-insulated buildings with light structures the difference is about 1.7 °C ÷ 1.9 °C. These values are conservative, since the calculation was limited to the period from December to February, which is the one which provided the lowest efficiencies in terms of losses and hence the greatest values of the temperature difference $\Delta T_{i,emb} + \Delta T_{i,ctr}$.

3.4.2 Energy analysis

Besides the embedded and control efficiency, the overall energy consumption should also be evaluated. Concerning the supply water temperature control modality, the climatic control has the undeniable advantage of reducing its seasonal mean value of about 4 °C in non-insulated buildings, 2.5 °C in insulated buildings and 2 °C in well-insulated buildings (Figure 3.8). The ceiling systems need higher water temperatures than floor systems because of the lower convective heat transfer coefficient and of the smaller active surface; for this reason the ceiling systems show the greatest temperature reductions among the 3 kinds of radiant systems when going from the constant supply temperature to variable supply temperature related to outside air (climatic control strategy). As regards the operation time, the climatic control obviously shows an increase, which is equal to 58%, 46% and 41% for the non-insulated, insulated and well-insulated buildings respectively.

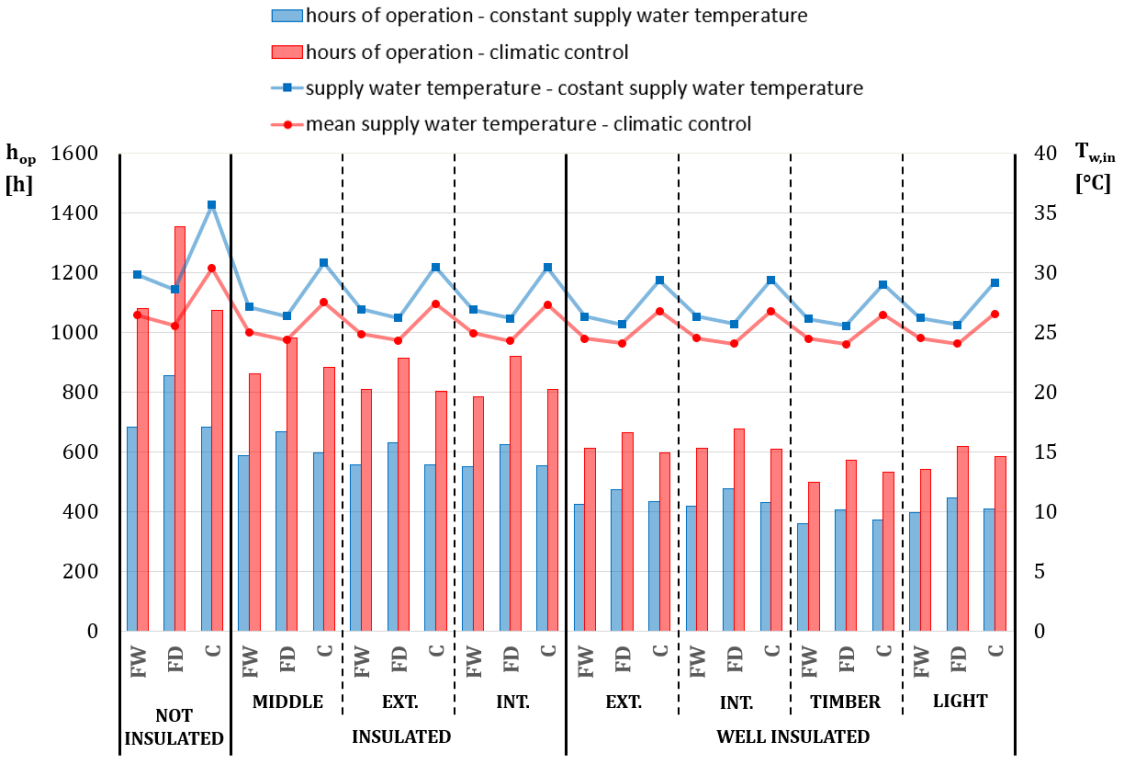

Figure 3.8 - Hours of operation of the radiant systems and mean value of the supply water temperature in the different cases.

A simplified evaluation of the energy consumption of the entire heating system was done considering a water-to-water heat pump as generator, a primary loop and a secondary loop with their pumps (Figure 3.9).

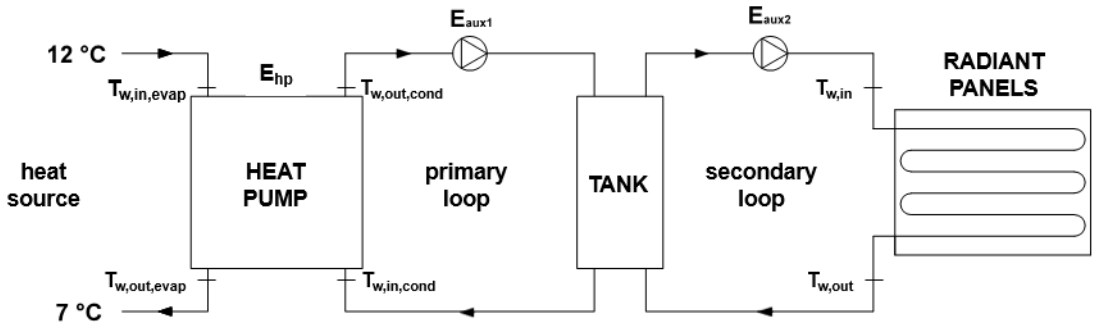

Figure 3.9 - Simplified layout of the considered heating system.

Table 3.9 - Nominal data of the considered water-to-water heat pump.

Heat pump data		Nominal condition	
$P_{el,nom}$	1.6 kW		
$P_{t,nom}$	6.8 kW	$T_{w,in,evap}$ = 12 °C	$T_{w,out,evap}$ = 5 °C
COP_{nom}	4.25	$T_{w,in,cond}$ = 30 °C	$T_{w,out,cond}$ = 35 °C

The electric energy consumption of the heat pump was estimated considering a heat source constantly at 12 °C and a temperature difference at the evaporator of 5 °C (water source temperature from 12 °C to 7 °C). The nominal conditions in Table 3.9 from a commercial datasheet were considered to evaluate the coefficient of performance (COP) in conditions different from the nominal ones.
For evaluating the COP of the heat pump the ideal coefficient of performance of a Carnot cycle was used:

$$COP_{id} = \frac{T_{cond}}{T_{cond} - T_{evap}} \tag{3.3}$$

where the condensing and evaporating temperatures of the cycle were evaluated as follows:

$$T_{cond} = \frac{T_{w,in,cond} + T_{w,out,cond}}{2} + 5 \tag{3.4}$$

$$T_{evap} = \frac{T_{w,in,evap} + T_{w,out,evap}}{2} - 5 \tag{3.5}$$

By using Equations 3.3, 3.4 and 3.5, in nominal condition the ideal Carnot cycle gives $COP_{id,nom}$ = 9.41.
At each time step of the simulations the ideal coefficient of performance COP_{id} was calculated considering the mean value of the water temperature in the condenser equal to the supply water temperature $T_{w,in}$ of the radiant panels. The COP of the heat pump was then estimated as follows:

$$COP = COP_{id} \frac{COP_{nom}}{COP_{id,nom}} \tag{3.6}$$

At each timestep the electric energy consumption of the heat pump E_{hp} can be calculated as:

$$E_{hp} = \frac{Q_w}{COP} \tag{3.7}$$

From the seasonal thermal energy and the corresponding electric consumption, the mean value of the COP can be calculated. This is called seasonal performance factor (SPF) and its value can be seen in Figure 3.10 (right axis) together with the electric energy require by the heat pump (left axis).

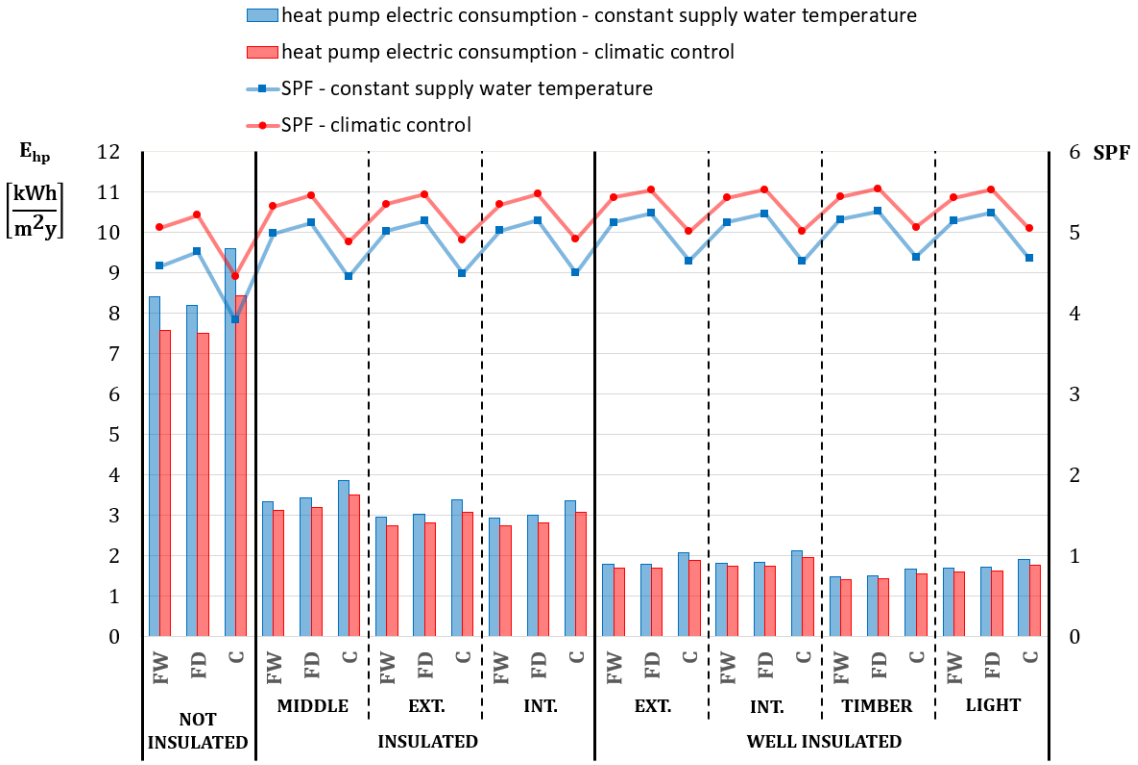

Figure 3.10 - Heat pump electric energy consumption and seasonal performance factor with constant supply water temperature and climatic control.

The higher SPF which can be achieved with the climatic control of the supply water temperature makes the heat pump electric consumption lower, but also the electric consumption of the auxiliaries should be evaluated. As already seen in Figure 3.8, the number of hours of operation of the pump of the secondary loop is much higher in the case of climatic control instead of constant supply water temperature. The pressure drops of each combination of radiant system and building type were calculated and the electric power of the pump was then evaluated from the chart of a common high efficiency pump for domestic use. For the primary loop the number of hours of operation of the pump was calculated from the seasonal thermal energy need and the nominal thermal power of the heat pump.

The resulting total electric energy consumption E_{tot} can be seen in Table 3.10, where also the electric energy consumption of the heat pump E_{hp}, of the primary pump $E_{aux,1}$ and of the secondary pump $E_{aux,2}$ are listed.
If the generator of the heating system is a heat pump and the radiant circuits are properly designed, the increase of the operation time of the secondary loop with climatic control instead of constant supply water temperature is in any case balanced by the reduction of the consumption of the heat pump due to the lower water temperature. Considering the ceiling system, the climatic control modality ensures a reduction of the total electric energy consumption of about 11%, 8% and 7% for the non-insulated, insulated and well-insulated buildings respectively. With the floor systems the reduction is about 8%, 5% and 4% respectively.

Table 3.10 - Electric energy consumptions and percentage difference between climatic control and constant supply water temperature.

Type of building	Type of radiant system	Constant supply water temperature				Climatic control				ΔE_{tot}
		E_{hp} [kWh]	$E_{aux,1}$ [kWh]	$E_{aux,2}$ [kWh]	E_{tot} [kWh]	E_{hp} [kWh]	$E_{aux,1}$ [kWh]	$E_{aux,2}$ [kWh]	E_{tot} [kWh]	
N	FW	841	31	11	883	757	31	17	806	-8.7%
	FD	820	32	16	868	750	32	26	807	-6.9%
	C	960	30	13	1003	844	30	21	896	-10.8%
I-M	FW	333	13	4	351	313	13	6	333	-5.1%
	FD	342	14	8	365	318	14	12	344	-5.6%
	C	385	14	7	406	351	14	11	375	-7.6%
I-E	FW	295	12	4	311	275	12	6	293	-5.9%
	FD	303	13	7	323	282	12	10	304	-5.6%
	C	338	12	6	356	307	12	9	329	-7.7%
I-I	FW	292	12	4	308	274	12	5	291	-5.3%
	FD	300	12	7	319	281	12	10	304	-4.8%
	C	337	12	6	355	307	12	9	329	-7.6%
WI-E	FW	179	7	3	189	169	7	4	180	-4.9%
	FD	180	8	4	191	169	8	5	182	-4.8%
	C	208	8	4	220	189	8	5	202	-8.1%
WI-I	FW	181	7	3	191	173	8	4	185	-3.1%
	FD	184	8	4	196	173	8	6	187	-4.6%
	C	212	8	4	223	196	8	5	209	-6.4%
WI-X	FW	148	6	2	156	141	6	3	150	-4.0%
	FD	151	6	3	160	143	6	4	154	-3.7%
	C	168	6	3	177	156	6	4	167	-6.0%
WI-L	FW	170	7	2	179	159	7	3	170	-5.4%
	FD	171	7	4	182	161	7	5	173	-4.8%
	C	191	7	3	202	176	7	5	189	-6.6%

3.4.3 Overtemperature analysis

An analysis was carried out on the operative temperature in the point P (Figure 3.2) in the period from December to February, considering the degree hours criteria described in Annex F of EN 15251 (2007) [50]. A temperature range was defined and the degree hours outside the upper boundary of the range ($T_{o,ul}$) was used as a performance indicator of the building for the cold season in relation to the overtemperature. The weighting factor for overtemperature WF^+ can be calculated as:

$$WF^+ = \sum(T_o - T_{o,ul}) \qquad \text{for } T_o > T_{o,ul} \qquad (3.8)$$

Since the simulations were performed maintaining in the convective ideal case the air temperature constant at 20 °C, the operative temperature differs in all the cases. Hence a specific range of acceptability was defined for each radiant case, centred on the mean value of the operative temperature, which is the same of the ideal convective cases, and with an amplitude of 1.0 °C (i.e. ±0.5 °C). A small band was chosen, with the same amplitude of the on-off thermostat, since the purpose was not the evaluation of comfort conditions, but simply the evaluation of the periods with the operative temperature rising outside the control band of the air temperature and the comparison of these periods with different envelopes and type of radiant systems, as well as the comparison between the building with the radiant systems and the same building with an ideal convective heating system. A larger band was not suitable for a fully exhaustive evaluation, since it was found that, in the worst cases (well-insulated timber envelope and light envelope with dry floor system), the operative temperature exceeded more than 1.5 °C its mean value for only about 3% of the time, i.e. no discomfort has been found for overheating in all the cases.

In Figure 3.11 the WF^+ calculated from the results of the radiant simulations are represented. As can be noticed, the constant supply water temperature control modality always gives a higher WF^+ than the climatic control modality, except for the well-insulated buildings, where the WF^+ are similar. The ceiling systems present a WF^+ which is, on average, more than 5 times the WF^+ of the floor systems in the non-insulated building and 2.5 times of the floor systems in the insulated and well-insulated masonry buildings. In the well-insulated lighter buildings the dry-floor system presents the highest WF^+, almost 1.5 times the WF^+ of the wet-floor and ceiling systems.

It is interesting to notice that the 50% of the WF^+ of the well-insulated light buildings can be already found in the ideal convective simulations. This percentage decreases to 27% for the well-insulated masonry buildings, 12% percent for the insulated buildings and only 2% for the non-insulated buildings. In a convective system controlled with an on-off band like the simulated radiant systems, these percentages would certainly be higher, showing that the problem of overheating in well-insulated buildings is not strictly related to the radiant system itself, but it is inevitable especially in case of light structures (even in ideal conditions). Moreover, the control modality may affect the overheating.

In Figure 3.12 the value WF^+/h^+ of the overheating is represented; h^+ is the number of hours which contribute to the overall value of WF^+, i.e. the number of hours in which the operative temperature exceeds the threshold value defined. In the insulated buildings the overheating intensity is the same of the ideal convective cases, except for the constant supply water temperature ceiling systems which show much higher values. The well-insulated masonry buildings with wet-floor radiant system show a overheating intensity lower than that of the ideal convective system. The same occurs in the well-insulated light buildings for the wet floor radiant systems and also for the ceiling systems but not for the dry-floor systems.

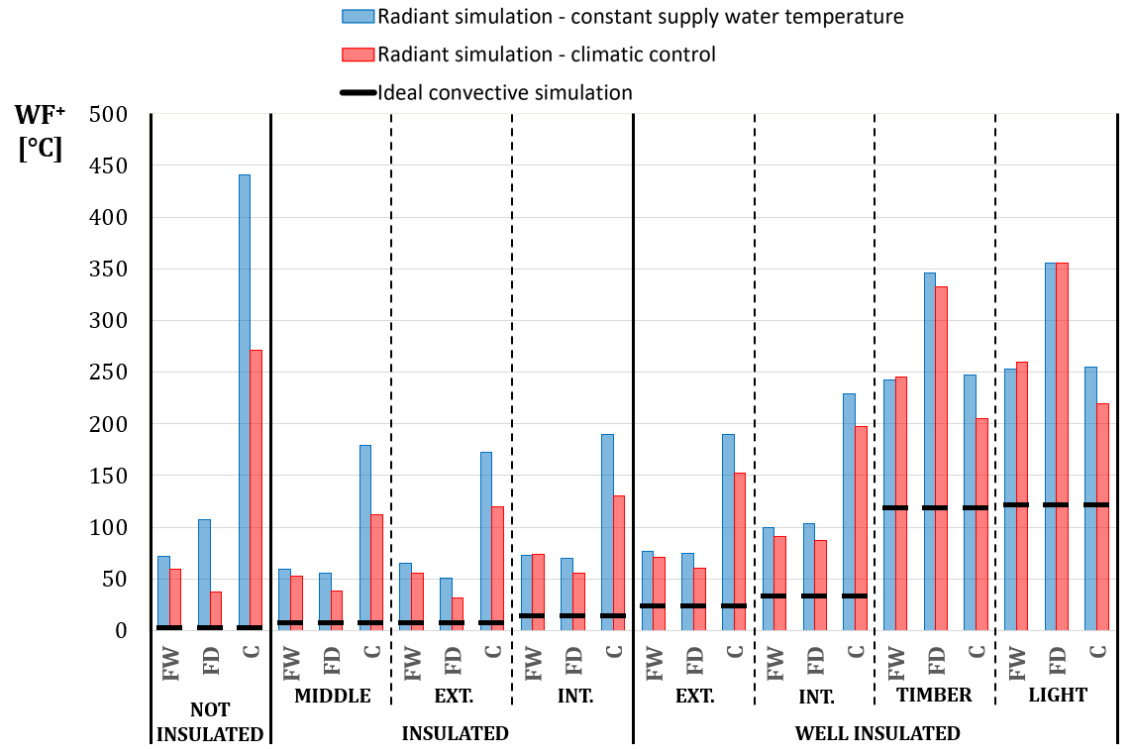

Figure 3.11 - Weighting factor in the radiant cases and in the equivalent ideal convective ones.

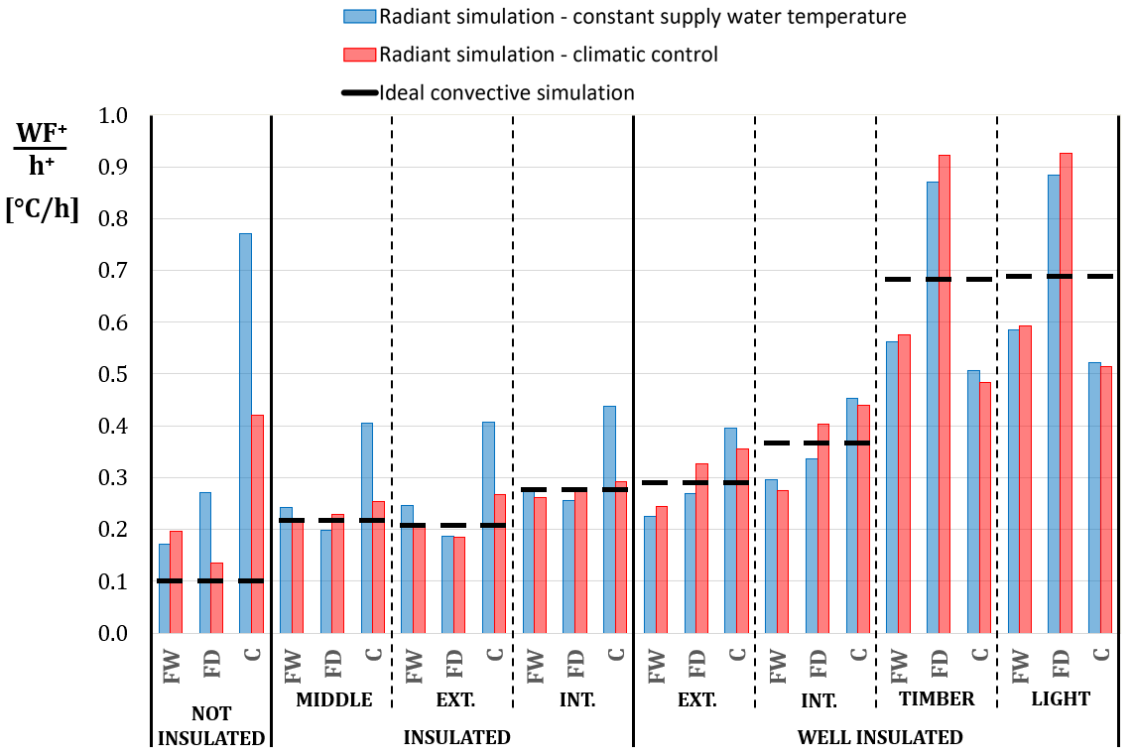

Figure 3.12 - Mean value of the specific overtemperature in the radiant cases and in the equivalent ideal convective ones.

3.5 CONCLUSIONS AND DISCUSSION

The work carried out is based on simulation of a room of about 100 m^2 which represents a flat in a multi-storey building where three types of radiant systems have been modelled: two radiant floors (one with usual pipes embedded in wet screed and one with low thickness dry screed) and a radiant ceiling. The work looks at the performance of these systems in heating conditions with three insulation levels of buildings: no insulation, insulated building and well-insulated building. Three types of insulated buildings (with internal, intermediate and external insulation) and four types of well-insulated buildings (masonry with external and internal insulation, timber structure and light structure) have been analysed. Dynamic simulations of the radiant systems with fixed temperature and with variable temperature according to outdoor temperature have been compared with an ideal convective dynamic simulation. Results have been analysed in terms of control and embedded efficiency of the radiant system, energy performance of the radiant system with a water-to-water heat pump at constant source temperature as well as thermal comfort.

About the embedded and control efficiency, the climatic control strategy performs slightly better than the constant supply temperature control modality. In well-insulated light buildings the efficiency of the two control strategies is almost the same (98-99%) regardless of the type of radiant system used. These buildings present 2% higher efficiency compared to masonry structures; with these last structures the different types of radiant systems show the same efficiency value in case of climatic control strategy, while with constant temperature the wet floor performs slightly better. In non-insulated buildings and in insulated buildings usually the dry floor radiant system performs about 2% less than both the wet floor and the ceiling system (which present an efficiency of about 96%).

The embedded and control efficiency calculated via dynamic simulations has been compared to the embedded efficiency calculated in steady-state conditions via FDM simulations. In light well-insulated structures the emission efficiency of dynamic simulations is 1.5% better than the one estimated via FDM. In masonry well-insulated buildings the emission efficiency of dynamic simulations is 3.5% better than the one estimated via FDM with constant supply temperature, while climatic control simulations provide 4.5% better emission efficiency than the one estimated via FDM. In insulated buildings the difference is almost 4% regardless to the water supply temperature, while for non-insulated buildings the difference is 6%.

The old version of the standard EN 15316-2 (2007) [92] provides an embedded and control efficiency of 90% for the wet floor and ceiling systems and 91.3% for the dry floor system. The dynamic simulations provide for the wet floor and the ceiling as average 96% in non-insulated buildings, in insulated buildings and in masonry well-insulated buildings, 98% in well-insulated buildings with light structures. The dry floor presents an embedded and control efficiency of about 93% in non-insulated buildings and in insulated buildings, 95% in masonry well-insulated buildings and 98% in well-insulated buildings with light structures.

As regards the new version of the standard EN 15316-2 (2017) [93], the current values of the temperature difference $\Delta T_{i,emb} + \Delta T_{i,ctr}$ are higher than the ones calculated in the present work. Based on the dynamic simulations, the suggested values for the joint embedded and control temperature differences are the ones reported in Table 3.8, which should substitute the existing default values.

Moreover, the efficiency calculated in transient conditions is higher than the efficiency calculated under steady-state conditions. This result is due to the fact that, over the season, the radiant systems work for some hours and then they switch off. Part of the thermal energy embedded in the structures is not lost when the water stops flowing in the pipes, but it is later released to the room.

When considering the overall energy consumed by a water-to-water heat pump (including the auxiliaries), the increased amount of hours of pumping in the case of variable temperature is counterbalanced by the higher COP of the heat pump; overall the climatic control leads to 5-6% better performance in floor heating systems and 7-8% better performance in radiant ceilings. Overall the radiant ceiling consumes always more than the two floor systems, due to the higher supply temperature (about 11% in the case of variable temperature and 15% in case of fixed temperature). Of course the higher the insulation the higher the performance, hence the light structures perform better than the masonry structures due to the lower U-values.

Looking at long-term comfort evaluation results, no particular problem was found in the period from December to February according to EN 15251 category II. The analysis carried out was mainly related to check the overtemperature, i.e. the periods when the temperature was above the set-point temperature plus the dead band (0.5 °C in the present work). The results show that overtemperature rises when the insulation increases. In masonry structures radiant ceiling has always the highest values of WF^+, especially in case of constant supply temperature. This is due to the higher water temperature supply, although the radiant structure is light. In well-insulated light structures the dry floor shows the highest overtemperature. Anyway, it must be underlined the overtemperature found with the ideal convective system is comparable with the overtemperature found with the radiant systems. In particular when dividing WF^+ by the number of hours h^+ when the overtemperature occurs, the intensity of overtemperature (WF^+/h^+) is about of the same magnitude in the cases with radiant systems and in the ideal convective case. This means that the amount of hours when the overtemperature occurs is higher with radiant systems than in the ideal convective case, but the intensity of the overtemperature is similar.

Resuming the results, the work carried out shows that in general the better the quality of the envelope the better the overall performance of the radiant system. Evaluating the efficiency in dynamic conditions leads to higher efficiencies compared to steady state conditions, former standard EN 15316-2 (2007) and also new standard EN 15316-2 (2017), and new values are suggested. Working at variable temperature leads to lower consumptions compared to fixed supply temperature over the season. No problems of comfort have been found in the period from December to February and overtemperature effects are not especially due to radiant system, but they happen in any case also with ideal convective systems.

In general, the radiant ceilings perform worse than radiant floor systems in heating conditions and there is no evidence that dry floor systems perform better than wet screed systems in all the types of buildings regardless of the level of insulation and thermal inertia.

As final remarks, it would be interesting to analyse the same building in cooling conditions, where the radiant ceiling could work better than the radiant floor system. Moreover, the present work considers an undivided room and it would be interesting to look in detail on the distribution of the internal spaces and check the different possible control strategies.

4 EXPERIMENTAL AND THEORETICAL ENERGY ANALYSIS OF TWO TYPES OF RADIANT FLOOR HEATING SYSTEMS

Abstract
Numerical simulations and field measurement analyses on a traditional radiant floor heating system and a radiant floor system with a reduced thickness of the screed are presented in this chapter. The two systems have been installed in a new building in adjacent flats with the same internal distribution. Continuous and intermittent operation were considered, with a limited and unlimited water temperature difference available from the generation side. The performance of the two floor systems in terms of final energy need, operative and air temperatures, floor surface temperature, mean supply water temperature, mean water temperature difference, number of hours of operation and eventual overheating were compared.

4.1 INTRODUCTION

Radiant floor heating system is the most widespread kind of radiant system, especially in residential buildings. Besides traditional floor systems and dry floor systems, a new type of floor system is recently spreading in the market. It is a wet floor system with a reduced thickness of the screed, which is useful in situations where there are problems of height (e.g. retrofit of existing buildings) and which has a faster thermal response if compared to a traditional floor system. Despite being part of a well-known technology, designers and practitioners frequently ask if these newly-developed systems perform better than the traditional ones and if energy saving can be achieved when they are used in intermittent operation. Moreover, it is argued if they allow better comfort conditions for the occupants in new and retrofitted buildings, where the insulation level of the envelope is high and overheating can occur in mid-seasons.
To investigate the energy performance of this new type of radiant floor, measurements are needed, along with dynamic simulations properly taking into account the dynamic behaviour of building structures as well as the transient operation of water in the embedded pipes. Dealing with field measurements involving systems like heating/cooling plants coupled with buildings is generally a complex matter and most of the times the mere energy measurements cannot lead to immediate conclusions on the energy performance of the analysed systems. In particular, when two systems are under comparison, it is very difficult to perform measurements in exactly the same conditions, because different orientations of the buildings, different internal loads when the buildings are inhabited, different weather conditions and different boundary temperature are elements which cannot usually be all avoided. Simulations are therefore needed to compare the systems under the same boundary conditions and data from measurements are very useful to tune the models.

4.2 METHOD

The floor radiant heating systems of two flats in a new building not yet inhabited were considered for the analyses, a traditional one and a thin-screed one. Continuous energy and temperature

monitoring in continuous and intermittent operation and with different supply temperature was planned, and the measurements were used to a rough tuning of the model. Dynamic simulations of the two systems were then performed under the same boundary conditions. A cold month and a mid-season month with mild temperatures and higher solar radiation were simulated, using a step of 10 minutes. Both continuous and intermittent operation were considered. Two possibilities were taken into account for the temperature difference from the generation side, which could be limited to 5 K or unlimited. The resulting energy need, operative and air temperatures, floor surface temperature, mean supply water temperature, mean water temperature difference, number of hours of operation and the eventual overheating were compared.
The numerical model DIGITHON [78] was used, as in the previous chapter, to perform the detailed simulations of the radiant systems and the building. Further details can be found in 3.2.
The commercial software HEAT2 [87] was used to calculate the heat transfer response factors, to evaluate the water temperature in design conditions and for the estimation of the response time of the two systems.

4.3 CASE STUDY

4.3.1 Building geometry and structures

Two flats of about 110 m^2 were considered as case study, located on the ground floor of a new building (year 2017) in Padova. Only two rooms where considered in the analysis, as highlighted in Figure 4.1. The choice was made considering that these two rooms have the same orientation and are not contiguous to the garages. Rooms 1 have wooden floor, while rooms 2 are bathrooms with ceramic tiles. The overall heated floor surface during the measurements was about 17 m^2 for each flat (Table 4.1).

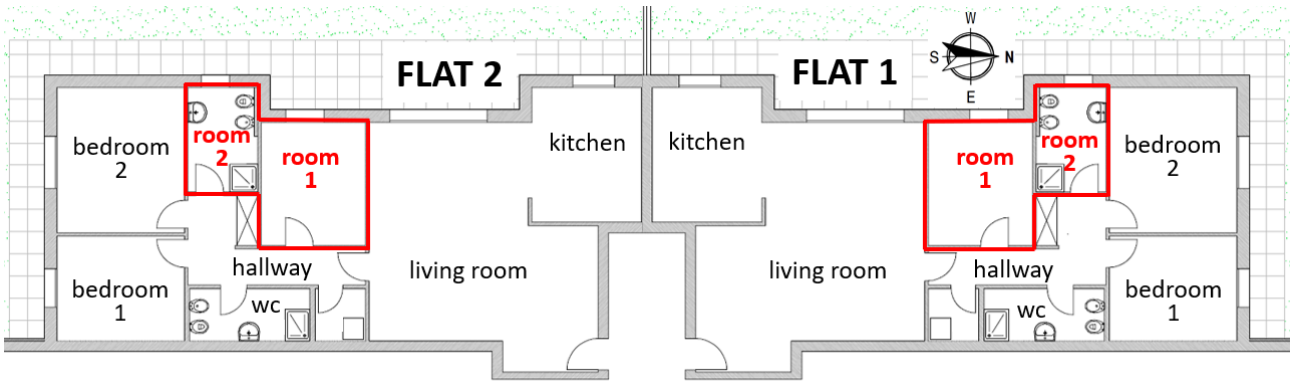

Figure 4.1 - The flats and the 2 rooms considered for measurements and simulations.

Table 4.1 - Dimensions of the 2 analysed rooms.

Room	Width [m]	Length [m]	Height [m]	Floor surface [m^2]	Volume [m^3]
1	3.00	3.54	2.70	10.62	28.67
2	2.01	3.01	2.70	6.05	16.34

The dimensions and the main properties of the windows are listed in Table 4.2.

The external walls are made of wood-fiber cement formwork blocks (Figure 4.2). Since the EPS layer and the concrete layer present slats in wood-fiber cement, the equivalent properties of those layers were calculated for the implementation in the models.
The stratigraphies of the different building structures of the 2 flats are presented from Table 4.3 to Table 4.7. For the horizontal structures, the stratigraphies of Rooms 2 with ceramic flooring are listed. Rooms 1 present the same layers, except for the flooring, which is a wooden one with a thermal resistance of 0.17 $m^2 K W^{-1}$ (thickness of 9 mm and thermal conductivity of 0.053 $W m^{-1} K^{-1}$), density of 700 $kg m^{-3}$ and thermal capacity of 2.40 $kJ kg^{-1} K^{-1}$.

Table 4.2 - Main features of the windows.

Room	Dimensions [m]	g-value [-]	U-value [$W m^{-2} K^{-1}$]		
			glass	frame	window
1	1.10 x 2.40	0.5	0.5	1.0	0.71
2	0.80 x 1.40	0.5	0.5	1.0	0.71

Figure 4.2 - Wood-fiber cement formwork block of the external walls.

Table 4.3 - Stratigraphy of the external walls.

Layer	s [mm]	ρ [$kg m^{-3}$]	λ [$W m^{-1} K^{-1}$]	c [$kJ kg^{-1} K^{-1}$]	R [$m^2 K W^{-1}$]
Internal liminar layer					0.13
Plaster	25	900	0.32	0.91	0.08
Wood-fiber cement	42.5	707	0.21	1.88	0.20
EPS with graphite *	106	175	0.031	1.84	3.42
Concrete *	131	2706	1.91	0.94	0.07
Wood-fiber cement	42.5	707	0.21	1.88	0.20
Plaster	25	1450	0.40	0.91	0.06
External liminar layer					0.04
	372				4.19
			U-value = 0.238 $W m^{-2} K^{-1}$		

* equivalent properties

Table 4.4 - Stratigraphy of the internal walls.

Layer	s [mm]	ρ [kg m^{-3}]	λ [W m^{-1} K^{-1}]	c [kJ kg^{-1} K^{-1}]	R [m^2 K W^{-1}]
Internal liminar layer					0.13
Plaster	15	900	0.32	0.91	0.05
Hollow brick	80	666	0.40	0.84	0.20
Plaster	15	900	0.32	0.91	0.05
Internal liminar layer					0.13
	110				0.54
U-value = 1.839 W m^{-2} K^{-1}					

Table 4.5 - Stratigraphy of the floor of Room 2, Flat 1.

Layer	s [mm]	ρ [kg m^{-3}]	λ [W m^{-1} K^{-1}]	c [kJ kg^{-1} K^{-1}]	R [m^2 K W^{-1}]
Internal liminar layer	-	-	-	-	0.13
Ceramic tiles	10	2300	1.00	0.84	0.01
Sand and cement screed	56	1600	1.31	1.00	0.04
EPS insulation *	48	25	0.031	1.45	1.55
Acoustic floor mat	5	35	0.036	1.40	0.14
Light concrete	100	315	0.08	1.40	1.25
Slab	450	2400	2.5	1.00	0.18
Lean concrete	100	2200	0.93	0.88	0.11
	769				3.40
U-value = 0.294 W m^{-2} K^{-1}					

* equivalent thickness

Table 4.6 - Stratigraphy of the floor of Room 2, Flat 2.

Layer	s [mm]	ρ [kg m^{-3}]	λ [W m^{-1} K^{-1}]	c [kJ kg^{-1} K^{-1}]	R [m^2 K W^{-1}]
Internal liminar layer	-	-	-	-	0.13
Ceramic tiles	10	2300	1.00	0.84	0.01
Self-leveling screed	32	2000	1.87	1.00	0.02
PIR insulation *	30	35	0.023	1.40	1.30
Acoustic floor mat	5	35	0.036	1.40	0.14
Sand and cement screed	45	1600	1.31	1.00	0.03
Light concrete	100	315	0.08	1.40	1.25
Slab	450	2400	2.5	1.00	0.18
Lean concrete	100	2200	0.93	0.88	0.11
	772				3.17
U-value = 0.316 W m^{-2} K^{-1}					

* equivalent thickness

Table 4.7 - Stratigraphy of the ceiling of Room 2, Flat 1 and Flat 2.

Layer	s [mm]	ρ [kg m^{-3}]	λ [W m^{-1} K^{-1}]	c [kJ kg^{-1} K^{-1}]	R [m^2 K W^{-1}]
Internal liminar layer					0.13
Plaster	25	900	0.32	0.91	0.08
Concrete and masonry slab	330	1009	0.89	0.84	0.37
Light concrete	100	300	0.065	1.40	1.54
Acoustic floor mat	5	35	0.036	1.40	0.14
EPS insulation *	27	30	0.035	1.45	0.77
Sand and cement screed	58	1600	1.31	1.00	0.04
Ceramic tiles	10	2300	1.00	0.84	0.01
Internal liminar layer					0.13
	555				3.20
U-value = 0.312 W m^{-2} K^{-1}					

* equivalent thickness

4.3.2 Radiant systems

The floor radiant system of Flat 1 is a traditional one, with cement and sand screed, while the radiant system of Flat 2 presents a reduced thickness of the screed, which is a self-leveling one, and a higher conductivity. In this case the total thickness of the screed is 32 mm (10 mm above the clew), against the 55 mm (40 mm above the clew) of the first case. Another difference is about the clew of the insulation panels, which is solid in System 1 and empty in System 2, allowing a uniform thickness of the screed.

The same typology of pipe is used in the two flats. It is a PE-RT pipe with an internal diameter of 13 mm. Also the pipe spacing is the same in the two flats: 15 cm in Room 1 and 5 cm in Room 2.

The main technical features of the two radiant systems are summarized in Table 4.8. Other properties of the materials of the screed and of the insulation panels were already listed in the stratigraphies in Table 4.5 and Table 4.6.

Table 4.8 - Technical features of the two radiant floor systems.

		System 1	System 2
Screed	Thickness above the clew	40 mm	10 mm
Insulation panel	Thickness (clew included)	52 mm	64 mm
	Minimum thickness	30 mm	42 mm
	Equivalent thickness	30 mm	48 mm
Screed	Thermal conductivity	1.31 W m^{-1} K^{-1}	1.87 W m^{-1} K^{-1}
	Thermal resistance	0.043 W m^{-2} K^{-1}	0.017 W m^{-2} K^{-1}
Insulation panel	Thermal conductivity	0.031 W m^{-1} K^{-1}	0.023 W m^{-1} K^{-1}
	Thermal resistance	1.55 W m^{-2} K^{-1}	1.30 W m^{-2} K^{-1}
Pipe	External diameter	17 mm	
	Internal diameter	13 mm	
	Thermal conductivity	0.40 W m^{-1} K^{-1}	
	Spacing, Room 1	0.15 m	
	Spacing, Room 2	0.05 m	

4.4 PRELIMINARY ANALYSIS

A pre-analysis on the two floor heating systems was performed by means of HEAT2 to calculate the water temperature in design conditions and the backward thermal losses, as well as the thermal response time.

The mean value of the water temperature in design conditions $T_{w,m}$ is the temperature value which gives a heat flux towards the considered room equal to the design heating load. The two considered rooms have different heating load, pipe spacing and flooring; the water temperature was calculated for both the rooms and the higher value was then considered. A mean value of 31.9 °C was found for Flat 1 and 30.9 °C for Flat 2. The useful heat flux towards the considered room q_u and the losses q_l in steady-state conditions can be seen in Table 4.9. A ground temperature of 10 °C, an operative temperature of 20 °C and a heat exchange coefficient between the radiant surface and the room operative temperature of 11 W m^{-2} K^{-1} [14] were used as boundary conditions.

Table 4.9 - Calculation of the mean water temperature and the losses in design conditions.

Flat	System	Room	Flooring	Pipe spacing	Design heating load		$T_{w,m}$	q_u	q_l	Losses
				[m]	[W]	[W m^{-2}]	[°C]	[W m^{-2}]	[W m^{-2}]	
1	1	1	parquet	0.15	354	33.3	31.9	33.4	6.2	15.6%
		2	ceramic tiles	0.05	296	49.0	27.1	49.2	5.2	9.6%
		2	ceramic tiles	0.05	296	49.0	31.9	82.6	6.6	7.4%
2	2	1	parquet	0.15	354	33.3	30.9	33.4	6.3	16.0%
		2	ceramic tiles	0.05	308	50.9	26.0	50.8	5.3	9.5%
		2	ceramic tiles	0.05	308	50.9	30.9	90.4	6.7	6.9%

A parameter that can evaluate the dynamic thermal performance of radiant systems is the so-called time constant or response time. The time constant is usually referred as the time it takes a parameter of a system to reach 63.2% of its final value after a step input. The concept of time constant typical of lumped heat capacity systems is not suitable for radiant systems involving large amount of thermal mass. Schiavon et al. [94] proposed to consider also the time for the surface temperature to reach 95% of the difference between the initial value and the steady-state value, which helps to more clearly describe the dynamic behaviour of radiant systems. A new classification was proposed according to this value:

- τ_{95} < 10 min: fast response radiant systems;
- 1 h < τ_{95} < 9 h: medium response radiant systems;
- 9 h < τ_{95} < 19 h: slow response radiant systems.

In Figure 4.3 the evaluation of this parameter for the systems involved in the present analysis is represented. The calculation was performed by means of HEAT2 considering an increase of water temperature from 15 °C to 35 °C and is based on the assumption that the room thermal conditions are constant. As can be seen, the considered systems can be classified as medium response radiant systems. In Table 4.10 also the response time calculated according to the usual definition are listed.

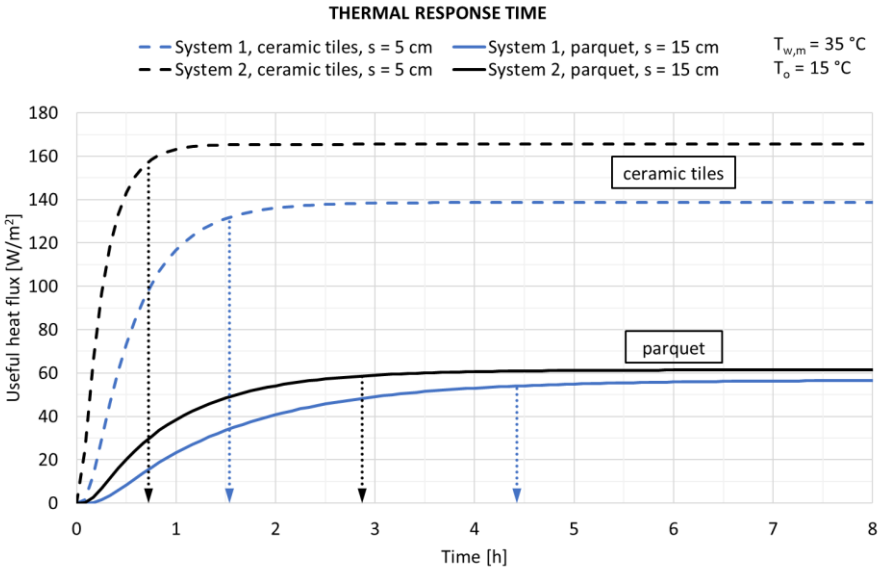

Figure 4.3 - Evaluation of the thermal response time τ_{95} of the two radiant floor systems.

Table 4.10 - Response time τ_{63} and τ_{95} of the two radiant floor systems.

	System 1		System 2	
	Room 1	Room 2	Room 1	Room 2
τ_{63} [h]	1.6	0.6	1.0	0.3
τ_{95} [h]	4.4	1.5	2.9	0.7

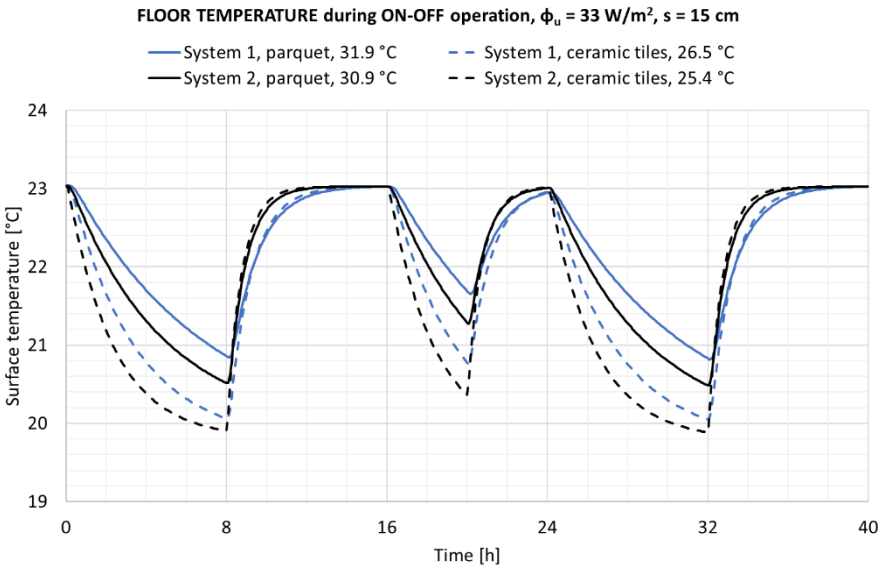

Figure 4.4 - Surface temperature during on-off cycles.

Finally an on-off cycle was simulated considering the same pipe spacing for the two systems and the same useful heat flux, i.e. different water temperature. The temperature boundary conditions

were set to 20 °C for the heated room and 10 °C under the slab. In steady state condition the systems with parquet covering require a water temperature level about 5 °C higher than with ceramic tiles. Starting from steady-state conditions, the systems were turned off and on for a cycle of 8-8-4-4 hous (Figure 4.4). Considering the same covering, System 2 cools down faster than System 1 and warms up faster. After 4 or 8 hours off, System 2 reaches the design surface temperature in 4 hours, while System 1 does not, even if restarting from a slighly higher value. Considering the same system, the parquet covering makes it slower than the ceramic tiles.

4.5 MEASUREMENTS

4.5.1 Measurement set-up and plan

Two rooms of each flat were considered in the present analysis. Their radiant loops were controlled by the same thermostat, placed in Room 1, while the other rooms of the flat were unheated.
Besides the external air temperature, the following parameters were measured for each flat:

- state of the thermostat and air temperature of its sensor;
- air temperature of the 2 heated rooms;
- air temperature of the 4 adjacent rooms;
- air temperature of the 2 rooms above the heated ones;
- floor surface temperature in 5 points of Room 1;
- floor surface temperature in 2 points of Room 2;
- supply and return water temperature in the manifold;
- mass flow, supply and return water temperature near the air-to-water heat pump by means of a thermal energy meter.

The measuring points can be seen in Figure 4.5, where Flat 2 is represented. For Flat 1 the measuring points were the same.

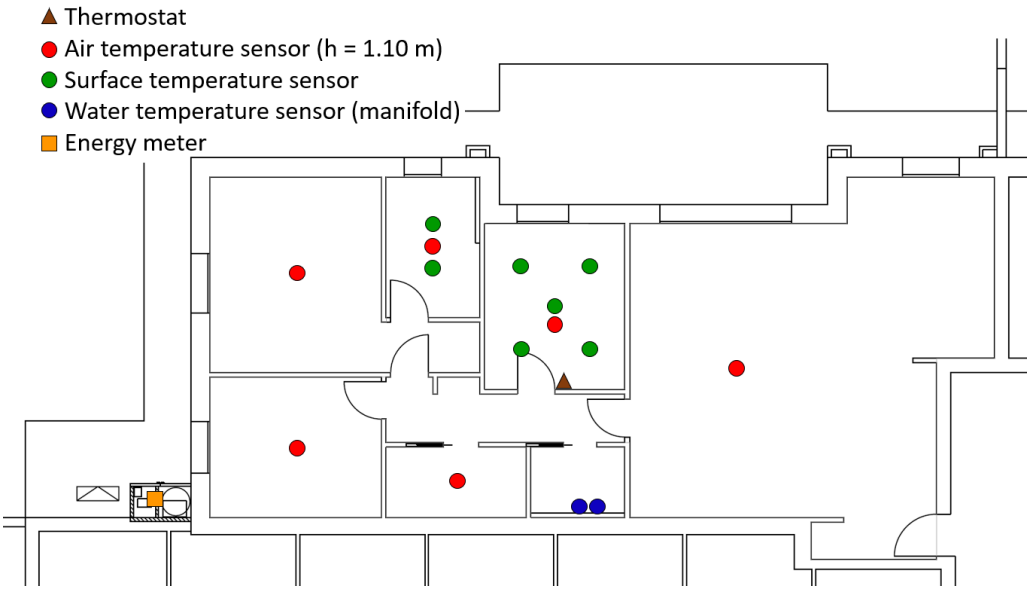

Figure 4.5 - Measurement set-up: position of the sensors.

The choice of the kind of sensors and acquisition system, the installation and the management of the measurements included the download of the data were arranged by a company and not all the

necessary information about the sensors and the acquisition system was provided. The temperatures were monitored with NTC thermistors and the acquisition system recorded the data with a frequency of 5 minutes. Also the air temperature in the rooms above the heated ones was measured, with an accuracy of ±0.35 K. Some images of the installation of the sensors can be seen in Figure 4.6: as can be noticed, the water temperatures in the manifold were measured on its external surface and not by means of immersion sensors. It is important to underline that the research activity started when the HVAC system was already installed and it was not possible to change it for performing better measurements.

Figure 4.6 - Installation of the temperature sensors (from left to right: Room 1, Room 2, manifold).

The energy meter used was a compact device consisting of an ultrasonic flow sensor, two Pt500 temperature sensors and a calculator with integrated circuits for temperature measurement, flow calculation and energy calculation (Table 4.11). Data were recorded on an hourly based interval.

Table 4.11 - Main technical specifications of the energy meter.

Technical specifications	
Maximum flow rate q_s	3.0 m^3/h
Nominal flow rate q_p	1.5 m^3/h
Minimum flow rate q_i	0.015 m^3/h
Flow sensor temperature range θ_q	5÷130 °C
Temperature measuring range θ	0÷180 °C
Temperature difference measuring range Δθ	3÷150 K
Accuracy	Class 2 (EN 1434)
Measuring cycles, volume	1 s
Measuring cycles, temperature and energy	16 s

Measurements were planned for 4 weeks from the middle of February to the middle of March according to the plan in Table 4.12. Then it was necessary to extend the measurements for another week, since the data recorded until 5th March were uncomplete or missing. The supply water

temperature set on the heat pumps was also increased because the 2 previous weeks were unusually cold for the period. During continuous operation the room thermostat was set to 21 °C for the entire day, while the schedule of intermittent operation can be seen in Table 4.13.

Table 4.12 - Measurement plan.

Period	Supply water temperature	Operation modality
14.02 - 21.02	35 °C	continuous
21.02 - 28.02	35 °C	intermittent
28.02 - 07.03	30 °C	continuous
07.03 - 15.03	30 °C	intermittent
15.03 - 22.03	40 °C	continuous

Table 4.13 - Schedule for the air temperature set-point during intermittent operation.

Time	Air temperature set-point Room 1
6:00 - 9:00	21 °C
9:00 - 16:00	15 °C
16:00 - 22:00	21 °C
22:00 - 6:00	18 °C

4.5.2 Analysis of measured data

Many unexpected events occurred during the measurements, managed by a third party. All the environmental data until 5th March were completely lost because of recording problems, along with the hourly data of the energy meters until 12th March because of downloading problems. Moreover, the heat pump of Flat 2 did not work from 14th March h 12:00 to 15th March h 9:00. Considering the time needed to reach in both the flats the desired internal conditions, data of environmental sensors and energy meters could be analysed from 15th March h 9:00 to 22nd March h 9:00. As regards only the environmental data, 6 complete days of intermittent operation are available, from 8th March to 13th March. The periods analysed, the operation modalities and the data available are summarized in Table 4.14.

Table 4.14 - Periods analysed and available data.

Period	Supply water temperature	Operation modality	Data available
08.03 h 0:00 - 14.03 h 0:00	30 °C	intermittent	environmental measurements
16.03 h 9:00 - 22.03 h 9:00	40 °C	continuous	energy meter and environmental measurements

The measured external air temperature is shown in Figure 4.7, along with the mean values over 24 hours in the two significant periods. The mean value was 8.6 °C in the first period and 5.2 °C in the second period.

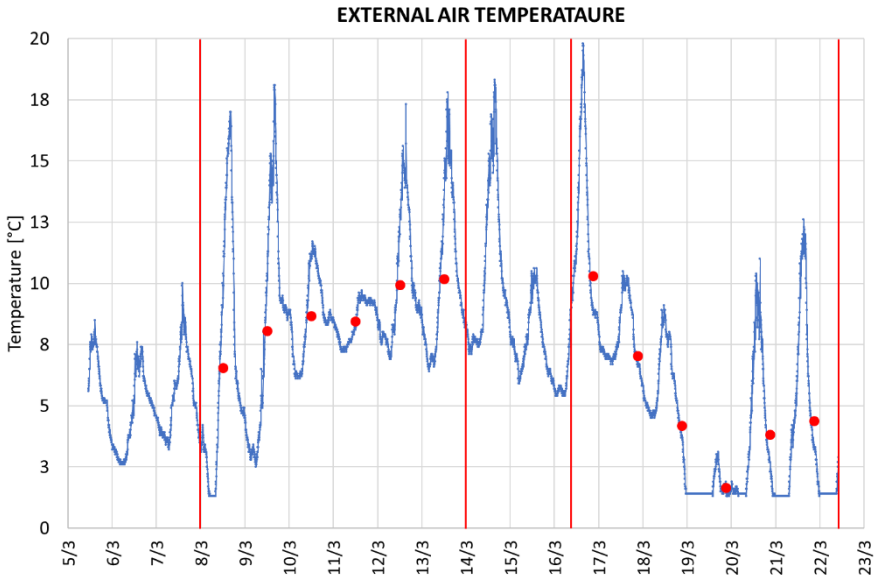

Figure 4.7 - External air temperature from on-site measurements.

As regards the period of continuous operation, the air temperature measured in the heated rooms and in the adjacent ones can be seen in Figure 4.8. During this week the thermostat, placed in Room 1, was set to 21 °C. The mean value of the air temperature in Room 1 was equal to 20.7 °C in Flat 1 and 20.9 °C in Flat 2 (from 16th March h 9:00). In Flat 2 the set-point was followed in a better way than in Flat 1 because of the much higher fluctuations of the sensor of the thermostat, which was placed near the door and was probably affected by higher air movements due to infiltration from the unheated hallway. The radiant loop of the other heated room, Room 2, was controlled by the thermostat of Room 1; the mean air temperature in this room was equal to 21.2 °C in Flat 1 and 24.1 °C in Flat 2. The higher air temperature level of this room in Flat 2 will be discussed later.
From the thermostat state, also monitored with a time step of 5 minutes, an operation time of 110 hours was deduced for the radiant system of Flat 1 and 95 hours for Flat 2. Flat 2 has the system with lower inertia and higher useful heat flux when the water temperature is the same, but also a better orientation (South-West instead of North-West for Flat 1) which ensured a higher temperature in the unheated rooms adjacent to Room 1 and Room 2. From the analysis of the data of the thermostat, a band of only ± 0.1 °C was found and thus *on-off* were very frequent: rarely the systems were *on* for more than one consecutive hour and most of the time they were *on* for less than half an hour, with many periods *on* only 10-15 minutes.
Various anomalies can be seen in the data. The sensors in the living room of Flat 1 and in the living room and bedroom of Flat 2 gave the same value for most of the time, showing some problems in the acquisition system. The data of the smaller bathroom of Flat 1 were missing for a period and in the same bathroom of Flat 2 a sudden fall of about 1.5 °C was found in a single 5-minute step; this fall cannot be explained since there are no windows in that room, the ventilation system was switched off during the measurement period and the eventual closing of the door would have produced a much slower decrease. Also the temperature of Room 2 in Flat 2 seems to be anomalous, especially if looking at the data of the previous period (Figure 4.9): until 10th March the temperatures of Room 1 and Room 2 were more or less the same and then a difference of almost 2 °C can be seen in the following days. This increase is difficult to be explained, since no change of setting was done and the door of the room was always closed.

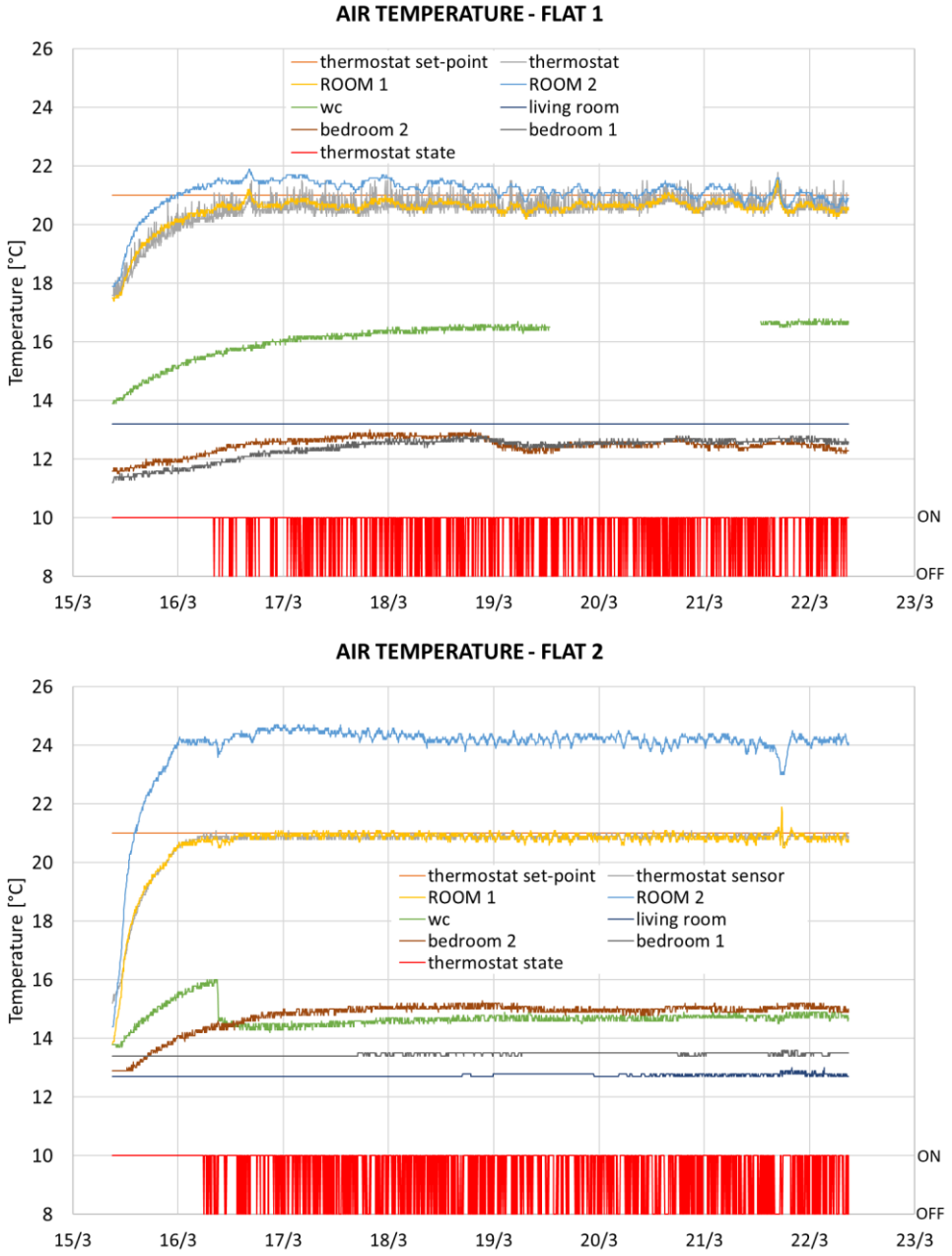

Figure 4.8 - Air temperature in the rooms and thermostat state from 15th March to 22th March.

As can be seen in Figure 4.9, at the beginning of March the temperature level of the supply water, set to 30 °C, was not adequate to reach the desired air temperature. This was due to the unusual very cold period at the end of February, wedded with the unheated rooms adjacent to Room 1 and Room 2. When the intermittent operation started, the situation obviously did not get better. From 8th March to 13th March the two radiant floor systems were *on* for about the same amount of time (98 hours in Flat 1 and 93 hours in Flat 2).

Differently from the following period of Figure 4.8, when there was no difference between the mean value of the thermostat sensor and the mean value of the sensor in the middle of the room, in Figure 4.9 there is a difference of 0.4 °C in Flat 1 and 0.6 °C in Flat 2.

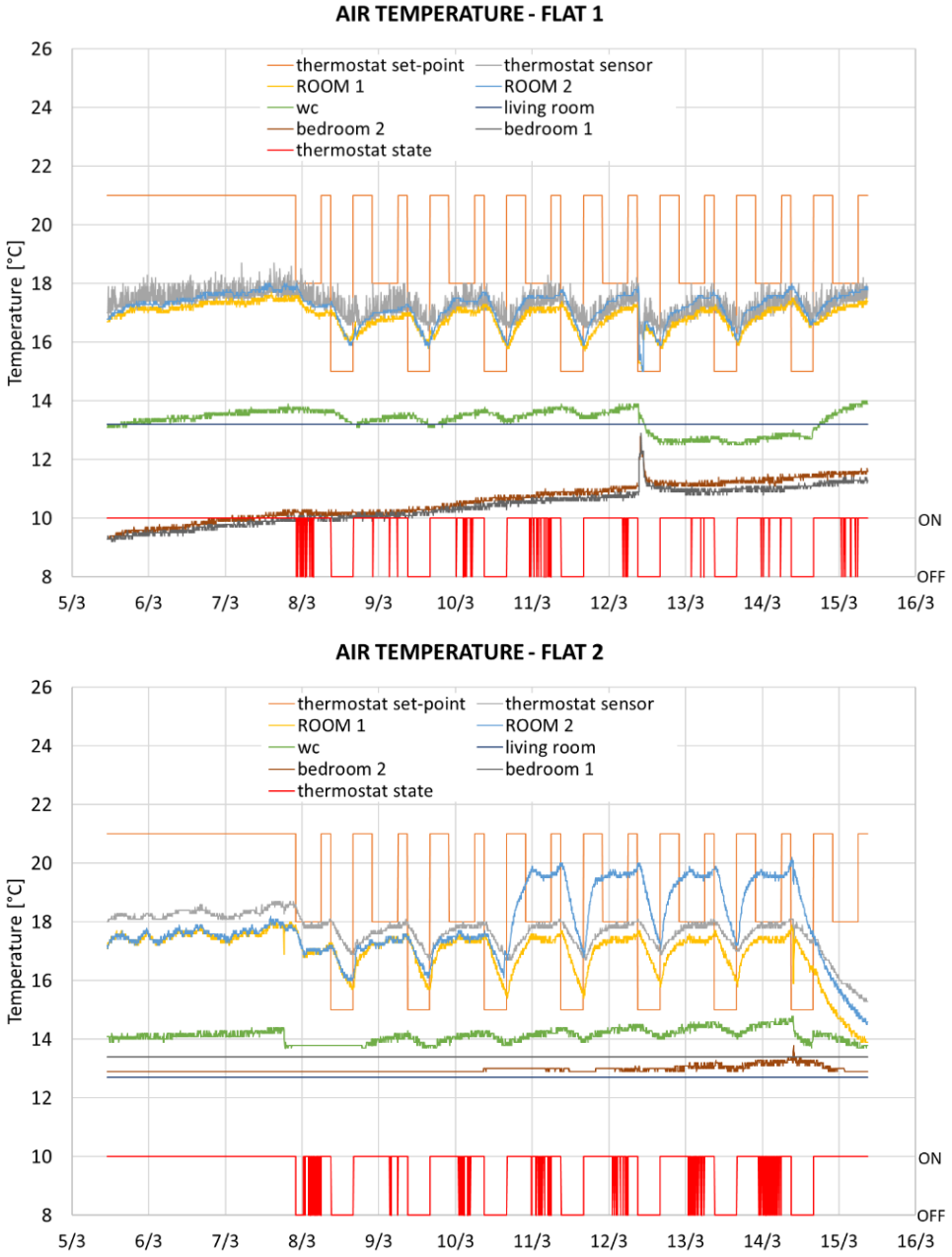

Figure 4.9 - Air temperature in the rooms and thermostat state from 5th March to 15th March.

The surface temperatures of the floor in the two flats are plotted in Figure 4.10. Two sensors were placed in Room 2 (ceramic tiles, pipe spacing 5 cm), five in Room 1 (parquet, pipe spacing 15 cm). The sensors were simply taped on the floor with the help of an infrared camera, but in the room with parquet it was difficult to see the position of the pipes. Moreover, the sensors were calibrated before the installation by the third party, but there was no information on how this process was carried out. Therefore, the differences which can be seen in both the flats for some sensors of Room 1 should be ascribed to a combination of these reasons.

The radiant floor system with the thinner screed (Flat 2) presented a higher number of oscillation, i.e. a higher number of *on-off* (almost 20% more, looking at the state of the thermostat during continuous operation). The amplitude of the oscillation was lower with parquet covering.

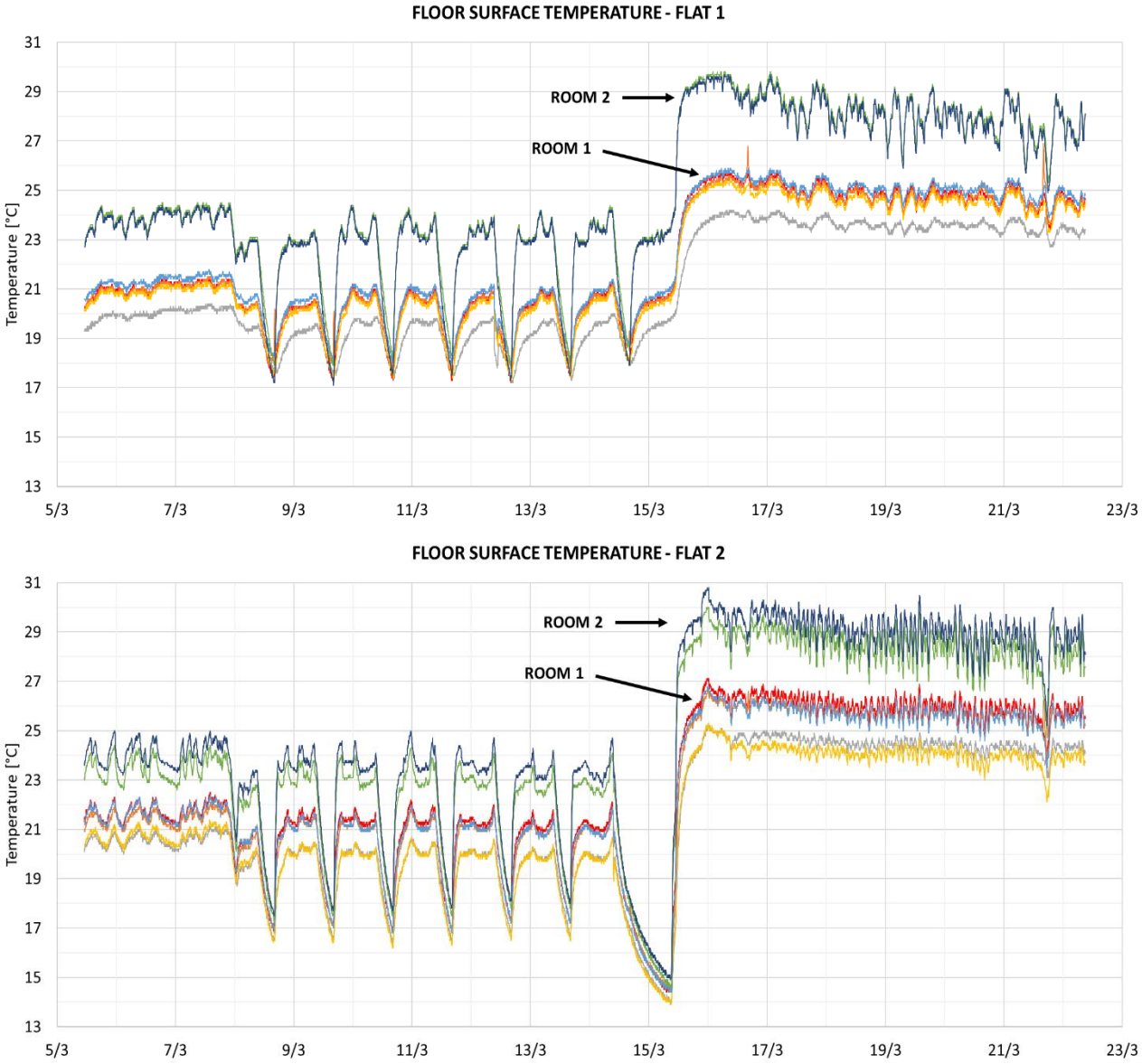

Figure 4.10 - Surface temperature of the radiant floor systems.

Table 4.15 - Mean values of the measured surface temperature of the floor.

Period	Mean temperature of each sensor [°C]				Mean temperature of all the sensors [°C]			
	Flat 1		Flat 2		Flat 1		Flat 2	
	Room 1	Room 2	Room 1	Room 2	Room 1	Room 2	Room 1	Room 2
from 08.03 h 0:00 to 14.03 h 0:00	19.8 19.9 18.9 19.6 20.1	22.2 22.0	20.4 20.2 19.3 19.2 20.2	21.9 22.4	19.7	22.1	19.9	22.2
from 16.03 h 9:00 to 22.03 h 9:00	24.8 24.8 23.6 24.6 25.1	28.1 28.0	26.0 25.7 24.5 24.0 25.6	28.4 29.0	24.6	28.1	25.2	28.7

Considering the mean value of all the sensors of each room (Table 4.15), the surface temperature of the thin-screed radiant floor system during continuous operation was 0.6 °C higher than the traditional system, with both the coverings.

As regards the temperature sensors placed on the surface of the manifolds, a much higher number of oscillations (i.e. on-off) can be seen, during continuous operation, for the thin-screed system. A higher temperature difference was found for the thin-screed system: in the period from 16th March its mean value is 2.5 °C, against 1.0 °C for the traditional system.
When the water was not flowing in the manifold of Flat 1 during the period of intermittent operation, negative values of the temperature difference were recorded. After many hours without water flowing in the manifold of Flat 2, a difference of 1.0 °C was found between the sensors. These facts could be due to acquisition or calibration errors.

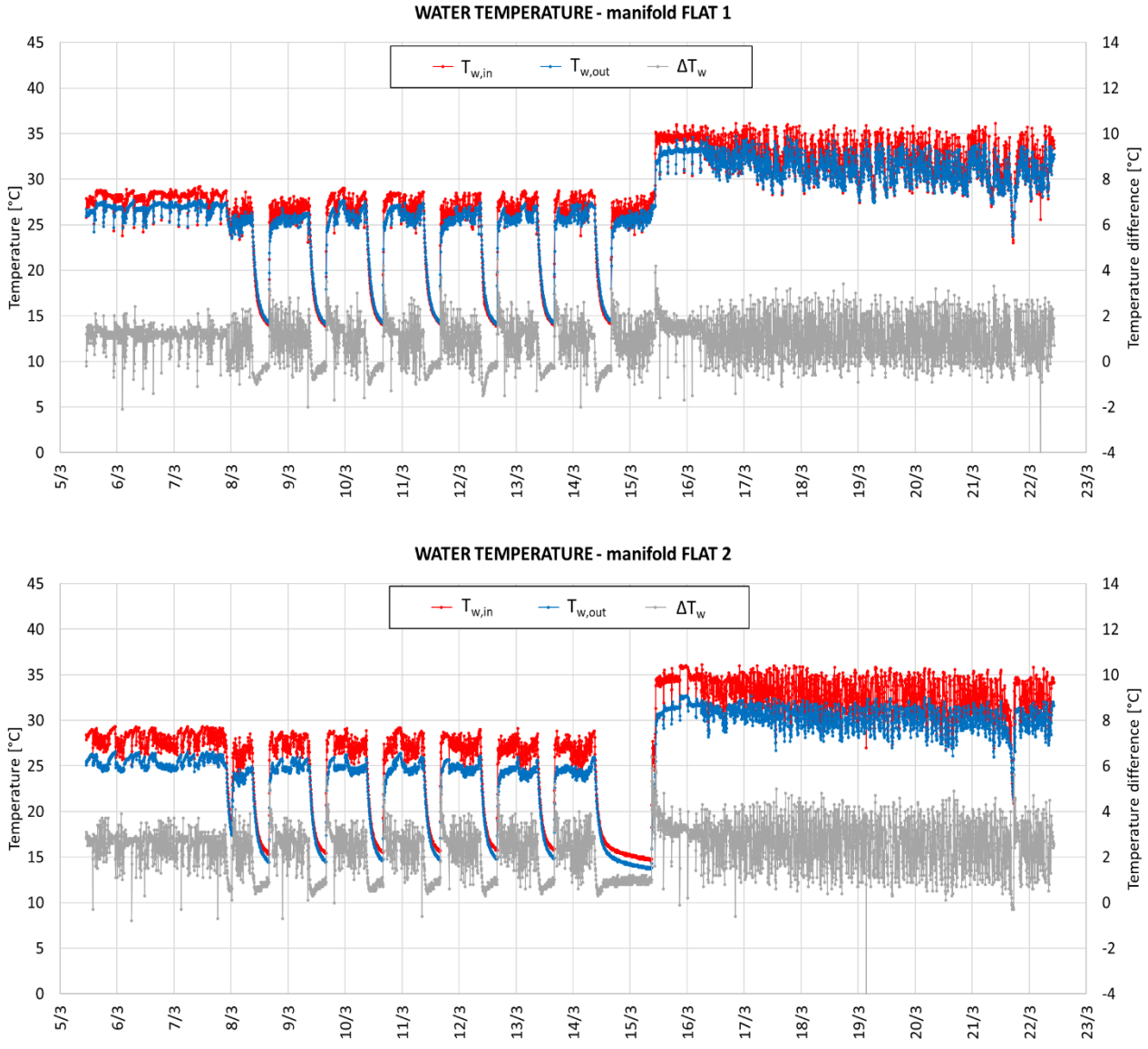

Figure 4.11 - Supply and return water temperature measured on the manifolds.

Comparing the water temperatures measured in the manifolds every 5 minutes with the mean hourly values from the energy meters, plotted in Figure 4.12, the mean values of the temperature difference in the period of continuous operation were 1.6 and 2.2 °C for Flat 1 and Flat 2 respectively, against 1.0 and 2.5 °C measured on the manifolds.
When there was no water flowing, the temperature values are strange. In Flat 1 an inversion of temperature can be noted, while in Flat 2 there was a significant difference between the sensors when the heat pump is off (between 14th and 15th March).

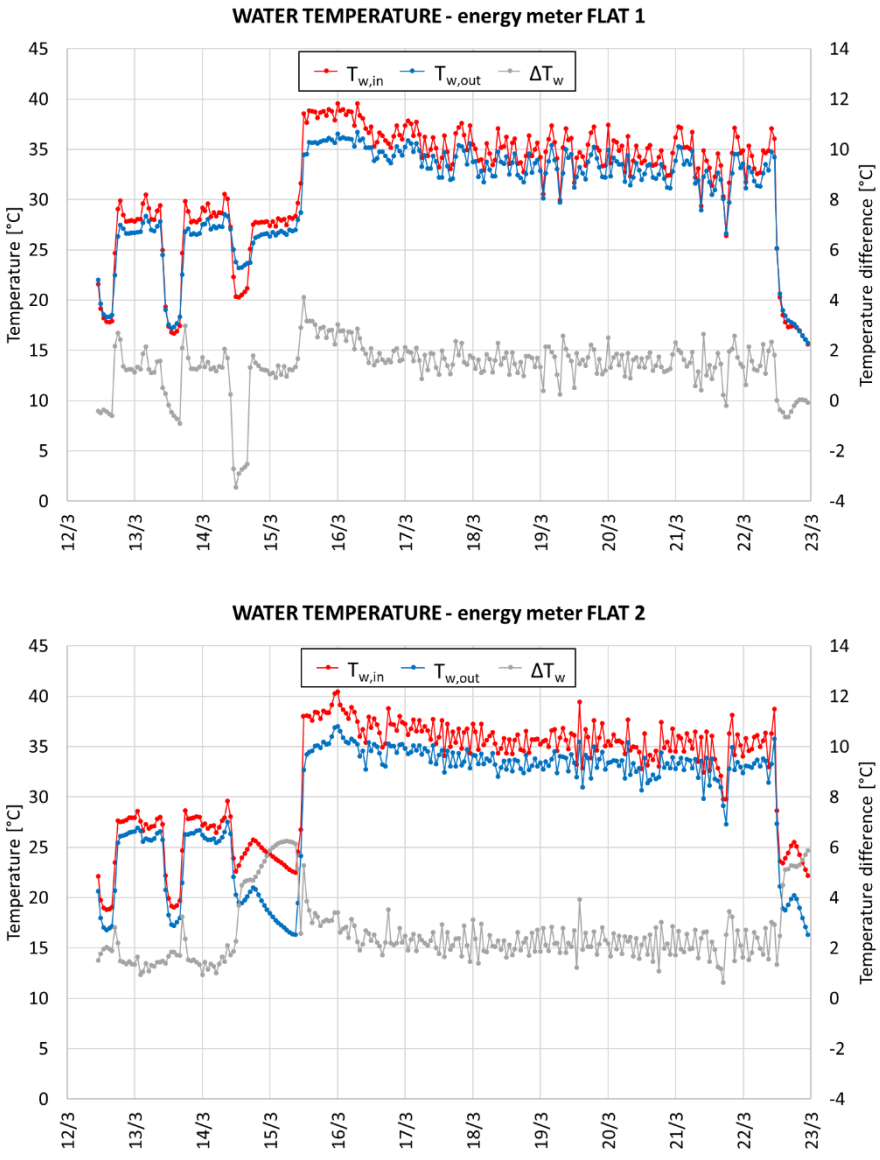

Figure 4.12 - Mean hourly values of the supply and return water temperature calculated by the energy meters.

Between 15th and 16th March both the systems were always on (i.e. the flow rate was never zero) for more than 20 consecutive hours: the mean values of the supply and return water temperature measured on the surface of the manifolds and by the sensors of the energy meters near the heat

pumps are compared in Table 4.16. The water temperature difference was equal to 3.2 °C in both the measurement points of Flat 2, while for Flat 1 a difference of 2.9 °C was found by the energy meter and 1.6 °C in the manifolds. Looking at the supply and return water temperature values, the temperature measured on the surface of the manifold is always about 4 °C lower than the temperature measured by the immersion sensors of the energy meters, except for the return of the radiant system of Flat 1. From this analysis, it can be concluded that there was a problem in the sensor measuring the return temperature in the manifold of Flat 1.

Table 4.16 - Water temperature values when flow rate is never zero (between 15th and 16th March).

Flat	Measurement point	$T_{w,in}$ [°C]	$T_{w,out}$ [°C]	ΔT_w [°C]
1	energy meter	38.3	35.4	2.9
	manifold (surface)	34.3	32.7	1.6
2	energy meter	38.6	35.4	3.2
	manifold (surface)	34.7	31.5	3.2

The mean hourly values of the flow rate measured by the energy meters are plotted in Figure 4.13, along with the minimum and maximum values recorded in each hour. The same for the average hourly thermal power, plotted in Figure 4.14.
As can be seen, from 16th March to 22nd March, when the thermostats were set on continuous operation, the water stopped flowing in the radiant systems for at least one time in each hour, except for two isolated hours. The mean flow rate was higher in Flat 1 (527 l/h against 437 l/h in Flat 2), and also the maximum flow rate, although the heat pumps were identical and so were the radiant loops. Also the mean hourly thermal power in Flat 2 was higher than in Flat 1 (1.4 kW against 1.1 kW). The mean values of the measurements of the energy meters are summarized in Table 4.17.

Between 15th and 16th March, the water flowed in the radiant loops for 20 complete hours without interruption with a mean value of 507 l/h in Flat 1 and 523 l/h in Flat 2 and a mean hourly thermal power of 1.7 kW and 1.9 kW respectively. The higher thermal power absorbed by the water in the pipes by the screed of Flat 2 is due to the fact that the heat pump of Flat 2 was off for almost an entire day between 14th and 15th°March; on 15th March, when the 20-hour period of uninterrupted water flowing started, the temperature of the screed was much lower than in Flat 1 and also the temperature inside the controlled room (about 14 °C against 17.5 °C) and thus the screed adsorbed more energy.
Looking at the mean hourly thermal power in Figure 4.14, the maximum and minimum hourly values in this 20-hour period are, for most of the hours, in a band of ± 0.5 kW for Flat 1 and ± 0.6 kW for Flat 2 from the mean hourly value and the mass flow is constantly equal to the minimum value which can be seen in Figure 4.13 (479 l/h for Flat 1 and 491 l/h for Flat 2). About every 3-4 hours peaks of positive and negative thermal power occurred in the same hour, with the heat pump modulating the mass flow rate between the minimum and the maximum values; in these hours a sudden decrease of the supply and return water temperatures can be seen for about 15 minutes from the sensors in the manifold (the straight lines in Figure 4.11). The supply and return water temperatures fell down to very similar values, thus the error on the temperature difference could be high, leading to errors in the calculated thermal power. From the 16th March the heat pumps turned off at least one time every hour and the very frequent change of flow rate as well as the related change of water temperatures could be a not negligible source of error in the calculation of the thermal power.

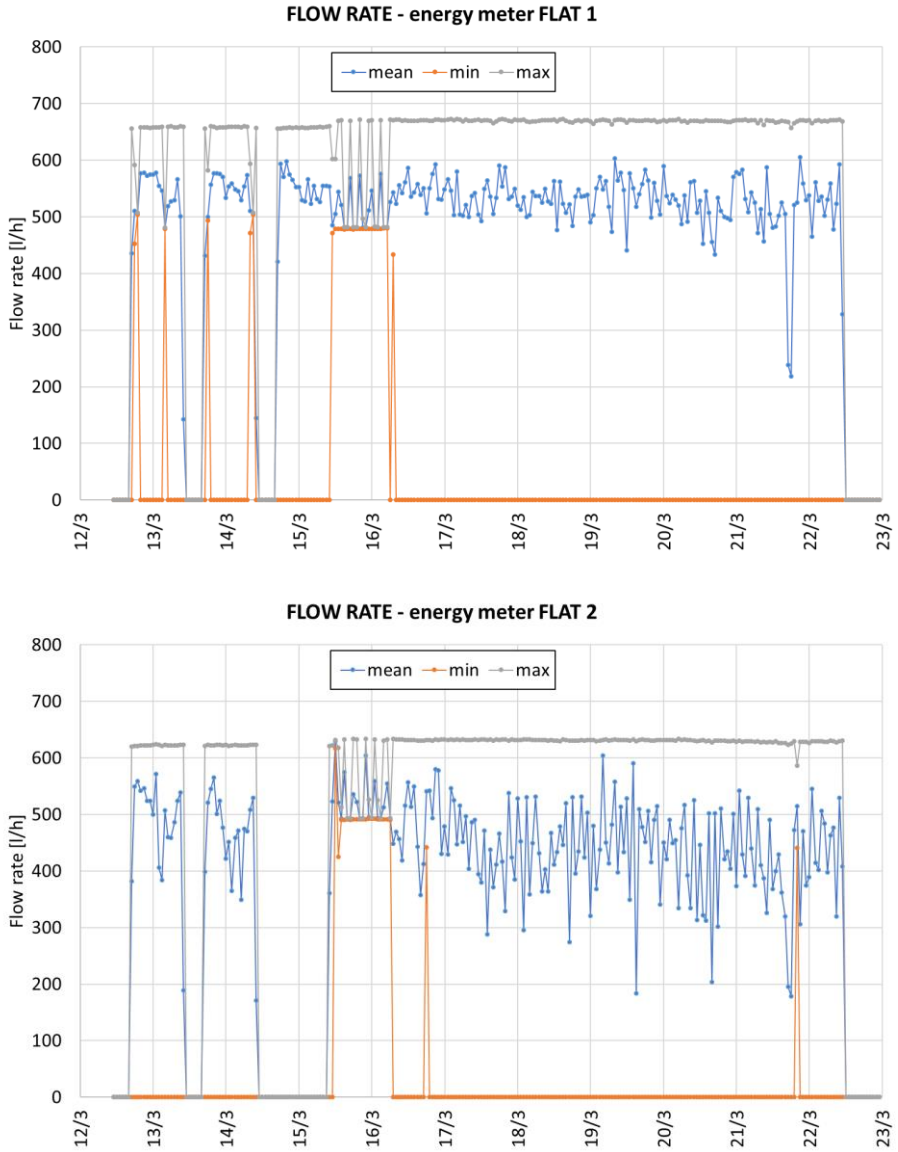

Figure 4.13 - Maximum, minimum and mean hourly values of the flow rate calculated by the energy meters

Table 4.17 - Mean value of water temperature difference, flow rate and thermal power measured by the energy meters from 16th March h 9:00 to 22nd March h 9:00.

Flat	ΔT_w [°C]	Flow rate [l/h]		Thermal power [kW]		
		Mean	Max	Mean	Max	Min
1	2.9	527	670	1.1	4.5	-0.7
2	3.2	437	630	1.4	4.5	-0.4

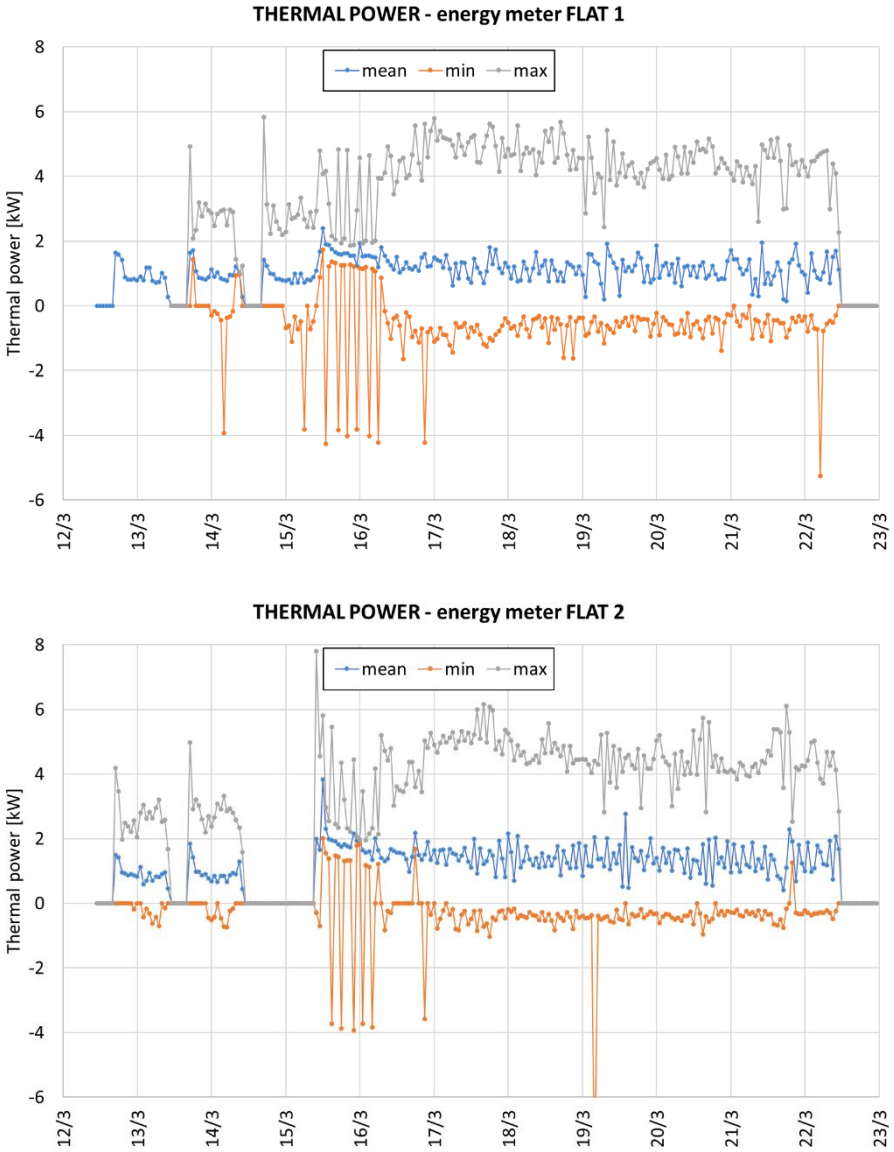

Figure 4.14 - Maximum, minimum and mean hourly values of the thermal power calculated by the energy meters.

To conclude, the thermal energy coming from the hourly data of the energy meters is presented in Table 4.18. In the period from 16th March to 22nd March for the flat with the thin-screed radiant floor system (Flat 2) the energy meter recorded an amount of thermal energy adsorbed 23% higher than for the flat with the traditional radiant floor system (Flat 1). The data of 14th March cannot be compared since the heat pump of Flat 2 was *off* and restarted on 15th March. The 12th and 13th March the systems were working with a schedule for the thermostat and the flat with the thin-screed system presented a lower thermal energy consumption than the flat with the traditional system.
In the period before 12th March only the daily data of the energy meters were available, without any hourly detail. The thermal energy adsorbed during 4 periods of 6 days is shown in Table 4.19. The difference between the consumption of the flat with the thin-screed radiant floor system and the flat with the traditional radiant floor system was between -5% and +4%. No further consideration can be

done without hourly data and without any data from the environmental measurements inside the flats, which were lost for the period before 5th March by the company who managed the installation of the instruments, as well as the acquisition and recording of the data.

Table 4.18 - Thermal energy consumption from the available hourly data of the period 12th March - 22nd March.

Day *	Thermal energy [kWh]		Difference
	Flat 1	Flat 2	(2 - 1)
12.03	17.0	15.9	-7%
13.03	17.7	16.8	-5%
14.03	15.6	0.4	-97%
15.03	38.7	44.6	+15%
16.03	29.9	36.5	+22%
17.03	27.6	34.0	+23%
18.03	27.0	33.1	+23%
19.03	27.1	33.7	+25%
20.03	25.5	32.1	+26%
21.03	25.7	30.9	+20%
from 16.03 to 21.03	162.7	200.2	+23%

* from 9:00 to 9:00 of the following day

Table 4.19 - Thermal energy consumption from the available daily data of the period 15th February - 13th March.

Period *	Thermal energy [kWh]		Difference
	Flat 1	Flat 2	(2 - 1)
15.02 - 20.02	146.2	138.4	-5%
22.02 - 27.02	118.3	122.5	+3%
01.03 - 06.03	127.1	132.8	+4%
08.03 - 13.03	101.8	104.1	+2%

* from 0:00 of the first day to 24:00 of the last day

4.5.3 Comparison of simulations against measurements

As presented and discussed in paragraph above4.5.2, the data from the environmental measurements present many problems and also many aspects of the data recorded by the energy meters are not completely clear, also because of a lack of information on the operation modalities of the heat pump. The data of two 6-day periods were used as input for the dynamic simulations of the two radiant floor systems by means of DIGITHON: from 16th to 22nd March for continuous operation and from 8th to 14th March for intermittent operation.
Two kinds of simulations were performed for each period and each system: in one simulation a thermostat was set using the same schedules of the measurements and the radiant system turned

on/off according to the air temperature reached in the room (ST simulation), in the other simulation the state of the radiant system was defined as input and the air temperature was not controlled (SO simulation).
The two heated rooms of the present work were controlled by the same thermostat, but the numerical model, already described in paragraph 3.2, requires that the thermostat is in the controlled room; thus for the ST simulations an iterative process was followed to reproduce the control only by the thermostat of Room 1 like in the field measurements.
The most important parts of the model and the settings are summarized in the following points:

- geometry: Room 1 and Room 2, described in paragraph 4.3.1, were implemented considering also their adjacent wall;
- response factors of the building structures and of the radiant systems: calculated using the data from Table 4.3 to Table 4.8 following the process described in paragraph 3.2;
- boundary temperatures: the air temperature data from the measurements were used, 10 °C was set as constant ground temperature;
- infiltrations: an air change of 0.15 h^{-1} was set;
- internal gains: not considered, since the rooms were empty;
- flow rate of the radiant loops: the mean value of the period of uninterrupted operation in Figure 4.13;
- supply water temperature of the radiant floor systems: according to Table 4.14;
- thermostat schedule: as defined in Table 4.13 for intermittent operation;
- thermostat type: on-off, with a band of ± 0.1 °C, like in the field measurements;
- simulation step: 10 minutes.

As regards the weather data, the outdoor air temperature was measured in the building site, while for the solar radiation the data provided by the regional environmental protection agency *ARPAV* were used. Solar radiation is taken by *ARPAV* at 15-minute intervals on a horizontal surface, while for the simulations the direct normal solar radiation and the diffuse solar radiation on the normal plane were needed as input with a step of 10 minutes. For this purpose, TRNSYS was used, by means of Type16, which takes the total horizontal solar radiation and computes the diffuse fraction using an algorithm that estimates cloudiness based on dry bulb and dew point temperature.
The results of SO simulations in terms of air temperature (T_{air}), surface temperature of the floor (T_s) and thermal power (P_w) are plotted in Figure 4.15. In the graphs also the mean values of the surface temperature sensors of the field measurements are shown. As regards the surface temperature, a good agreement was found in Room 1, which has parquet as covering, especially during intermittent operation. In Room 2, which has ceramic tiles as covering and a lower pipe spacing, the difference is higher.
In Table 4.20 the results of all the simulations are shown. In general, a good compliance with measured air temperature was found in Room 1, with a mean difference of 0.4 °C during continuous operation and 1.1 °C during intermittent operation. In Room 2 the difference is higher, up to 2.2 °C, but in the model all the surface of the floor was thermally active, while part of the real room was not, since it was a bathroom.
As regards the thermal energy consumption, SO simulations of the period of continuous operation gave 79% and 68% of the measured energy consumptions of Flat 1 and Flat 2 respectively. For the period of intermittent operation the percentage was 87% and 85% respectively.

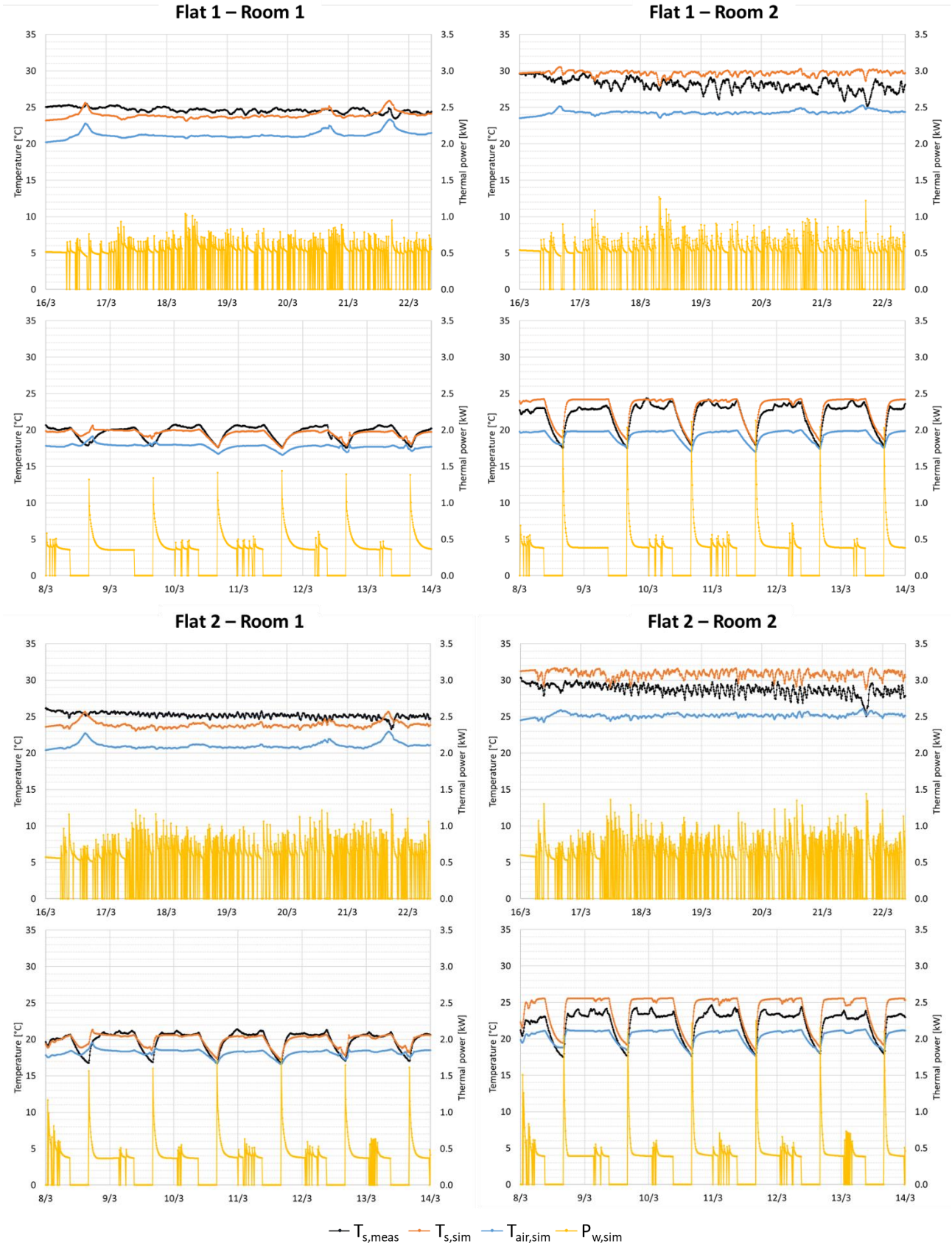

Figure 4.15 - Results of the SO simulations in continuous and intermittent operation and comparison with the measured surface temperature of the floor.

Table 4.20 - Comparison between measurements and simulations: thermal energy consumption, air temperature and surface temperature of the floor.

Operation modality	Flat	measurements/ simulation	Q_w [kWh]		T_{air} [°C]		T_s [°C]	
					Room 1	Room 2	Room 1	Room 2
continuous	1	meas.	163		20.7	21.2	24.6	28.1
		ST	125	77%	21.0	23.8	23.6	28.8
		SO	129	79%	21.3	24.3	23.9	29.7
continuous	2	meas.	200		20.9	24.2	25.2	28.7
		ST	135	67%	21.0	25.0	23.8	30.5
		SO	136	68%	21.1	25.2	23.9	30.9
intermittent	1	meas.	102		16.7	17.0	19.7	22.1
		ST	89	87%	17.8	19.3	19.6	23.0
		SO	89	87%	17.8	19.3	19.5	23.0
intermittent	2	meas.	104		17.0	18.2	19.9	22.2
		ST	84	81%	18.0	20.2	19.7	23.6
		SO	88	85%	18.2	20.4	19.9	24.0

The results of the simulations can be considered good, since:

- the temperatures used as boundary conditions in the simulations came from field measurements with low quality data (some temperature data were lacking, others were questionable);
- some input data were assumed (ground temperature, infiltration rate);
- the beam and diffuse part of the solar radiation were calculated using an algorithm which estimates cloudiness;
- the material properties of the building structures were partly assumed and their influence, especially for the floor, are not negligible;
- a constant supply water temperature was used, without considering the effects of the heat pump operation on the water temperature;
- a constant flow-rate was used, since from the field measurements only the mean hourly value was known (considering also the time when there was no water flowing) and only for the period of continuous operation.

The models of the two rooms were then used to compare the performance of the two different kinds of radiant floor heating systems under the same boundary conditions.

4.6 ADDITIONAL SIMULATIONS

4.6.1 Input data

The simulations were performed using the weather data of Padova provided by *ARPAV* for the heating season 2017-2018. From the analysis of the air temperature and solar radiation, two months were chosen for the simulations (Table 4.21):

- December 2017, which is the month with the lowest mean air temperature;
- March 2018, which is a mid-season month with high global solar radiation.

The air temperature trend of the selected months is shown in Figure 4.16.

Table 4.21 - Weather data of the heating season 2017-2018 in the city of Padova.

Month	Mean external air temperature [°C]	Heating Degree Days	Normal solar radiation [kWh/m^2]		
			Direct	Diffuse	Global
10 (15th - 31st)	12.7	125	52	23	75
11	8.1	356	64	29	93
12	2.8	534	68	30	98
1	5.5	449	56	28	84
2	3.8	454	59	36	95
3	7.1	399	91	51	142
4 (1st - 15th)	13.1	104	63	32	95

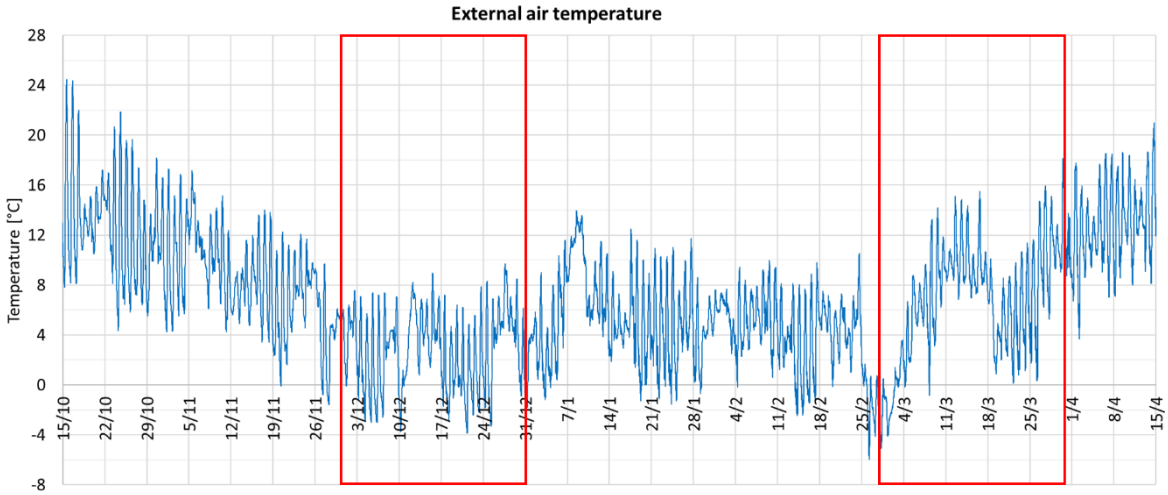

Figure 4.16 - External air temperature and months chosen for the simulations.

The traditional radiant floor system (System 1) and the thin-screed radiant floor system (System 2) were simulated in continuous and intermittent operation considering the geometrical model of Flat 1 (Figure 4.1).
The settings for the simulation are summarized in the following points:

- air temperature set-point: during continuous operation 20 °C in Room 1 and 24°C in Room 2, during intermittent operation according to Table 4.22;
- control: on-off, ± 0.5 °C;
- temperature of the adjacent rooms: the same of Room 1;
- internal gains: according to Table 4.23;
- infiltration and ventilation: 0.3 h^{-1} with external air temperature.

Table 4.22 - Schedule of the thermostat during intermittent operation.

Time	Air temperature set-point [°C]	
	Room 1	Room 2
6:00 - 9:00	20	24
9:00 - 16:00	16	20
16:00 - 22:00	20	24
22:00 - 6:00	18	22

Table 4.23 - Schedule of internal gains.

Time	Internal gains [W]	
	Room 1	Room 2
7:00 - 22:00	10	10
22:00 - 7:00	70	10

4.6.2 Working parameters of the radiant systems

The supply water temperature and the mass flow rate are needed as input for the model. As first step for the evaluation of these parameters, the design heating load of the two rooms was calculated, considering 0.5 h^{-1} as air change and 10 °C for the ground temperature and also for the rooms above the simulated ones. The resulting heating load is shown in Table 4.24, where the heat flux between Room 2 and Room 1 was not taken into account.

Table 4.24 - Design heating load of the two rooms.

Room	Design air temperature	Design heating load	
	[°C]	[W]	[W m^{-2}]
1	20	264	24.8
2	24	320	52.9

HEAT2 simulations were then performed to evaluate the mean water temperature, which depends on Room 2. The simulations gave the mean temperatures in Table 4.25, i.e. 31.7 °C for System 1 and 30.4 °C for System 2. Choosing a temperature difference between supply and return in design conditions equal to 3°C, the supply temperature is 33.2 °C for System 1 and 31.9 °C for System 2. By using these supply water temperatures for both rooms, in Room 2 the useful heat flux is about 53 W m^{-2} in agreement with design conditions, while in Room 1 the specific useful heat flux is about 30% higher than the one calculated in design conditions.

Table 4.25 - Evaluation of the supply water temperature for the two radiant systems.

System	$T_{w,m}$ [°C]	ΔT_w [°C]	$T_{w,in}$ [°C]
1	31.7	3	33.2
2	30.4	3	31.9

Considering the useful heat flux towards the heated rooms and the losses towards the ground, a mass flow rate of 90 kg/h and 103 kg/h was calculated for Room 1 and Room 2 respectively. Two kinds of simulations were performed, one with no limits on the power available from the water side and one with a limit of 5 K in the temperature difference between supply and return, i.e. 525 W and 600 W for Room 1 and Room 2 respectively. The second case is representative of a radiant system directly connected to a heat pump, while the first one is more representative of a heating system with a tank or with a gas-fired generator.

4.6.3 Results

Two floor radiant systems, two months (December and March), two schedules for the thermostat (continuous and intermittent operation) and two possibilities for the generation (limited and unlimited thermal power available) were considered, for a total of 16 simulations. First a brief overview of the results is provided, then the details are examined, analyzing thermal energy need, hours of operation, supply water temperature and water temperature difference, air and operative temperature, to conclude with the possibility of overheating.

The two adjacent rooms simulated were heated at a different temperature, with the set-point of Room 2 (bathroom) 4 °C higher than the set-point of Room 1 and all the surrounding rooms at the same temperature of Room 1. For this reason, along with the high insulation level of the external walls, the radiant loop of Room 1 was found to be working only for 2-3 hours per day. Therefore the results of the simulation of Room 2 are more interesting to be shown. In Figure 4.17 the air temperature, the surface temperature of the floor, the supply water temperature, the temperature difference between supply and return and the thermal power exchanged by the water flowing in the pipes during the first 2 days of December are plotted.

As can be seen, the thin-screed radiant system (System 2) turns on more frequently than the traditional one (System 1), because of its lower thermal inertia, which makes the floor surface to warm up faster, but also to cool down faster after the set-point is reached. During intermittent operation of System 1, the set-point of the time slot from 6:00 to 9:00 is reached only at 9:00, even if the radiant system has already turned on at 3:00 and even if the set-back is only 2 °C lower. System 2 is faster, but it needs to be turned on earlier in order to reach the set-point.

When the water temperature difference which can be supplied by the generation system is limited (simulations with limited power) and the radiant system turns on, the supply water temperature does not reach the set value because the temperature level of the water inside the pipes has decreased during the time period in which the radiant system was off and time is needed to heat up the structures. Gradually the screed warms up and the set value of the supply water temperature is reached; then the heat exchange between the screed and the water flowing in the pipes decreases (i.e. the water temperature difference decreases). As can be seen, the supply water takes also more than 3 hours (for System 1 in intermittent operation) to reach the set value.

When the generation has no limit (simulations with unlimited power) and the radiant system turns on, the supply water temperature is immediately the set value and the water temperature difference can reach up to 7 °C and 11 °C for continuous and intermittent operation respectively. As the screed warms up the difference decreases. In this second case the radiant system is obviously faster and the number of on-off is higher.

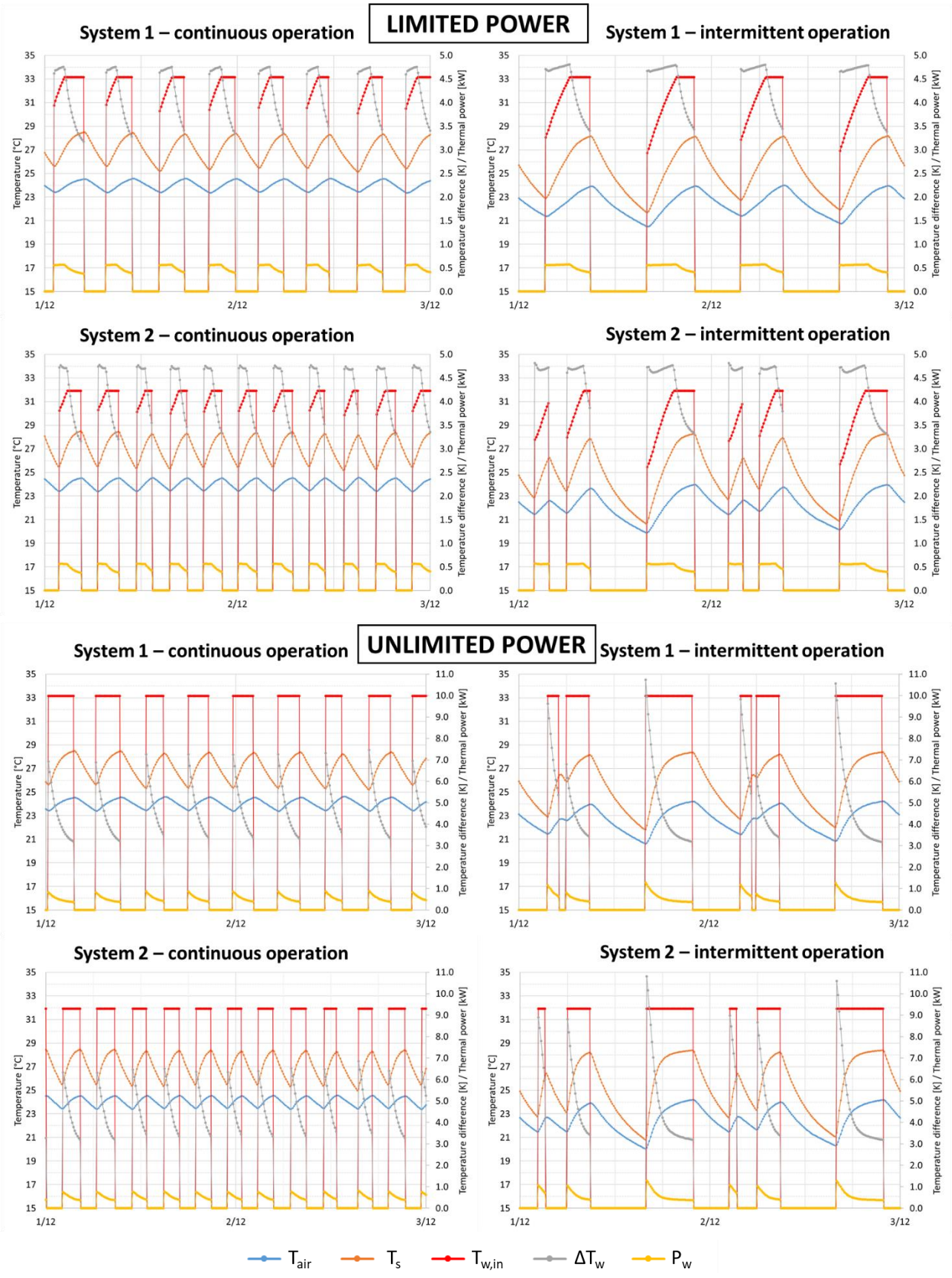

Figure 4.17 - Results of the simulations of December for Room 2 with System 1 and System 2.

The resulting thermal energy need is shown in Figure 4.18. As can be seen, no significant difference was found between the two kinds of radiant floor systems and between continuous and intermittent operation. It is useful to remember that in the case of intermittent operation the supply water temperature was the same which was set in the case of continuous operation and that the set-point was hardly reached.

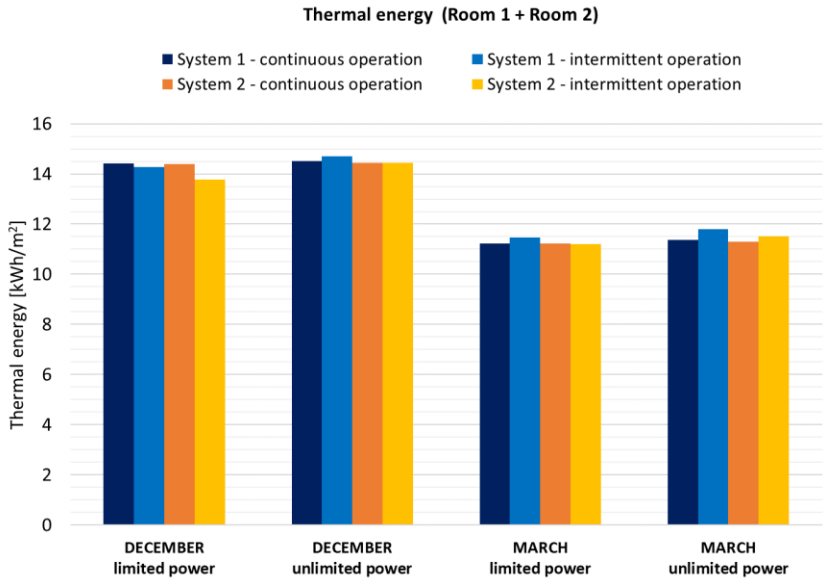

Figure 4.18 - Specific thermal energy need.

The mean daily amount of operation hours is shown in Figure 4.19 and Table 4.26.
As already said, the radiant system of Room 1 was off for most of the time because of the heat coming from the wall adjacent to Room 2. Adding the number of hours of Room 1 and Room 2, no significant difference is found between the thin-screed floor system and the traditional one.
Without limits on the water temperature difference from the generator side, both the radiant systems are working about 15% less time than with a limit of 5 °C.

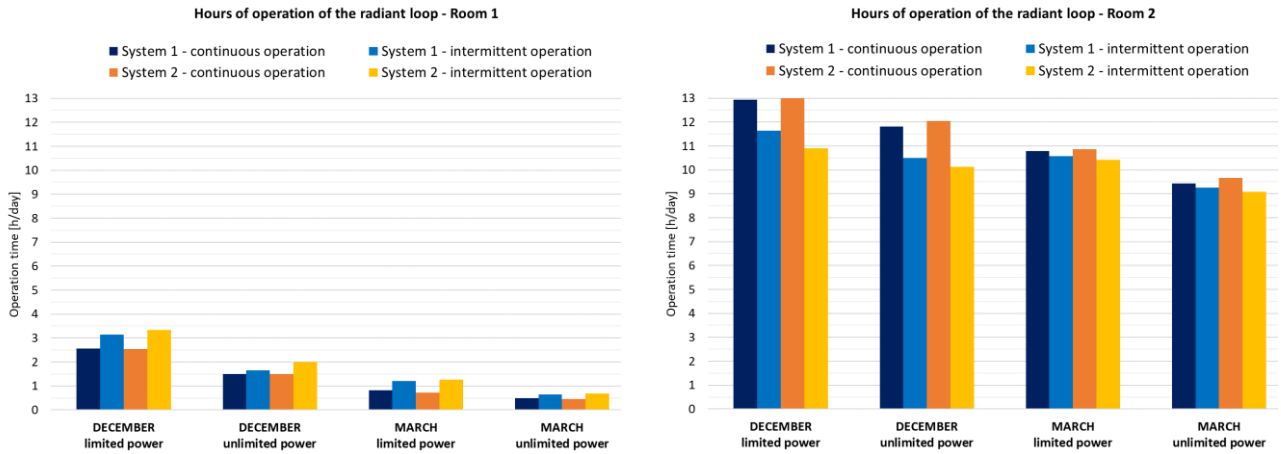

Figure 4.19 - Hours of operation of the radiant loops of Room 1 and Room 2.

As can be seen in Table 4.26, the average number of hours in which the radiant system of Room 2 is *on* before turning off is found to be higher with intermittent operation than with continuous operation (about 40% for System 1, about 60% for System 2). Instead, the radiant system of Room 1 stays of for less time, but more frequently.

Table 4.26 - Amount of operation hours on a daily basis and for every time the system turns on.

Room	System	Mean daily amount of operation hours [h]				Mean amount of consecutive operation hours [h]			
		December		March		December		March	
		L	U	L	U	L	U	L	U
1	1, cont.	2.6	1.5	0.8	0.5	4.0	2.6	4.2	2.6
	1, int.	3.1	1.7	1.2	0.7	2.4	1.8	3.1	2.2
	2, cont.	2.5	1.5	0.7	0.4	2.9	1.8	2.8	1.7
	2, int.	3.3	2.0	1.3	0.7	2.4	1.8	2.6	1.6
2	1, cont.	12.9	11.8	10.8	9.4	3.4	2.9	2.9	2.3
	1, int.	11.6	10.5	10.6	9.2	4.7	3.5	4.9	3.3
	2, cont.	13.0	12.0	10.9	9.7	2.5	2.1	2.1	1.7
	2, int.	10.9	10.1	10.4	9.1	3.6	3.4	3.5	2.8

cont = continuous operation, int = intermittent operation, L = limited power, U = unlimited power

When the power is limited, in the room with parquet (Room 1) the mean temperature of the supply water is 5.5 °C lower than the design value for the traditional system, 4.5 °C for the thin-screed system. In the room with ceramic tiles (Room 2) the difference from the design value is lower, about 1 °C (Table 4.27).
With limited power the mean temperature of the supply water of the thin-screed system is on average 0.4 °C and 1.2 °C lower than the temperature of the traditional system (27.3 °C against 27.7 °C in Room 1, 30.8 °C against 32.0 °C in Room 2).
The mean water temperature difference is about 4.7 °C in Room 1 and 4.3 °C in Room 2. If the thermal power is not limited it rises to 7.9÷9.0 °C and 4.5÷5.0 °C respectively.

Table 4.27 - Mean values of the supply water temperature, water temperature difference and thermal power.

Room	System	Supply water temp. [°C]				Water temp. difference [°C]				Thermal power [kW]			
		December		March		December		March		December		March	
		L	U	L	U	L	U	L	U	L	U	L	U
1	1, cont.	27.7	33.2	27.9	33.2	4.8	8.5	4.8	8.5	0.50	0.89	0.50	0.89
	1, int.	27.4		27.8		4.7	9.0	4.8	8.5	0.50	0.94	0.50	0.89
	2, cont.	27.3	31.9	27.3	31.9	4.7	8.1	4.7	8.1	0.49	0.84	0.49	0.84
	2, int.	27.3		27.5		4.7	7.9	4.7	8.0	0.49	0.83	0.49	0.84
2	1, cont.	32.6	33.2	32.3	33.2	4.2	4.6	4.4	5.0	0.50	0.55	0.52	0.60
	1, int.	31.6		31.5		4.4	5.1	4.4	5.2	0.52	0.60	0.53	0.62
	2, cont.	31.5	31.9	31.2	31.9	4.2	4.5	4.4	4.9	0.50	0.54	0.52	0.59
	2, int.	30.2		30.3		4.4	5.0	4.3	5.2	0.53	0.60	0.52	0.62

cont = continuous operation, int = intermittent operation L = limited power, U = unlimited power

In Table 4.28 the mean monthly values of the operative temperature, air temperature and surface temperature of the floor are listed. The operative temperature is calculated in the centre of the rooms at 1.10 m height as mean value of the air temperature and the mean radiant temperature.
Regardless of the month, the system and the operation modality, the difference between the air temperature and the operative temperature is maximum 0.1 °C, thanks to the good insulation level of the envelope. In continuous operation the rooms with ceramic tiles (Room 2) present substantially the same mean temperatures, while for the rooms with parquet (Room 1) the traditional system presents slightly higher air and operative temperatures than the thin-screed system (in each case always less than 0.2 °C).
The same can be seen also for the surface temperature of the floor. With intermittent operation the mean surface temperature of the thin-screed system is lower than that of the traditional one when covered with ceramic tiles (up to 0.5 °C in December with limited power) and also when covered with parquet (up to 0.2 °C in March with unlimited power).

Table 4.28 - Mean values of the operative temperature, air temperature andsurface temperature of the floor.

		Operative temperature [°C]				Air temperature [°C]				Floor temperature [°C]			
Room	System	December		March		December		March		December		March	
		L	U	L	U	L	U	L	U	L	U	L	U
1	1, cont.	20.3	20.4	21.0	21.1	20.2	20.4	21.0	21.0	20.5	20.6	21.0	21.1
	1, int.	20.1	20.3	20.8	20.8	20.0	20.2	20.7	20.8	20.3	20.5	20.8	20.8
	2, cont.	20.3	20.3	20.9	20.9	20.2	20.3	20.8	20.9	20.4	20.5	20.8	20.9
	2, int.	20.1	20.2	20.6	20.7	20.0	20.2	20.6	20.6	20.4	20.5	20.6	20.6
2	1, cont.	23.9	24.0	23.9	24.0	24.0	24.0	24.0	24.1	27.0	27.1	26.6	26.7
	1, int.	22.4	22.6	22.6	22.8	22.5	22.7	22.7	22.9	25.3	25.7	25.3	25.6
	2, cont.	23.9	23.9	23.9	23.9	24.0	24.0	24.0	24.0	27.1	27.1	26.6	26.7
	2, int.	22.1	22.4	22.4	22.6	22.2	22.5	22.5	22.7	24.9	25.4	25.0	25.3

cont = continuous operation, int = intermittent operation L = limited power, U = unlimited power

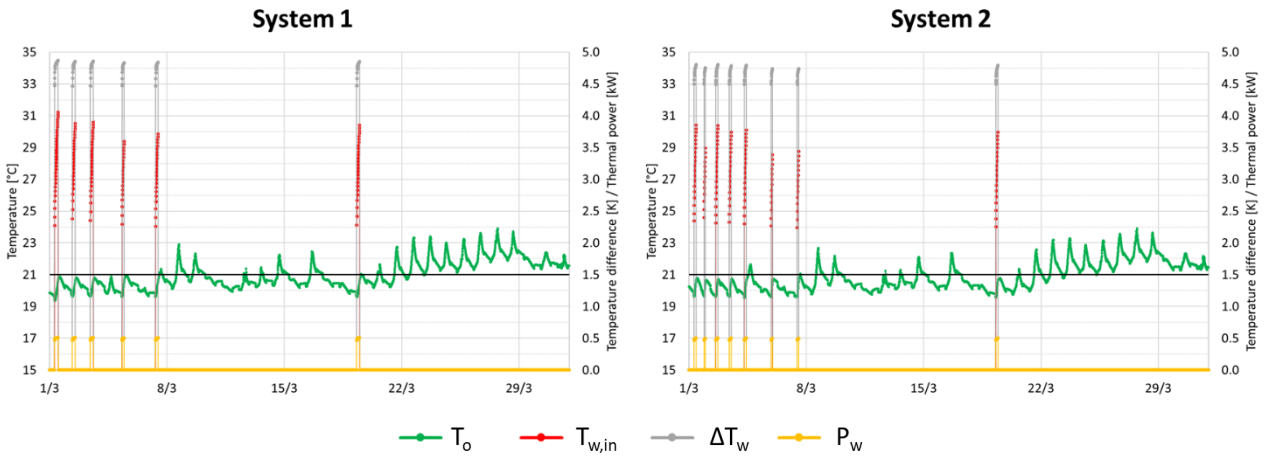

Figure 4.20 - Results of the simulations of March with continuous operation and limited power for Room 1.

The time periods in which the operative temperature exceeds 21 °C were examined, only for the room with parquet because adjacent to the bathroom, which has a higher set-point and act for this reason like a constant load for the other room. The results of two simulations of March are shown as an example in Figure 4.20, where the operative temperature is plotted. As can be seen, in this room the radiant system works only the first week, when the external air temperature was still low. Excluded the first part of the month, the operative temperature frequently exceeds 21 °C, especially in the afternoon since the room is West oriented.
The weighting factor for overheating WF^+, already described and used in 3.4.3, was considered as performance indicator of the building for the heating season in relation to the overheating risk. The monthly weighting factor WF^+, the number of hours which contribute to overheating h^+ and the mean monthly intensity of overheating WF^+/h^+ were calculated and can be seen in Table 4.29.
The WF^+ of December for the systems working in intermittent operation is negligible and is very low also in continuous operation. In March the room with the thin-screed radiant floor system in continuous operation presents a WF^+ which is more than 10% lower than in the room with the traditional radiant floor system when the power is limited, almost 20% lower when the power is unlimited. In intermittent operation the percentages are even higher (almost 20% and 30%)

Table 4.29 - Overheating: cumulative value, duration and intensity.

Room	System	WF^+ [°C]				h^+ [h]				WF^+/h^+ [°C/h]			
		December		March		December		March		December		March	
		L	U	L	U	L	U	L	U	L	U	L	U
1	1, cont.	20	34	272	309	53	110	322	359	0.38	0.31	0.85	0.86
	1, int.	3	13	152	183	36	65	273	299	0.08	0.19	0.56	0.61
	2, cont.	13	16	240	249	46	59	295	307	0.29	0.27	0.81	0.81
	2, int.	1	6	125	130	5	31	201	204	0.20	0.21	0.62	0.64

cont = continuous operation, int = intermittent operation L = limited power, U = unlimited power

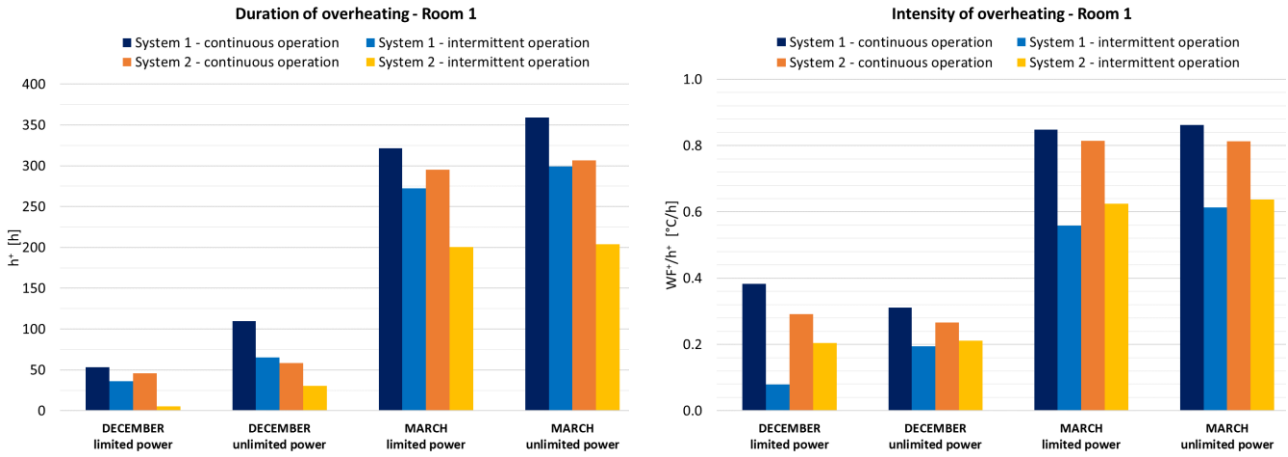

Figure 4.21 - Duration and intensity of overheating for Room 1.

The number of hours in which overheating occurs is significantly lower with System 2 than with System 1 (Figure 4.21). With continuous operation the mean intensity of overheating is 0.4 °C/h in

December and 0.9 °C/h in March for the traditional floor system, 0.3 °C/h and 0.8 °C/h for the floor system with reduced thickness of the screed. With intermittent operation the mean overheating decreases to 0.1 °C/h in December and 0.6 °C/h in March for the traditional floor system, 0.2 °C/h and 0.6 °C/h for the floor system with reduced thickness of the screed.

4.7 CONCLUSIONS AND DISCUSSION

In the present chapter the performance of a wet floor radiant system with a reduced thickness of the screed was studied in comparison to a traditional floor radiant system. The investigation was both experimental, by means of field measurements in two flats of a new building, and theoretical, by means of dynamic simulations of the two systems under the same boundary conditions. Two rooms for each flat were heated during the measurements; for each flat 9 sensors were used to monitor the air temperature, 7 for the surface temperature of the floor, 2 for the water temperature, all with a frequency of 5 minutes, and an energy meter which gave mean hourly data of supply and return water temperature, mass flow rate and thermal power. Despite the high number of measurement points and the choice of instruments and sensors with good accuracy level, the field measurements revealed to be quite complicated and, for some aspects, even misleading.
Four weeks of measurements were planned with continuous and intermittent operation of the two radiant systems and different supply water temperature, but towards the end of the measurements recording problems came to light from the third party who managed the acquisition of the data. Environmental data were available for only the last 10 days and the measurements were extended for a week.
During the period of continuous operation both the traditional floor heating system and the thin-screed floor system accurately followed the set-point for the air temperature. The number of hours of operation of the radiant loops was about 15% lower for the thin-screed system, but that flat was South-West oriented and thus presented higher temperatures in the adjacent rooms in comparison with the flat with the traditional system which was North-West oriented. During the period of intermittent operation both the systems had problems to reach the higher set-point temperature because of the high inertia, as well as for unexpected cold weather conditions and a consequently too low supply water temperature.
Analysing the water temperature measured in the manifold, a higher difference between supply and return temperature was found for the thin-screed system, but comparing these temperatures with the mean hourly values of the ones recorded by the energy meter a mismatch was found for one of the sensors.
From the analysis of the mean hourly, maximum and minimum values of water flow rate recorded by the energy meters, non-negligible oscillations were found, due to the operation of the heat pumps, which were directly connected to the radiant systems without inertial tanks. The evaluation of the flow rate for the time periods when water was flowing based on the mean hourly data was not possible, since the frequency of acquisition of the thermostat state was too low in relation to the mean duration of the periods in which they were *on*. This happened also because of a too low on-off band of the thermostat.
From the mean hourly values of the thermal power provided by the energy meters, the energy need of the flat with the thin-screed radiant system in the last week of continuous operation resulted to be about 20% higher than the energy need of the flat with the traditional radiant system. In the previous weeks, when only the daily data of the energy meters were available, the situation was much more

different, with only some percentage points of difference in the thermal energy provided to the two flats. Therefore no conclusion could be drawn from the field measurements.
The available environmental data presented many critical points, denoting probable calibration and/or acquisition errors, but also the data from the energy meters could not be used for a fine tuning of simulations reproducing the period of field measurements. Simulations have been anyway compared to measurements to check the trends of internal temperatures and it can be concluded that the distribution of indoor parameters is similar in the simulations compared to measurements.
Simulations under the same boundary conditions were performed for the two systems, taking into account the dynamic behaviour of building structures as well as the transient operation of water in the embedded pipes. From the results of the simulations, no significant difference was found in the thermal energy need of the two kind of floor radiant heating systems. The thin-screed system presents a lower response time, but intermittent operation does not lead to a lower energy consumption. Moreover, if the supply water temperature is the same used during continuous operation, the set-point is hardly reached during short time-slots. To ensure comparable indoor conditions in the occupied time periods, the radiant system should be turned on earlier or the supply water temperature should be increased, with resulting higher energy consumption.
From the analysis of the temperature inside the rooms, a negligible difference was found between air and operative temperature for both the radiant systems. A slightly lower risk of overheating was found for the thin-screed system, but the intensity of overheating is very low with both the systems and becomes significant only at the end of the heating season, when the external air temperature rises. In these periods the radiant system is working only sporadically and it is self-evident that the temperature inside highly insulated buildings would rise easily also with other kinds of heating systems.
The coupling of the emission system with the generation system is an interesting point to be further investigated, since the water temperature difference available from the generation system significantly influences the transient operation of the radiant system and the time needed to reach the indoor set-point. Also from the field measurements it was found that the generator can be quite critical for the proper operation of the radiant system.

5 EXPERIMENTAL ANALYSIS ON THERMAL COMFORT IN A TEST ROOM

Abstract

The experimental investigations on thermal comfort performed in a test room with vertical radiant asymmetry and air stratification are presented in this chapter. The work was carried out in the facility of the Technical University of Dresden. Thermal global and local sensations were assessed by means of questionnaires during 38 tests in which the surface temperatures of the upper and lower parts of the room were progressively increased and decreased, while inlet air temperature was kept constant. No relevant asymmetry problem was found in the analysis of the local sensations detected by the test subjects, while other factors played a significant role.

5.1 INTRODUCTION

Radiant floor is the most widespread kind of radiant system, but radiant ceiling is increasingly being used, especially in commercial buildings. As regards heating operation, the limit for the surface temperature of radiant floor is clearly defined in the standards: 29 °C in the occupied area and 35 °C in the peripheral area [14]. In the case of heating ceilings, physiological limitations concerning the surface temperature are connected not to the contact with the person, but to overhead radiation which can cause a warm sensation at the head and also a cold sensation at the feet. This local discomfort factor, which is known as asymmetric thermal radiation, is implemented in ISO 7730 [48] along with the other possible factors of local discomfort and Fanger's PMV-PPD model. Radiant temperature asymmetry is defined as the difference between the plane radiant temperature of the opposite sides of a small plane element [95, 96]; the plane radiant temperature is the uniform temperature of an enclosure in which the incident radiant flux on one side of a small plane element is the same as that in the actual environment.

As concerns asymmetric thermal radiation, in ISO 7730 the warm ceiling is the most critical among the possible heated or cooled surfaces of a room: to ensure a percentage of dissatisfied (PD) lower than 5%, the vertical radiant temperature asymmetry should be lower than 5 °C. A heating ceiling, if compared to a heating floor, shows a lower convective coefficient because of the effect of air stratification, and cannot generally be completely active. These two aspects lead to a surface temperature higher than the one required by a heating floor. Therefore, it is difficult to keep the radiant asymmetry low when the heating load is high. This is one of the reasons why heating ceilings are mainly used in buildings with a low heating load, i.e. new buildings or renovated ones.

Besides heating operation, the need for cooling during the summer is increasing also in countries with a predominant heating demand, due both to global warming and especially to the higher level of insulation of buildings. As a consequence, new buildings are generally designed to offer comfortable thermal conditions throughout the year and are therefore provided with cooling systems. This is true mainly for commercial buildings, where the increasing demand for more comfortable indoor environment is also aimed to achieve a better performance of the workers. To reduce

investment costs and space requirement, it is wise to use the same system to fulfil both heating and cooling demand.
These are the reasons for new investigations with test subjects in a climate room. The presented experimental analysis is focused on heating and cooling ceilings and floors and takes into account both radiant temperature asymmetry and air stratification, with the aim of detecting how the different factors affect the local sensations of the test subjects. As a matter of fact, even though radiant systems have been present for a long time in the market, there are still open questions in their use and design. The radiant asymmetry in particular is usually not calculated by practitioners, who prefer to deal with a limit on the maximum surface temperature of a heating ceiling. This habit introduced different limiting surface temperatures over the years and currently each producer declares different values in a range between 29°C and 35°C. In order to give answers to this particular issue, more research is needed for establishing the well-being of people under radiant heating ceilings and the present chapter is the first step of this research activity. Moreover, as shown hereunder the studies of Fanger were limited in number and some criticisms were moved by some authors in literature.

The first studies on sedentary persons exposed to radiant asymmetry dates back to 1950's, when Chrenko [97] investigated the subjective response of test subjects exposed to a heated ceiling, increasing the mean radiant temperature up to 12 °C and keeping air temperature at a constant value. Twenty years later, tests were performed the McNall [98] and Griffiths [99] by increasing the temperature of the ceiling, while lowering the temperature of the walls to keep the operative temperature constant. In later studies Fanger studied the asymmetric thermal radiation due not only to a heated ceiling [95], but also to a cooled ceiling, a heated wall and a cooled wall [96]. In these investigations both the air temperature and the temperature of the other surfaces were modified during the test according to the answers of the subject to keep him/her neutral. The air change was high to avoid air stratification and thus it was possible to study only the effects of the asymmetric temperature field. The skin temperature of the different parts of the body was monitored by 14 temperature sensors and a thermal manikin was later used to calculate the operative temperature of each of the tested level of radiant asymmetry.
In each investigation 16 college-age subjects (8 males, 8 females) were individually tested, except in the investigation on cooled wall which had 32 test subjects; they were wearing a uniform with a clo value of 0.6. After a first phase intended to find the comfort temperature for the subject according to his/her request, the surface temperature was changed every 30 minutes increasing the radiant asymmetry. From the answers of the test subjects to a questionnaire every 5 minutes, curves were derived showing the percentage of dissatisfied subjects as a function of the radiant temperature asymmetry. Among the studied surface, the warm ceiling was found to be the most critical. Accepting a 5% of uncomfortable subjects, the maximum allowable radiant temperature asymmetry is 4 °C with a warm ceiling, against 14 °C with a cool ceiling, 10 °C with a cool wall and 23 °C with a warm wall. The results of the studies on radiant asymmetry by Fanger are implemented in ISO 7730 (Figure 5.1, left). It should be noticed that the equations written in this standard for calculating the percentage of dissatisfied give curves (Figure 5.1, right) which are not in agreement with the curves in the image inside the standard (Figure 5.1, left).
Going back to Fanger study on heated ceiling [95], two interesting findings should be remarked. The first is about the mean skin temperature resulting from the thermal preference of the subjects, which was constant during the entire test, regardless of the temperature of the ceiling. The second is that people who felt an uncomfortable cold sensation on the feet were almost as frequent as people detecting a warm sensation on the head. Another interesting finding for all the studied cases [96] is

that no significant difference was detected in the response of males and females to asymmetric radiation.
Some critical remarks on the studies of Fanger were done by Glück [100], who noticed that the number of test subjects was small and the age distribution was limited. Moreover the subtraction of 3.5% from the logarithmic regression line of warm ceiling was not necessary because a linear regression with a good correlation coefficient was possible.
In addition Glück stated that the priority when dealing with radiant asymmetry should be given to the head. As a matter of fact, the local sensation detected by the persons on all the other parts of the body can be limited with an appropriate adjustment of the clothes, while for the head nothing can be changed. From this point of view considering the radiant asymmetry on a small surface at 0.60 m from the floor appears to be inadequate. For this reason he proposed to consider a small cube at 1.30 m from the floor as simplification of the head and to calculate the highest radiant temperature asymmetry between all the combinations of 2 faces of the cube. He also used the data from Fanger's test to calculate the corresponding limits according to his new definition of asymmetry.

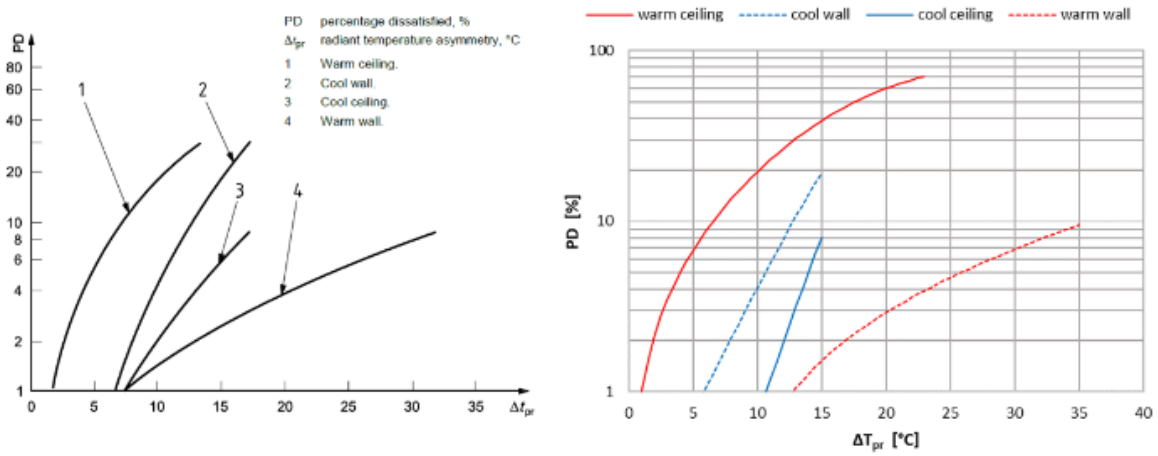

Figure 5.1 - Local thermal discomfort caused by radiant temperature asymmetry: image inside ISO 7730 (left) and plotted equations from the same standard (right).

5.2 DESCRIPTION OF THE TEST ROOM

The experiments took place in the new climate room at the Technical University of Dresden, Institute of Power Engineering, Building Energy Systems and Heat Supply Group.
The climate room (Figure 5.2) is part of the Combined Energy Lab 2.0, where complex technical systems of a building (generation, distribution and emission) can be investigated, along with the connection from the building to the upstream supply system.
The climate room has the following internal dimensions:

- length: 5.0 m;
- width: 4.0 m;
- height: 2.5 m.

All the surfaces of the room are made of modular elements with the dimensions of 1 m x 2.5 m and 8 cm thick. The modules are made of a water-based capillary system placed on a metal plate and the external side is insulated with a polyurethane foam. Temperature sensors are placed on the metal plate to measure the surface temperature (Figure 5.3). Each of the 9 modules of the walls is

made of 3 segments which can be controlled at independent temperatures, while the 16 modules of the ceiling and of the floor are made of one segment. Thanks to this kind of modules, the system has a very low response time and a great flexibility.
The supply water temperature of each capillary segment is controlled by a three-way valve, which mixes the hot and cold water mass flows provided by the hot and cold distribution networks. The surface temperatures of each segment can be regulated in a range from 10 °C to 50 °C with a heating/cooling rate up to 4 K/min.

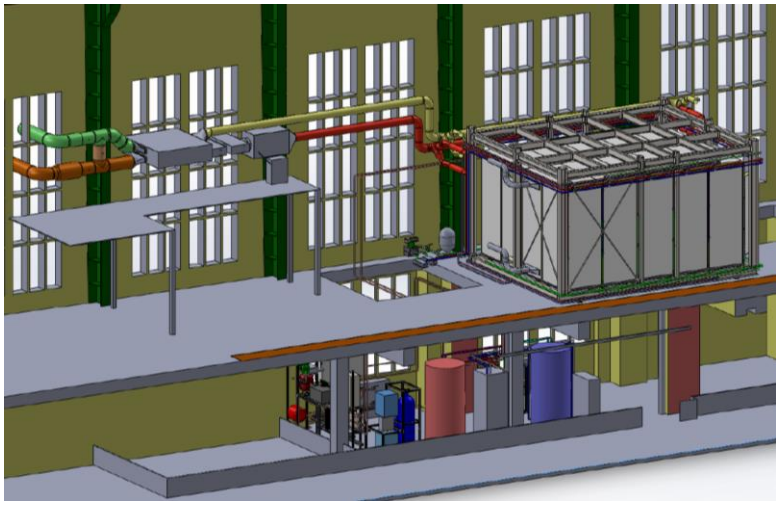

Figure 5.2 - Schematic structure of the test facility with the climate room on the right and the ventilation system on the left on the first floor and the generation system on the ground floor [101].

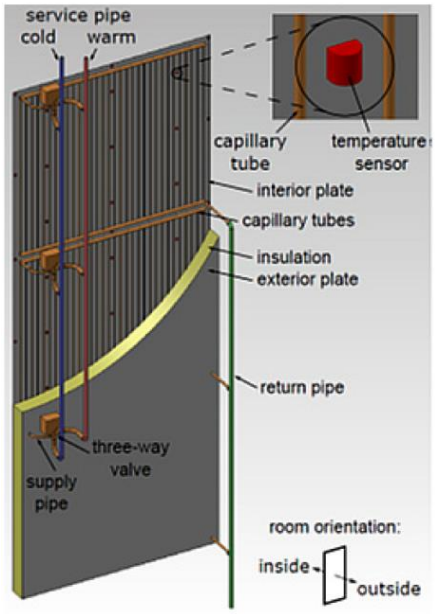

Figure 5.3 - Construction details of the modules of the climate room [102].

The climate room is connected to a ventilation and air conditioning systems with a maximum flow rate of 600 m³/h, which corresponds to an air change of 12 h^{-1}. The air temperature can be regulated in a range from 10 °C to 35 °C and the air humidity from 20% up to 90%. The air supply and extraction are provided through 4 grids placed in 2 opposite walls of the room, as can be seen in Figure 5.4.

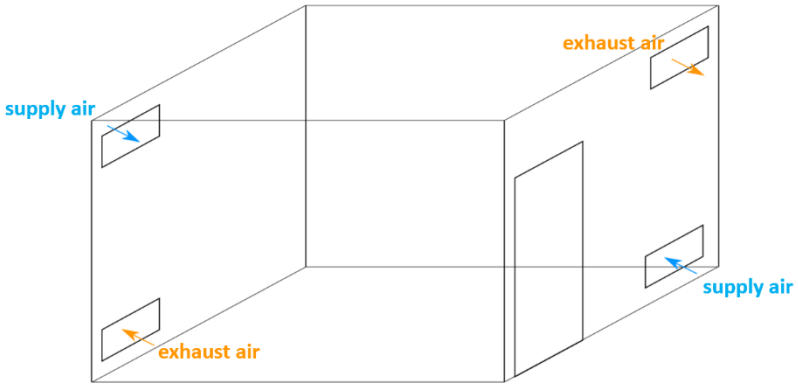

Figure 5.4 - Schematic view of the connection of the test room with the ventilation system.

From the tests done after the construction of the room, it can be seen that the actual temperatures can follow the set-points very well. The differences between the set-points and the actual values are lower than 0.2 K.
The uniform and independent temperature control of the segments can be seen from the thermographic images in Figure 5.5.

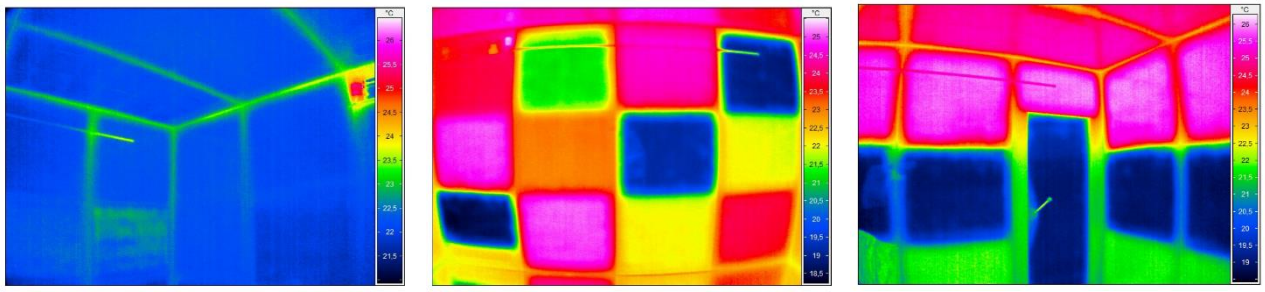

a b c

Figure 5.5 - Thermographic images of a corner of the room with homogeneous surface temperature distribution (a), proof of independent setting of the wall elements (b) and detail of the door element with non-temperable frame (c) [101].

5.3 DESCRIPTION OF THE TESTS PERFORMED

5.3.1 Experimental procedure

In the tests performed the subjects were not wearing a standard uniform, but they were asked to bring a T-shirt, a long pair of trousers, socks and closed shoes, which are equivalent to about 0.5 clo. They arrive to the test facility before the start of the experiment and eventually change their clothes there if dressed in a different way because of the external temperature. The hour at which the test started was not the same for all the subjects, but was agreed with each single one. All the

experiments took place in the morning or in the first hours of the afternoon in the period from June to August 2018. The subjects were asked to inform if they were feeling sick or tired, so that the test could be moved to another day.
The subject was seated in the centre of the room on a chair which had a negligible effect on the amount of heat losses from the body. In front of the subject there was a small stool where the tablet used to answer to the questionnaire was placed.

The experimental procedure is similar to that applied by Fanger et al. [95] [96] in their studies about radiant asymmetry.
At the beginning of the test the temperature of the supply air and of all the surfaces of the room was set to 22 °C. From previous tests on 84 people (Figure 5.6), this was the comfort temperature for almost 70% of the subjects (Figure 5.7).

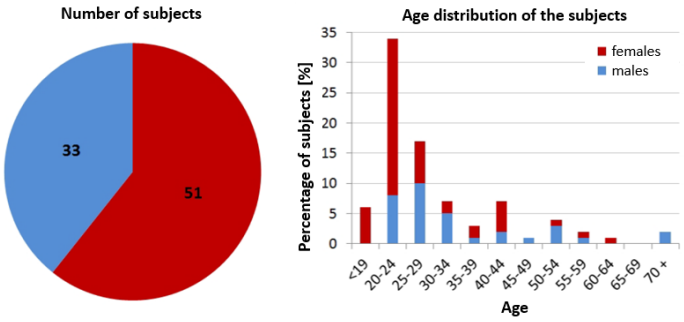

Figure 5.6 - Sex and age distribution in a previous study on comfort temperature [101].

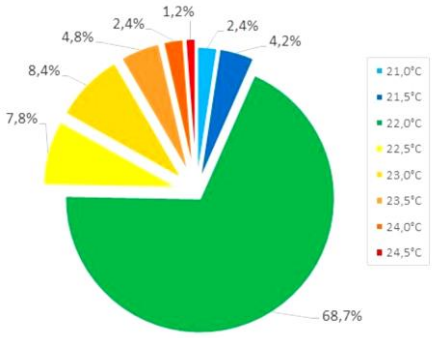

Figure 5.7 - Distribution of the comfort temperature from a previous study [101].

The first phase of the test was intended to reach the temperature at which the subject felt thermally comfortable. Every 5 minutes he/she was asked if he/she wanted a warmer or cooler environment (see 5.3.3) and then the temperature of the supply air and of all the surfaces was immediately increased or lowered of 0.5 °C according to his answer. The comfort temperature was considered to be reached when he/she did not ask for a change for at least two consecutive answers to the questionnaire. This first phase lasted at least 30 minutes, even if the subject never asked for a change, up to a maximum of 1 hour.

In the second phase of the test the surface temperatures of the upper part of the room and of the lower part of the room were changed, while the supply air temperature and the surface temperature of the central part of the walls were kept constantly equal to the comfort temperature (Figure 5.8). The angle factors of the 3 groups of surfaces from a point in the centre of the room at 0.6 m and 1.1 m from the floor were calculated according to [103] and are listed in Table 5.1.

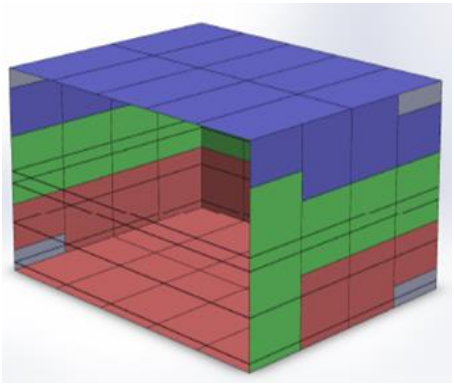

Figure 5.8 - Representation of the 3 groups of surfaces for the second part of the test: the lower part of the room (red), the central part of the walls (green) and the upper part of the room (blue).

Table 5.1 - Angle factors of the 3 groups of surfaces from a point in the centre of the room at 0.6 m and 1.1 m from the floor

Group of surfaces	h = 0.6 m	h = 1.1 m
upper half-room	0.30	0.40
central modules of the walls	0.15	0.17
lower half-room	0.55	0.43

Table 5.2 - The 2 types of test performed.

Type of test	Heated surfaces	Cooled surfaces	n. of tests
UH	upper half-room	lower half-room	20
LH	lower half-room	upper half-room	18

Two types of test were done, 20 tests with the upper half-room heated and the lower half-room cooled and 18 tests with the lower half-room heated and the upper half-room cooled (Table 5.2). Considering the case UH, every 30 minutes the surface temperature of the upper half-room was increased of 1.5 °C while the surface temperature of the lower half-room was lowered of 1.5 °C. This second phase lasted 2.5 hours, thus reaching a difference between the ceiling and the floor temperature equal to 15 °C. For the case LH the heated and cooled surfaces were reversed. In this second phase of the experiment the test subject was asked to answer to questions on thermal global sensation, thermal preference, thermal local sensations and air quality every 5 minutes (see 5.3.3).

A schematic summary of the experimental plan and the calculated resulting radiant asymmetry at 0.60 m above the floor can be seen in Table 5.3.

The air change during the entire test was about 3.5 h^{-1}.

Table 5.3 - Experimental plan.

Test phase	Time	Temperature difference between heated surfaces and neutral ones	Temperature difference between cooled surfaces and neutral ones	Calculated radiant asymmetry at 0.60 m
	[min]	[K]	[K]	[K]
1	0 - 30÷60	0	0	0
2	0 - 30	+1.5	-1.5	2.3
	30 - 60	+3.0	-3.0	4.5
	60 - 90	+4.5	-4.5	6.8
	90 - 120	+6.0	-6.0	9.1
	120 - 150	+7.5	-7.5	11.3

5.3.2 Measurement set-up

Due to the active control of the surfaces, the temperatures of each module or sub-module was recorded with a frequency of 10 s with five 1-wire digital temperature sensors integrated in the module. The accuracy of these sensors is ±0.5 K.
The air temperature during the tests was measured by 26 NTC sensors (Table 5.4) placed on a pole in the central part of the room, next to the subject. The spacing between the sensors, equal to 10 cm, ensures a detailed representation of the air stratification inside the room.
Three standard black globe thermometers (Table 5.4) were placed in the proximity of the sitting subject, at three relevant heights (0.10 m, 0.60 m and 1.10 m), in compliance with ISO 7726 for class C (comfort) [104]. The influence of the test subject on the temperatures measured by the globe thermometers has been analysed, as will be further discussed in 5.4.2.
Air velocity was not measured during the experiments with test subjects, but only in further tests with an unheated manikin. Three thermo-anemometers (Table 5.4) were used to evaluate the air velocity in proximity of the arms and the back, as will be presented in 5.4.5.

Table 5.4 - Measuring instruments and main technical data.

Measured parameter	Type of device	Designation	Measuring principle	Measuring range	Accuracy
Air temperature	Thermometer	*Ahlborn ZA9040FS*	NTC thermistor	-50 ÷ 125 °C	±0.05 K
Globe temperature	Globe thermometer	*Ahlborn FPA805GTS*	PT100 resistances	-40 ÷ 200 °C	Class B (DIN/IEC 751)
Air velocity	Thermo-anemometer	*Ahlborn FVA605TA1O*	heated thermistor	0.010 ÷ 1.000 m/s	±1% of final value

The arrangement of the instruments in the occupied area of test room during the experiments is shown in Figure 5.9.

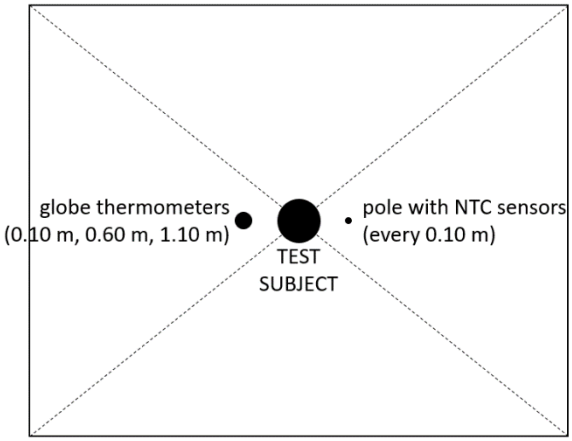

Figure 5.9 - Arrangement of the sensors in the test room.

5.3.3 Assessment of the comfort conditions by means of questionnaires

Since thermal comfort is not measurable, a subjective assessment of the climatic conditions by the subjects is necessary. This can be done using a suitable questionnaire to be answered by the test subjects. The possible answers to the questions to assess thermal global sensation, thermal preference, thermal local sensations and air quality were based on scales as can be seen in Table 5.5. The questionnaire was implemented in an online tool and followed the procedure shown in Figure 5.10.

Table 5.5 - Questions asked to the subjects, possible answers and evaluation scales.

Questions	Answers	Scale
How do you feel with the current room temperature?	cold, cool, slightly cool, neutral, slightly warm, warm, hot	from -3 to +3
Do you want to change the room temperature?	yes, no	1, 0
How do you want to change it?	warmer, cooler	+1, -1
Do you feel warm or cool somewhere on your body?	yes, no	1, 0
Select your sensation for the following body area (head, arms, hands, legs, feet)	cool, neutral, warm (for each body area)	-1, 0, +1
Is any of these sensations uncomfortable?	yes, no	1, 0
How do you perceive the room air?	very stuffy, stuffy, neutral, fresh, very fresh	-2, 0, +2

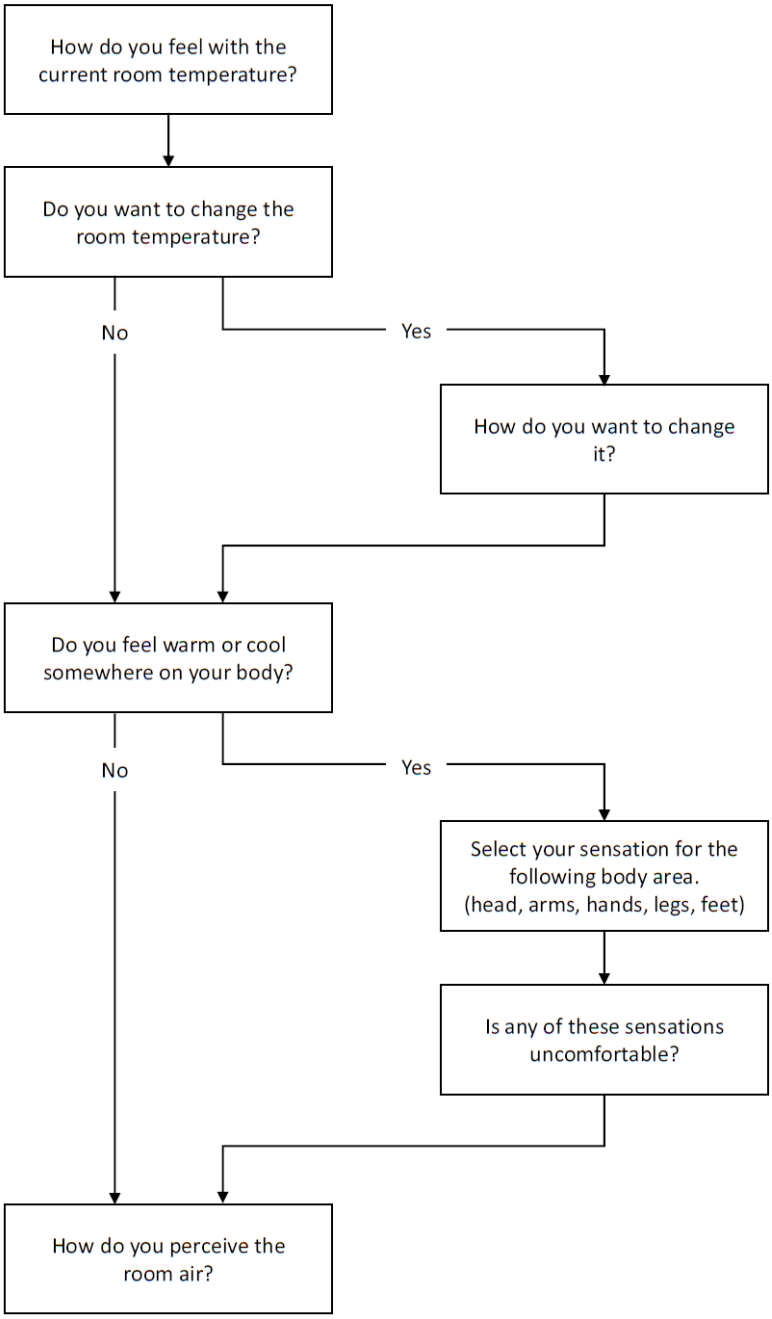

Figure 5.10 - Procedure implemented in an online tool to ask the subjects about their thermal global and local sensations and discomfort

5.4 ANALYSIS OF DATA

5.4.1 The test panel

Thirty-eight college-age people were used as test subjects (Figure 5.11): 14 males and 6 females in the UH tests, 13 males and 5 females in the LH tests. Anthropometric data of the subjects are listed in Table 5.6.

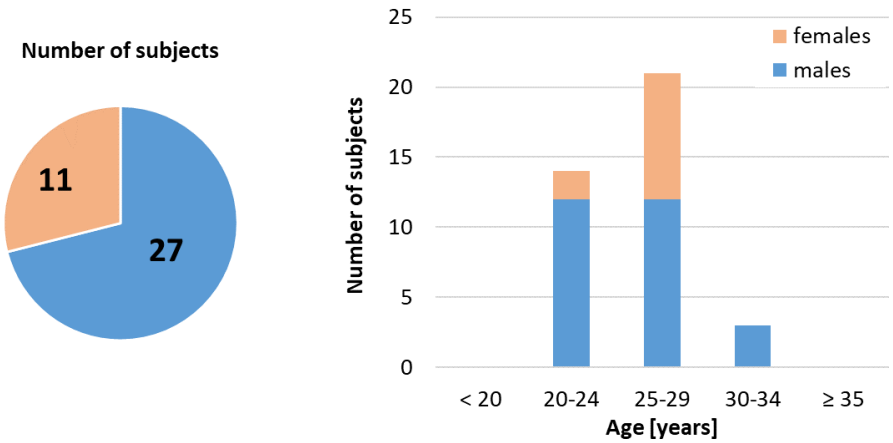

Figure 5.11 - Number of subjects and age distribution.

Table 5.6 – Anthropometric data of the subjects.

Sex	N. of subjects	Age [years]	Height [m]	Weight [kg]
Males	27	25.4 ± 3.2	1.83 ± 0.06	79.4 ± 13.4
Females	11	25.6 ± 2.3	1.69 ± 0.08	59.6 ± 14.1
Males and females	38	25.4 ± 3.0	1.78 ± 0.09	73.7 ± 16.2

In Figure 5.12 the distribution of the comfort temperature (air temperature and surface temperature) at the end of the first phase of the tests is shown. Almost 70% of the test subjects felt comfortable with a temperature of 22.0 °C. No relevant difference can be seen between females and males.

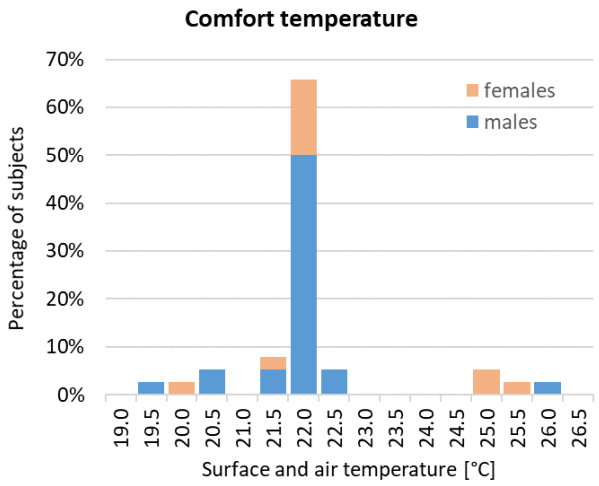

Figure 5.12 - Distribution of the comfort temperature (end of test-phase 1).

5.4.2 Globe thermometer measurements

The presence of the test subject near the globe thermometers influences the measured temperature values. The angle factors between the globes and the person are not negligible, especially for the globes placed at a height of 0.60 m and 1.10 m from the floor. For this reason, a test was performed without a person inside the room and the detected globe temperatures were compared with those measured with a test subject. This test was performed following the procedure defined for the tests with heated upper half-room and cooled lower half-room.
The measured globe temperatures are shown in Figure 5.13. As will be seen from the next paragraph, only the last 10 minutes of each step of the test (from minutes 20 to 30, 50 to 60, 70 to 90 and so on) were considered in the analysis of the results. In these periods the mean value of the difference between the two measurements is 0.1 °C at 0.10 m, 0.4 °C at 0.60 m and 0.4 °C at 1.10 m.

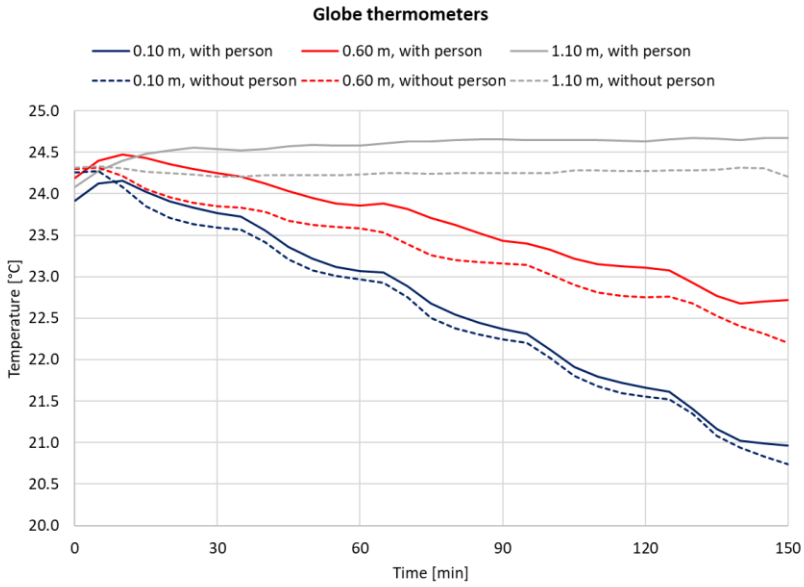

Figure 5.13 - The globe temperatures measured during a test with and without a person.

Starting from the measured globe temperature with the person inside the room, the procedure described in Annex B of ISO 7726 was followed to calculate the mean radiant temperature. The air temperature was known during the tests every 10 cm of height, while the air velocity was not measured. Assuming an air velocity of 0.1 m/s, the mean radiant temperature is 0.2 °C higher than the globe temperature at all the three heights (i.e. 0.10 m, 0.60 m and 1.10 m). With an air velocity of 0.05 m/s the same results were found.
For these reasons, along with the debated necessity of a more complete definition of the features of the globe thermometers designed to operate in asymmetric radiative fields [105] [106], the mean radiant temperature was not calculated in each test and the measured globe temperature will be directly shown in the results presented in the next paragraphs.

5.4.3 Example of results from two tests

In this section the results of two tests are shown, one for the tests with the upper half-room heated and the lower half-room cooled (Figure 5.14 and Figure 5.15) and one for the tests with the upper half-room cooled and the lower half-room heated (Figure 5.16 and Figure 5.17).
In Figure 5.14 the air temperature, measured every 10 cm from the floor to the ceiling, is shown. Only the values recorded at the beginning of the second phase of the test (0 min) and at the end of each 30-minute step of increment of the radiant asymmetry were plotted. The values are not the absolute ones, but they are plotted as difference from the starting operative temperature, which is the temperature of all the surfaces and of the inlet air at the beginning of the second phase. In this specific case the starting operative temperature preferred by the test subject was equal to 22 °C.

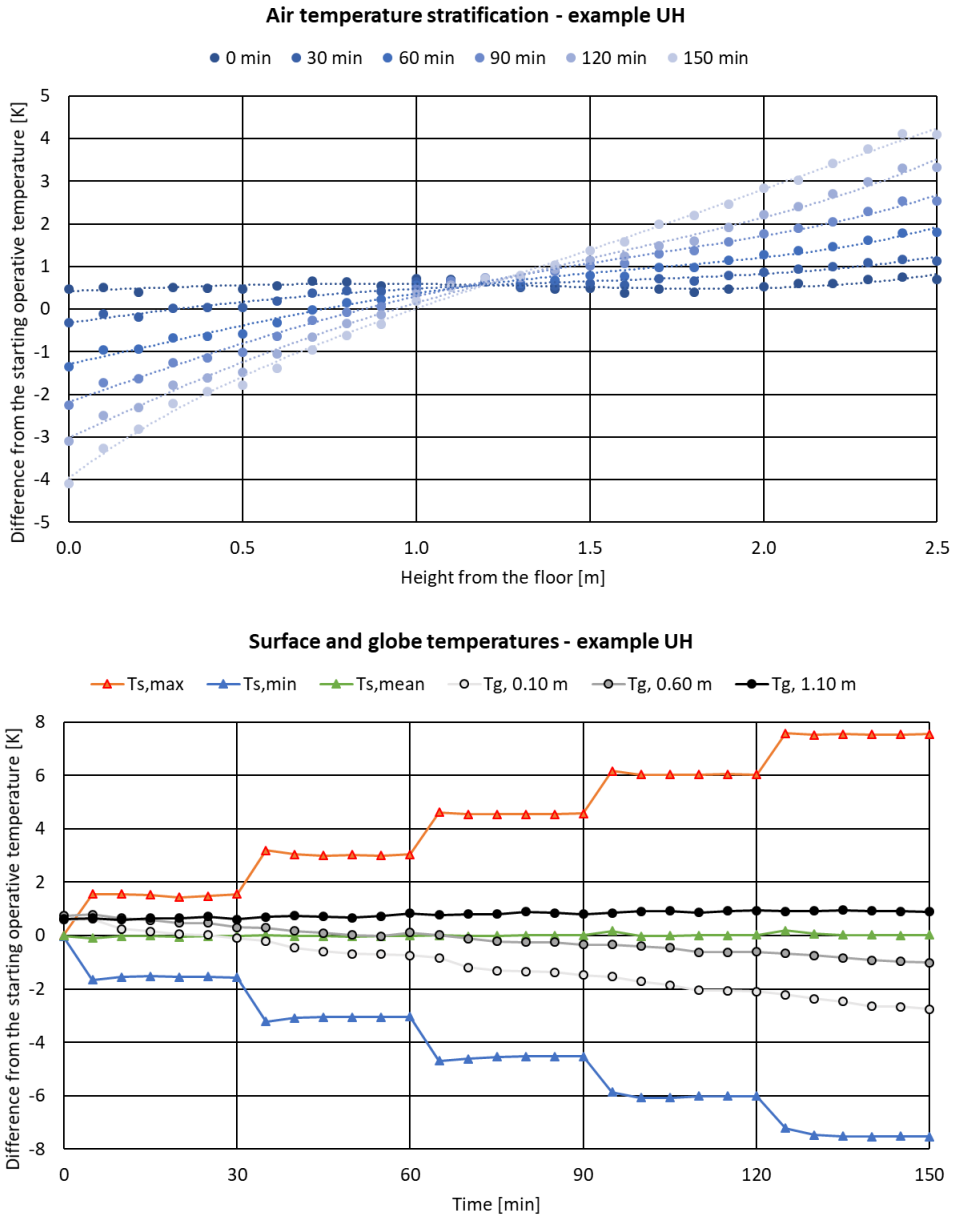

Figure 5.14 - Air stratification, surface and globe temperatures during one of the tests with the upper half-room heated and the lower half-room cooled.

Also the temperatures of the 3 globe thermometers and of the surfaces are plotted according to the same consideration. As can be seen, the temperature measured by the globe thermometer at 1.10 m of height is almost constant throughout the test.
As regards the surfaces:

- $T_{s,max}$ is the maximum value among the surface temperatures of all the modules and can be considered equal to the surface temperature of the heated half-room;
- $T_{s,min}$ is the minimum value among the surface temperatures of all the modules and can be considered equal to the surface temperature of the cooled half-room;
- $T_{s,mean}$ is the mean value of all the modules of the room, without consideration of their area.

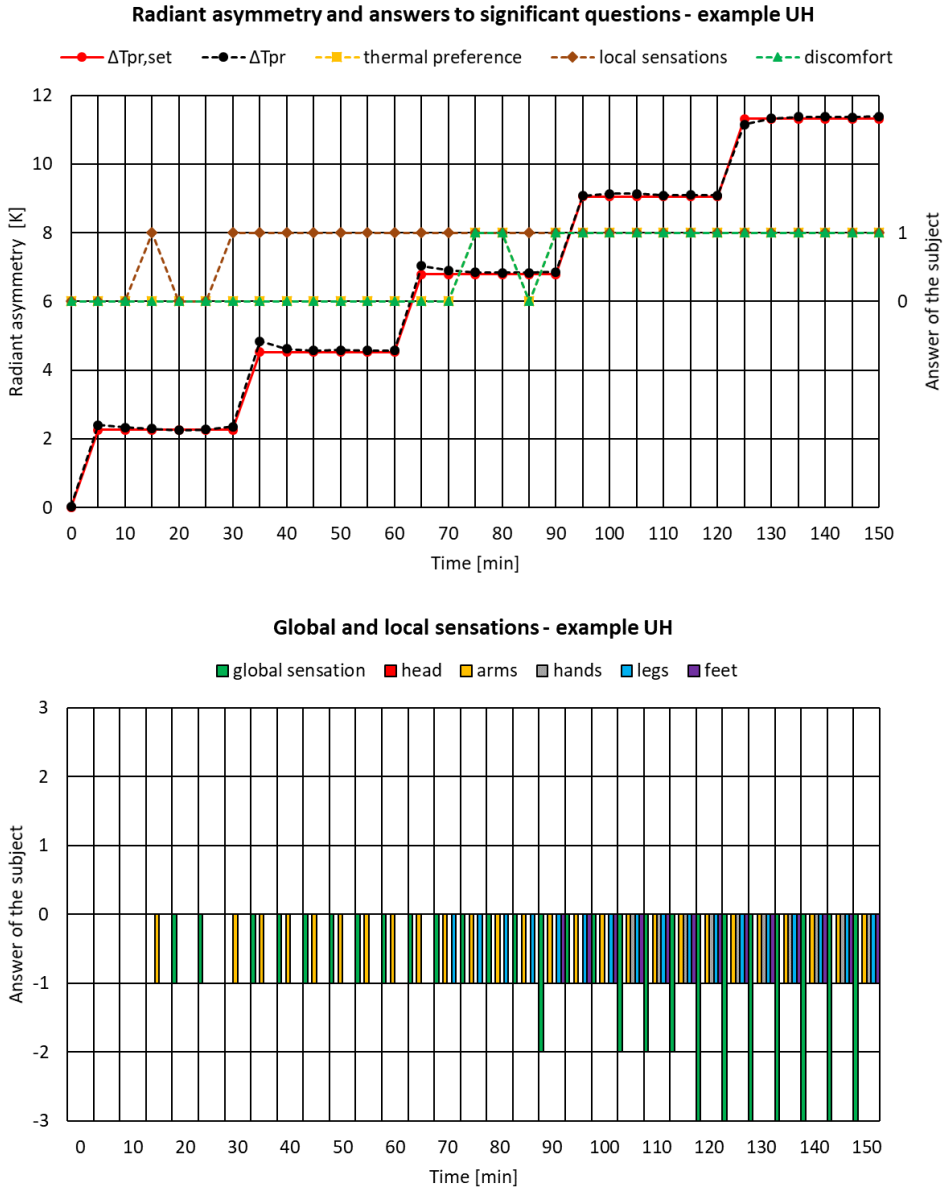

Figure 5.15 - Radiant asymmetry, answers to significant questions, global and local sensations during one of the tests with the upper half-room heated and the lower half-room cooled.

In Figure 5.15 the radiant temperature asymmetry is plotted. The desired value $\Delta T_{pr,set}$ is the one calculated with the design increments and decrements of the surface temperatures (Table 5.3), while ΔT_{pr} is the one calculated with the measured maximum temperature, minimum temperature and middle-wall temperature. As can be seen the system reaches the desired radiant asymmetry quickly. The answers of the subject to some significant questions are also plotted in this way:

- thermal preference: 1 if he/she desires a temperature change, 0 if not;
- local sensations: 1 if he/she detects any local sensation, 0 if not;
- discomfort: 1 if he/she feels thermally uncomfortable, 0 if not.

Also the answers about global and local sensations are plotted, according to the evaluation scales already seen in Table 5.5: from -3 to +3 for the global sensation and from -1 to +1 for the local sensations.

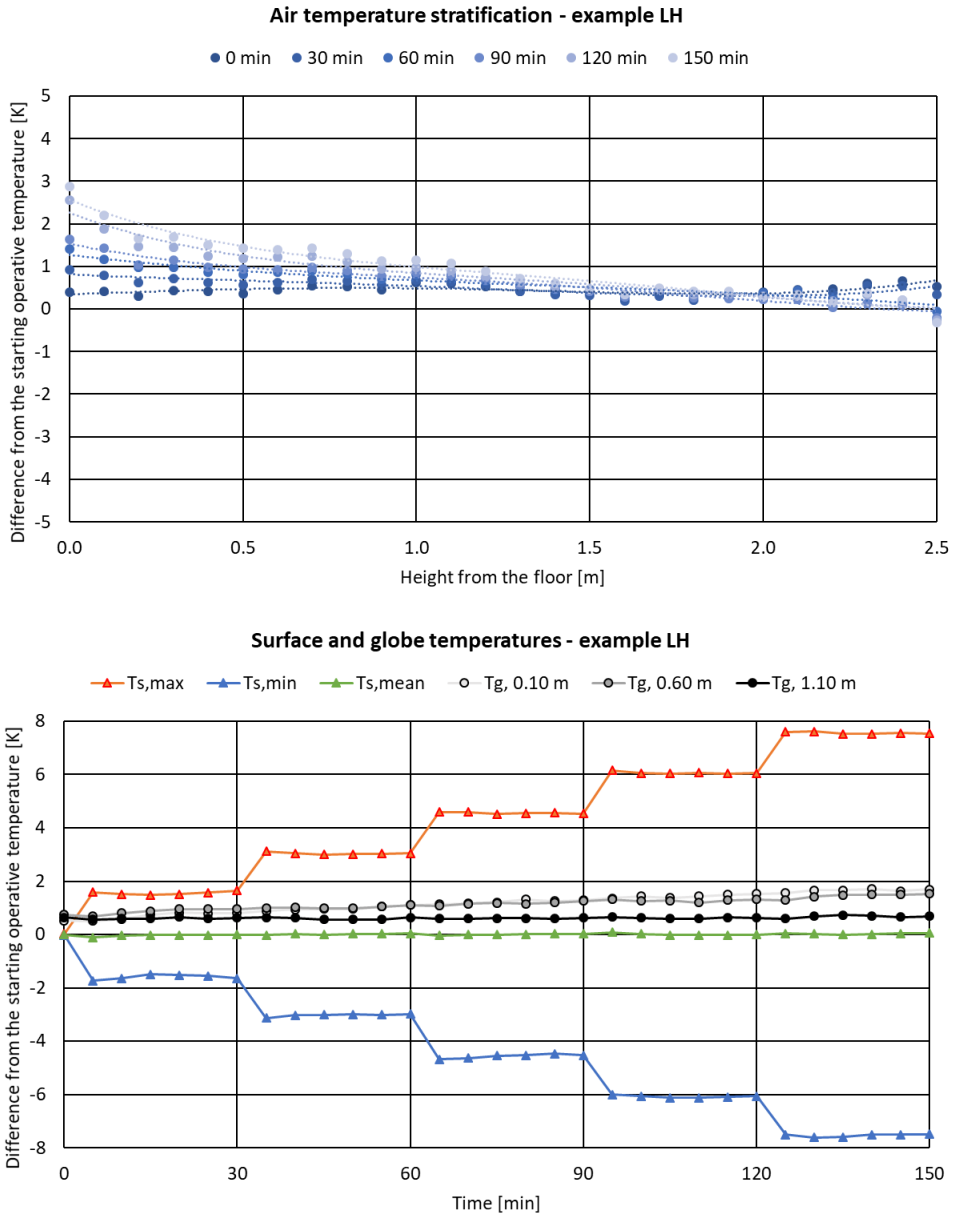

Figure 5.16 - Air stratification, surface and globe temperatures during one of the tests with the upper half-room cooled and the lower half-room heated.

In Figure 5.16 and Figure 5.17 the same results are plotted for a test with the upper half-room cooled and the lower half-room heated. In this case the air stratification is, as expected, much lower than in the example UH. The globe temperature at 1.10 m of height is almost constant as in the previous example. The globe temperature at 0.60 m of height is decreasing throughout the example UH, while in the example LH is slightly increasing. About the answers of the subjects, it should be noticed that the 6 answers given every 5 minutes during each step of radiant asymmetry are not always the same. For the analysis of the following paragraphs only the 3 answers given in the last 10 minutes of each step were considered (from minute 20 to 30, from 50 to 60 and so on) and only if at least 2 of 3 were identical.

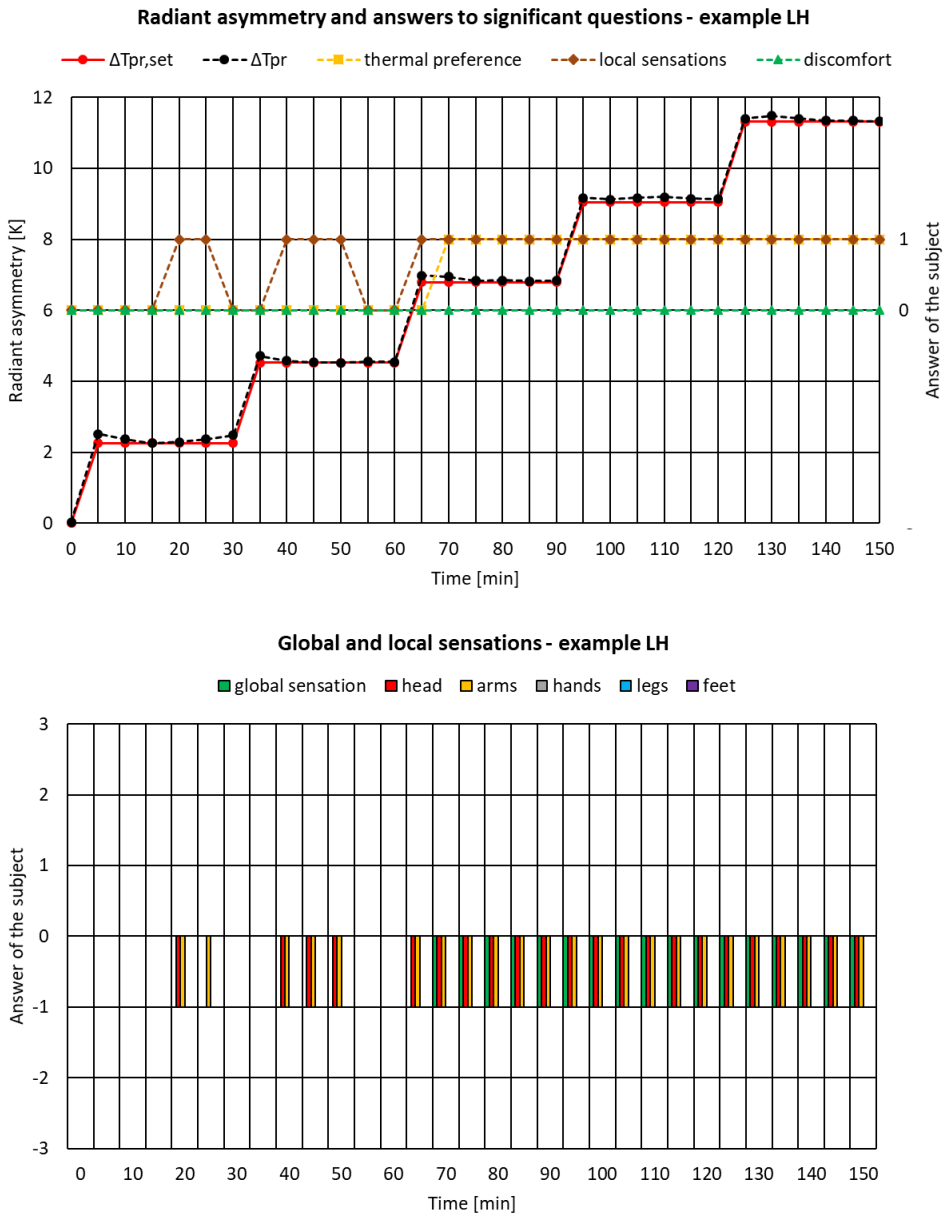

Figure 5.17 - Radiant asymmetry, answers to significant questions, global and local sensations during one of the tests with the upper half-room cooled and the lower half-room heated.

5.4.4 Overall results

The results of the measurements and of the questionnaires were analysed separately for the UH tests and the LH tests. They are presented in this section in terms of:

- air temperature stratification;
- air and globe temperature;
- radiant temperature asymmetry;
- global sensation;
- desired temperature change;
- local sensations;
- thermal discomfort.

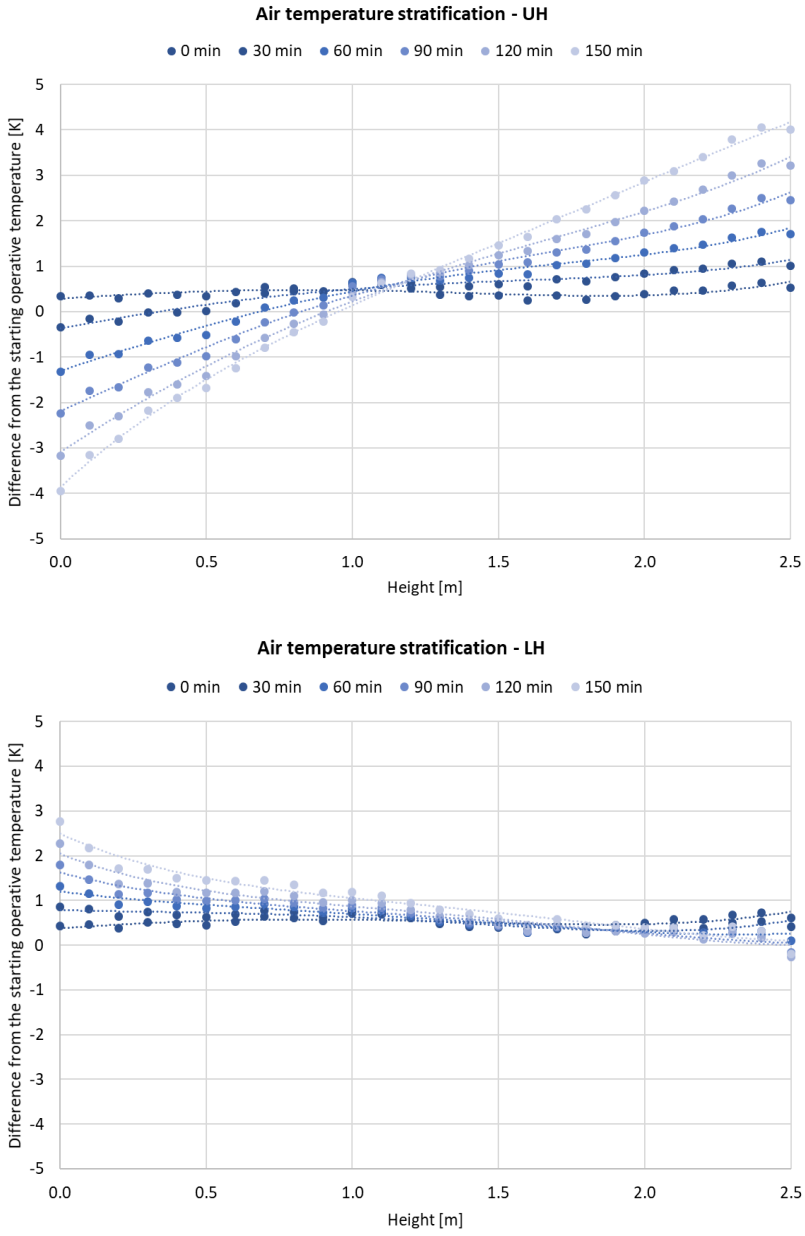

Figure 5.18 - Air temperature stratification during the two kinds of tests.

For the air temperature, the mean values at the end of each 30-minute step were calculated for each sensor. As can be seen in Figure 5.18, a much higher stratification was found at the end of the tests with heated ceiling and cooled floor, in which the air temperature difference between the higher and lower sensors was about 8 K, against about 3 K in the tests with cooled ceiling and heated floor. The air temperature difference between the neck (1.10 m) and the ankles (0.10 m) was equal to 3.8 K and 1.1 K respectively.
The globe temperatures and the air temperature at the same height are plotted in Figure 5.19. In the UH tests the air temperature at 1.10 m height is almost constant, while the globe temperature is slightly increasing. At 0.60 m and 0.10 m height the temperatures are progressively decreasing, up to 1.5 K and 3.5 K respectively from the beginning of the test. In the LH tests the globe temperature at 1.10 m height is almost constant, while the air temperature is slightly increasing. At 0.60 m height the air and globe temperatures of about 0.7 K.

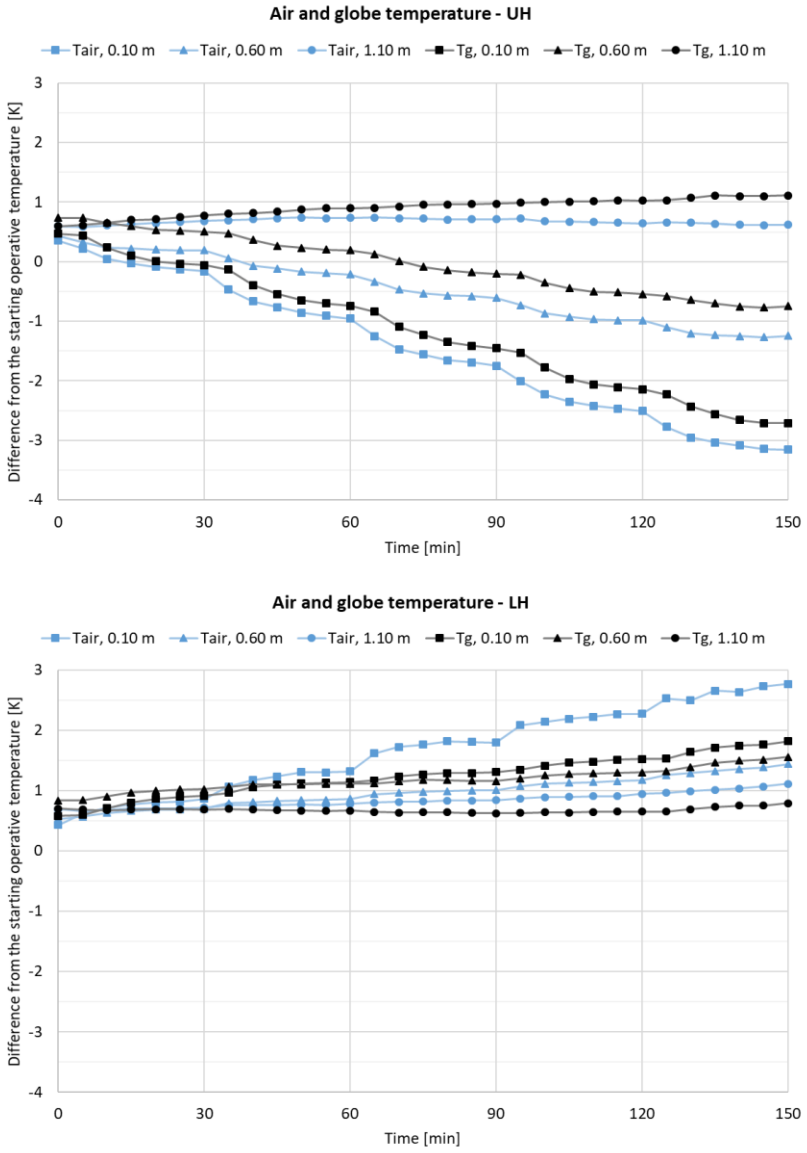

Figure 5.19 - Air and globe temperature during the two kinds of tests.

About the radiant temperature asymmetry, the calculated increments (Table 5.3) are verified. As already seen in the examples in Figure 5.15 and Figure 5.17, after 10 minutes from the surface temperature change the desired radiant asymmetry is reached.
As regards the analysis of the answers to the questionnaires, only the last 10 minutes (3 questionnaires) of each step of the test were taken into account. The option which was chosen by each test subject in at list 2 of the 3 questionnaires was considered to be the valid one. For the starting time (minute 0), that single answer was considered.
The reported global sensation shows for the UH tests 30% of the subject feeling cool after 30 minutes and 60% after 60 minutes till the end of the test, while for the LH tests 17% after 30 minutes, 33% after 60 minutes and 50% at the end of the test. No relevant percentage of subjects feeling warm and asking for a higher temperature was detected during the two type of tests (Figure 5.20).

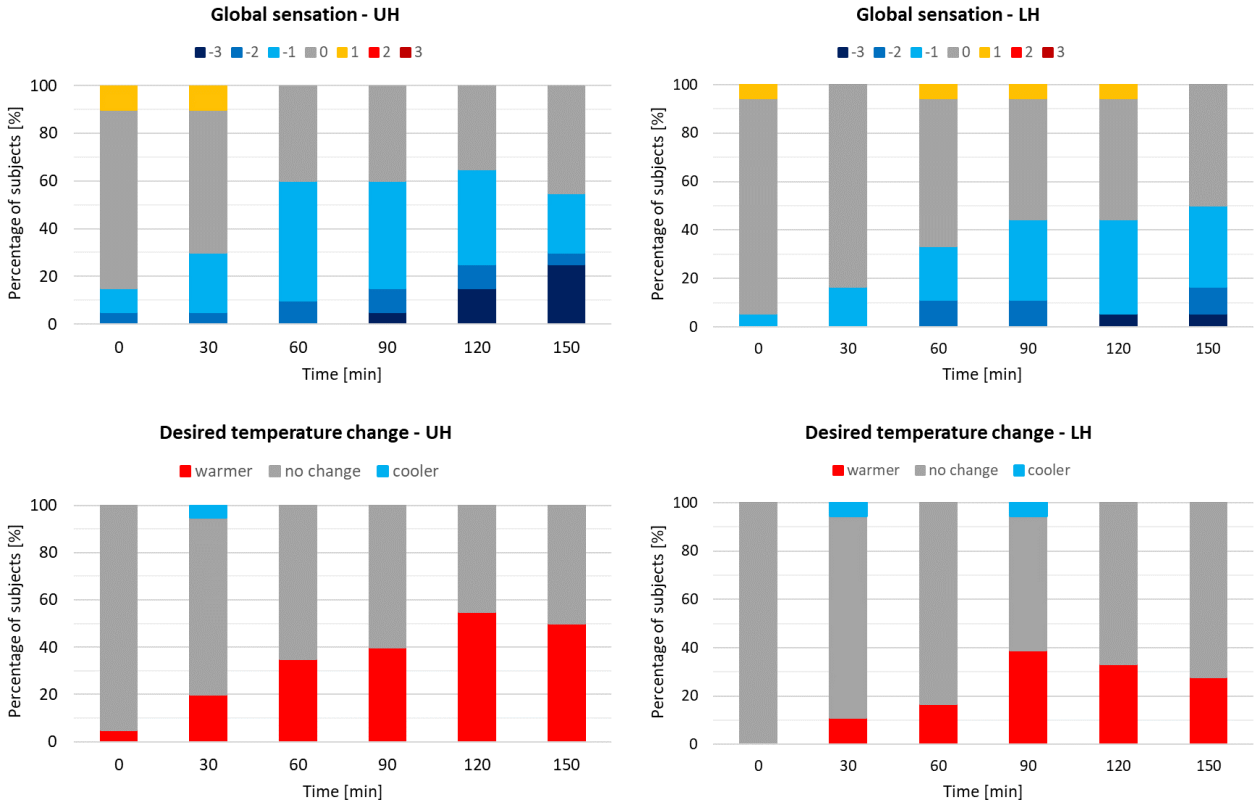

Figure 5.20 - Global sensation and desired temperature change during the two kinds of test.

In Figure 5.21 the local sensations detected by the test subjects are shown. At the end of the UH tests 55% of the subjects felt cool feet, 40% cool arms, 35% cool hands, 30% cool legs, 20% cool head and 10% warm head. At the end of the LH tests 44% of the subjects felt cool arms, 33% cool hands, 22% cool legs and 17% warm feet. It should be noticed that at the beginning of the tests there were some subjects feeling cool or warm on some parts of the body.
As concerns the question asking if any of the local sensations detected were uncomfortable, in the UH tests 30% of the subjects felt uncomfortable at the end of the first step, up to 50% at the end of the test (Figure 5.22). In the LH tests 17% of the subjects felt uncomfortable at the end of the second step, up to 33% at the end of the test.

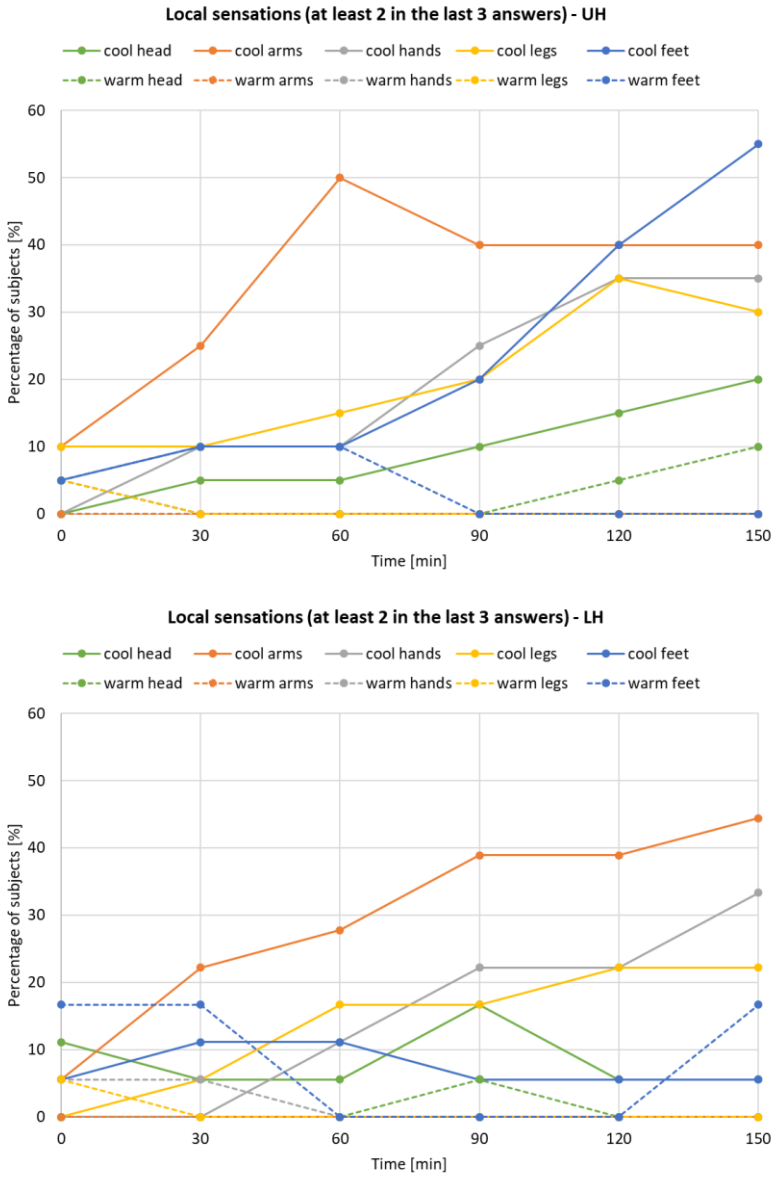

Figure 5.21 - Local sensations detected by the test subjects during the two kinds of test.

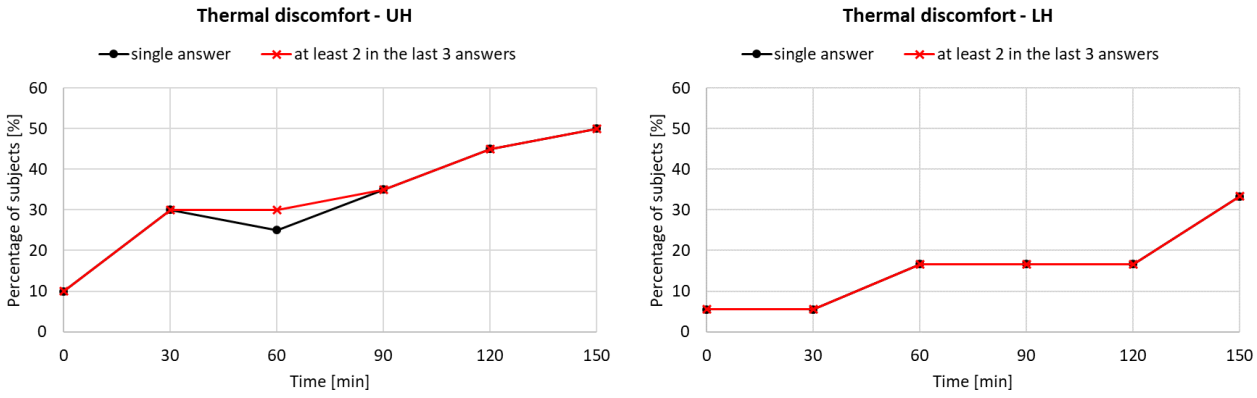

Figure 5.22 - Percentage of subjects feeling thermal discomfort during the two kind of tests.

The local sensations in Figure 5.21 are all the sensations detected by the test subjects, but not necessarily giving discomfort. In Figure 5.23 only the local sensations of the subjects feeling uncomfortable are collected. In the last 2 steps of the UH tests the cool sensation was, for an important part of the subjects, a global problem. Moreover, a cool sensation on the arms was sensed by the majority of the subjects feeling uncomfortable during the entire test. Cool feet complaint was increasing throughout the test, because of the contact with the floor, whose temperature was lowered: in most of the tests the final surface temperature of the floor was equal to 14.5 °C.

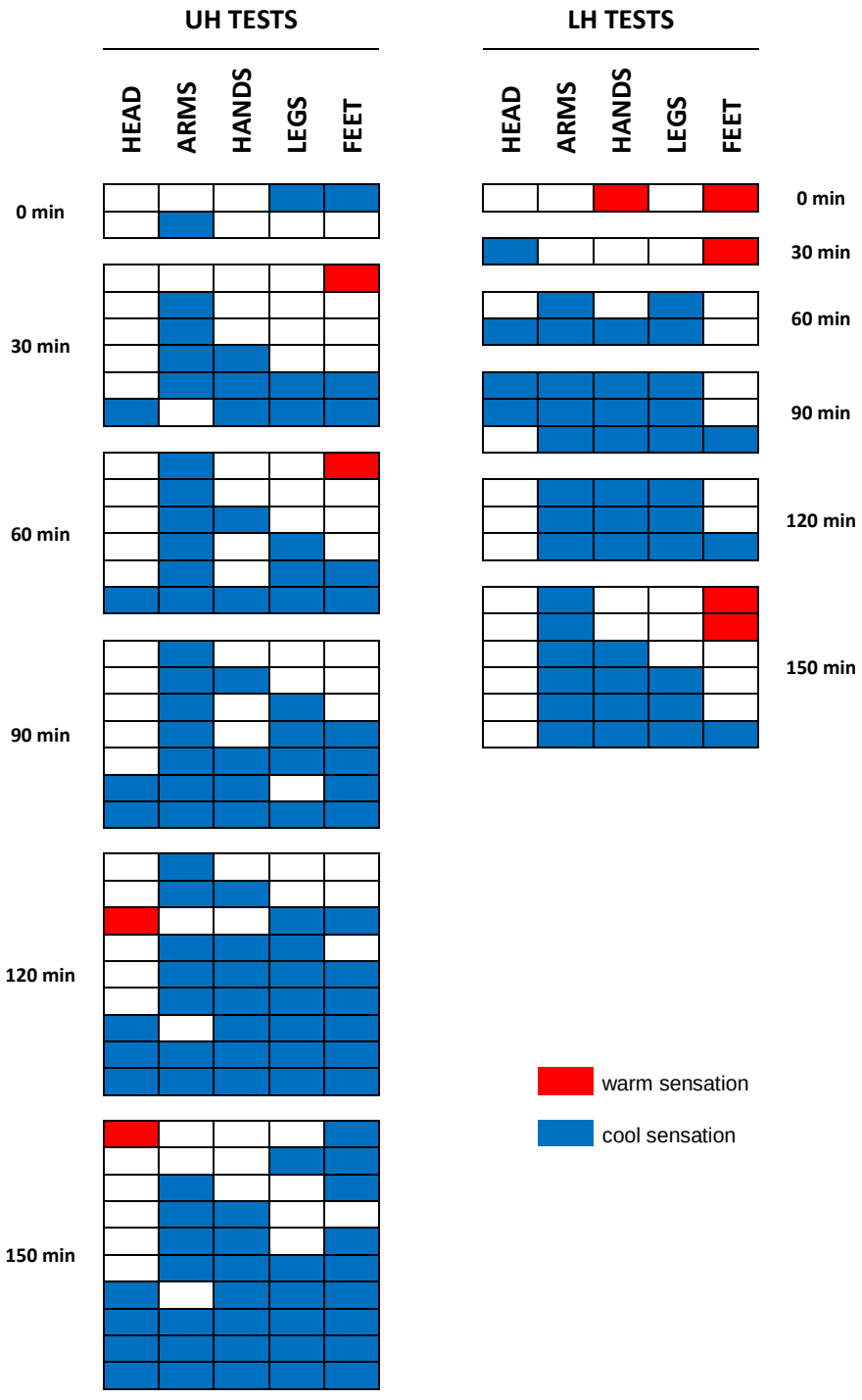

Figure 5.23 - Local sensations detected by the test subjects who felt uncomfortable.

It is interesting to notice that, in the last two steps of the UH tests, when the radiant temperature asymmetry was equal to 9.1 °C and 11.3 °C, only one person was feeling cool feet and warm head at the same time. In the LH tests the cool arms are the main problem, but also cool hands and cool legs are common. At the end of the tests 2 subjects felt warm feet, but no cool sensation at the head; the surface temperature of the floor was 29.0 °C in one case and 29.5 °C in the other.
As concerns the perceived air quality, positive answers were given in most of the cases, giving an average value between neutral and fresh. An increasing freshness was detected during both the tests, with a slightly better perceived air quality in the LH tests. For the subjects feeling uncomfortable the air freshness was, on average, even better than for the other ones.
Finally, an analysis on the differences between males and females was carried out, since the number of female test subjects was much lower than the number of males. The results for the tests with the upper half-room heated and the lower half-room cooled are presented. In these tests the females were 30% of the total subjects (14 males and 6 females). Considering the low absolute value of the female group, the results should be analysed only from a qualitative point of view, without looking at the percentage values. As can be seen in Figure 5.24, females felt cooler than males, despite the starting temperature of each test was chosen by the test subject. Also the intensity of the global sensation appears to be higher and thus they desired a warmer temperature more than in the male group. In the female group there was a subject who desired a warmer temperature at time 0; this is not an error, it was a single answer and she felt neutral from the following answer (5 minutes later) and even slightly warm from the middle of the first 30-minute step.

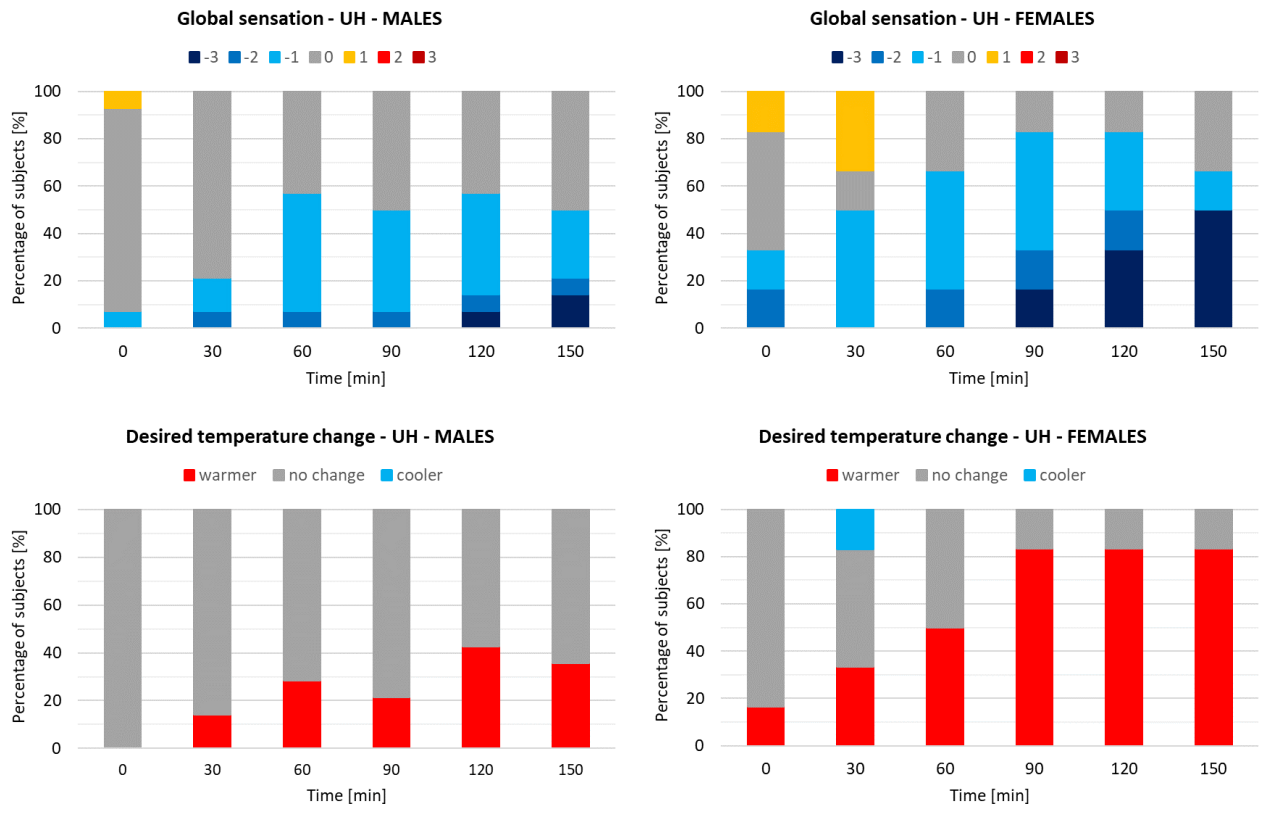

Figure 5.24 - Global sensation and desired temperature change for males and females during the UH tests.

Females were also more sensible from a local point of view (Figure 5.25). At the end of the test more than half of them felt cool on the arms, legs, feet and hands, while less than half of the male subjects detected cool sensations. As a result, the rate of females feeling uncomfortable was higher.

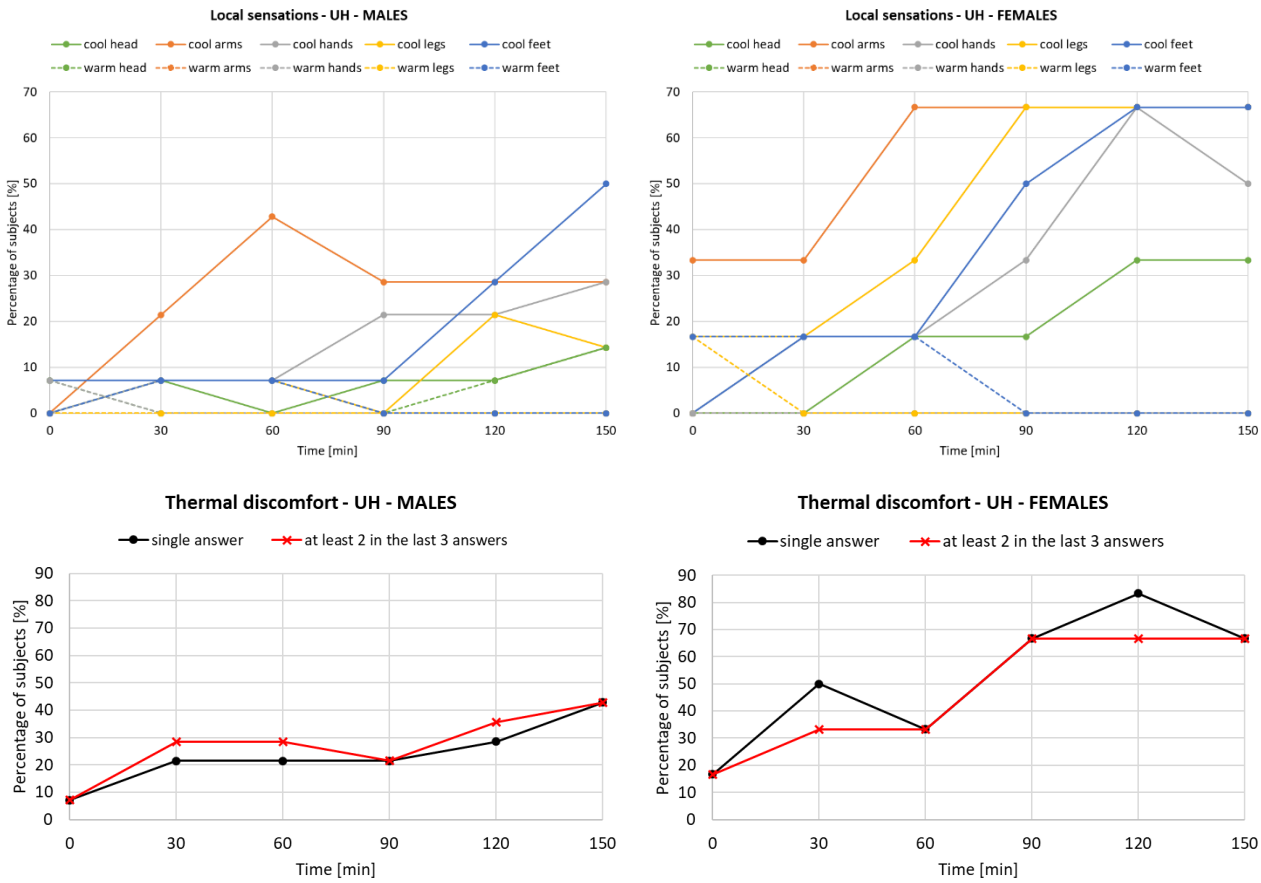

Figure 5.25 - Local sensations detected by males and females and related thermal discomfort during the UH tests.

5.4.5 Additional measures

Besides the investigations with test subjects, further measurements were performed in the test room using an unheated manikin. Two tests were done, one reproducing the UH tests and one LH tests, starting with a uniform temperature of the surfaces equal to 24 °C. During these tests, air velocity measurements were taken placing two thermo-anemometers on the arms of the manikin and one on the back (Figure 5.26). The mean value and the standard deviation of the values measured by the 3 instruments, calculated in the last 5 minutes of each step of the test, are shown in Figure 5.27. In the UH test (heated ceiling and cooled floor), the air velocity was equal to 0.02 m/s during the entire test, while in the LH test it was constantly increasing, going from 0.04 ± 0.02 m/s at the end of the first step to 0.08 ± 0.05 m/s at the end of the last step. Not only the mean value was significantly higher, but there was also a much higher turbulence level (higher standard deviation). This is the reason for the cool sensation on the arms during the LH tests, since the test subjects were wearing long trousers and a T-shirt and so the arms were uncovered.

Figure 5.26 - Position of the anemometers for air velocity measurements.

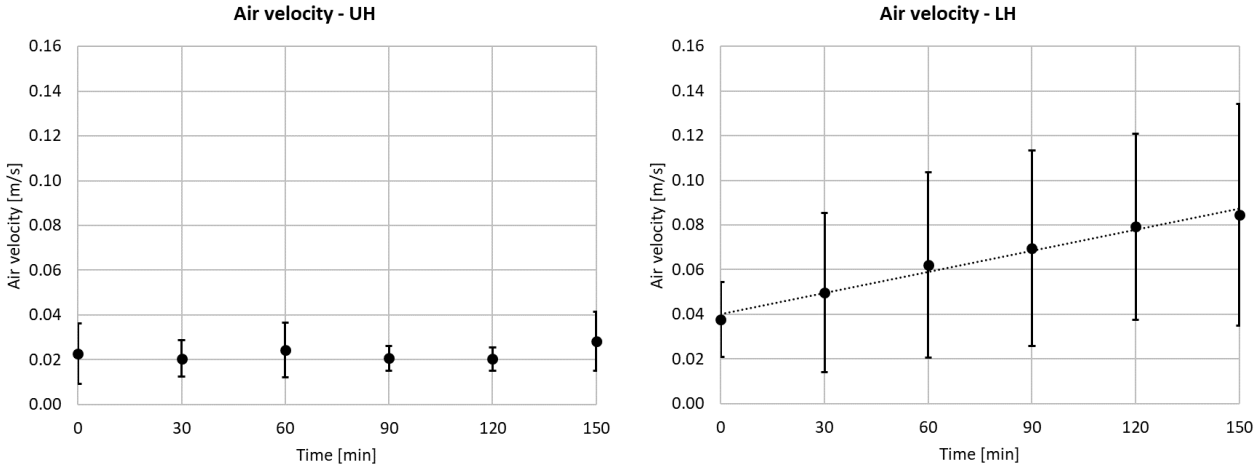

Figure 5.27 - Air velocity (mean value and standard deviation) measured at the height of the arms.

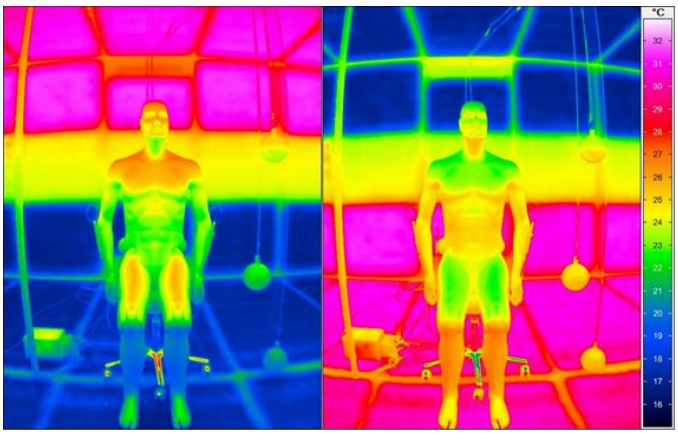

Figure 5.28 - Thermographic images of the final step of the UH test (left) and LH test (right).

A thermography was also performed during the two tests, simply to verify which area of the body are seen from the heated and cooled surfaces of the room. As can be seen in Figure 5.28, the surface temperature of the lower part of the room has a higher influence in terms of angle factor than the surface temperature of the upper part, which is important for the head, the shoulders and the upper legs. During the UH tests the arms were frequently felt cool by the test subjects because of their position and the resulting high view factor with the cooled lower part of the walls.

5.5 CONCLUSIONS AND DISCUSSION

When dealing with radiant heating and cooling surfaces, a particular attention should be paid to the surface temperatures to assure a comfortable thermal environment for the occupants. An important aspect to be taken into account is, especially in buildings with heating/cooling ceilings and high heating/cooling peak loads, the radiant temperature asymmetry. In these buildings occupants could be also in contact or in proximity of a cool/warm floor or wall. An experimental investigation on thermal comfort in a test room with both vertical radiant asymmetry and air stratification was presented in this chapter. Thermal global and local sensations were assessed by means of questionnaires during 38 tests in which the surface temperatures of the upper and lower parts of the room were progressively increased and decreased (+/- 1.5 K every 30 minutes for 2.5 h), while inlet air temperature was kept constant. The starting uniform comfort temperature was chosen by each test subject during a 30-60 minutes first phase. The radiant asymmetry at 0.60 m height was increased of 2.3 K at the beginning of each 30-minute step, up to 11.3 K at the end of the test.
In the tests with the upper half-room heated and the lower half-room cooled (UH) an important stratification was found in the occupied height, with a significant vertical temperature difference (3.8 K) between the neck and the ankles at the end of the test, while in the tests with upper half-room cooled and lower half-room heated (LH) the air temperature was, as expected, more uniform.
As consequence of the position of the heated and cooled surfaces, a constantly increasing air velocity (mean value and turbulence) was also found throughout the LH test, while in the UH test it was constant and negligible.
The operative temperature at the height of the head was almost constant during both of the tests; at 0.60 m height it was slightly increasing during the LH tests, while a drift of about -0.6 K/h occurred during the UH tests. According to a study of Kolarik et al. [107], such a moderate drift (in the range 23.8÷19.0 °C) is sensed by sedentary subjects only after 3-4 hours of exposure and so should not be influent in these tests.
The assessed global sensation showed that:

- in the UH tests 30% of the subjects felt cool after 30 minutes (2.3 K of radiant asymmetry) and 60% after 60 minutes till the end of the test (11.3 K of radiant asymmetry);
- in the LH tests 17% of the subjects felt cool after 30 minutes, 33% after 60 minutes and 50% at the end of the test.

No relevant percentage of subjects feeling warm and asking for a lower temperature was found during the tests.
As regards local sensations:

- at the end of the UH tests 55% of the subjects felt cool feet, 40% cool arms, 35% cool hands, 30% cool legs, 20% cool head and 10% warm head;
- at the end of the LH tests 44% of the subjects felt cool arms, 33% cool hands, 22% cool legs and 17% warm feet.

Because of the detected local sensations:

- in the UH tests 30% of the subjects felt uncomfortable at the end of the first step, up to 50% at the end of the test;
- in the LH tests 17% of the subjects felt uncomfortable at the end of the second step, up to 33% at the end of the test.

No relevant asymmetry problem resulting in opposite sensations on head and feet at the same time was found in the analysis of the answers, while other factors played a significant role. The feet were increasingly felt cool during the UH test, as floor temperature decreased, and uncovered arms were also a problem because of the high angle factor with the lower part of the walls, which was cooled. Uncovered arms were also the more relevant source of discomfort in the LH tests, because of the increasing air velocity.

Significant differences were found in the answers of males and females, who were much more sensible from a local point of view, highlighting the importance of a differentiated analysis with a proper number of female test subjects.

Despite the initial adaptation phase, the effects of the decreasing metabolic rate of the test subjects should probably be taken into account in the data analysis.

These experimental investigations were a very first step towards a better understanding of the complex matter of indoor thermal comfort in buildings with heated/cooled surfaces. Much more investigations are needed to fully understand all the effects on the test subjects and a multidisciplinary approach would be useful to solve some questionnaire-related interpretation matters. More realistic combination of surface temperatures should be analysed to understand the effects of a heated/cooled surface on the perceived thermal comfort and resulting productivity of people. In particular the maximum comfortable ceiling temperature is a crucial point to be investigated, since ceiling systems could be an easy and quite affordable solution in the renovation of existing buildings.

6 A NEW TEST ROOM FOR INDOOR ENVIRONMENTAL QUALITY ANALYSIS

Abstract
Scope of this chapter is to show the first steps of the set-up of a test room and the related control room. The novel test room equipped with radiant systems and fresh air with controlled flow rate, supply temperature and relative humidity. Although so far no results for publications have been produced, the work, time and effort during the Ph.D has been consistent.

6.1 INTRODUCTION

In recent years increased interest have been being paid in the IEQ and hence the group BETA-Lab of the Department of Industrial Engineering of the University of Padova has decided to build up a test room to make future analyses on well-being of people, perception of the indoor environment and productivity together with the Department of Psychology.
For this purpose a room with different set-up is currently under construction and should start operating in autumn 2018. The basic idea behind the room is to investigate different combinations of indoor parameters to check their influence on the perception of the environment by panels of users.
For doing this it has been decided to keep the environment as much neutral as possible so that it looks like more a real office than a test facility. Therefore the instruments which will be installed will be as far as possible limited.
Another important aspect is related to lighting. Existing windows have been maintained and new windows have been installed internally to increase to sound insulation of the façade leaving as unique parameter of the outdoor environment the incoming natural lighting.
Tests will be anyway performed in heating or cooling conditions according to the outdoor environment, i.e. tests will be performed with systems in heating operating conditions in winter and in cooling conditions in summer. All internal surfaces can be independently heated or cooled, but the idea is to control the indoor surfaces to maintain the indoor operating temperature under control during tests. This means that the external wall will be under strict control heated in summer and cooled in winter (as a usual external wall would be) and the other ones can be controlled in an independent way (heated, cooled or maintained at neutral temperature).
Also fresh air can be controlled in temperature in winter time and in temperature and relative humidity in summer time. That means that there is a coil in the outlet of the air handling unit which can heat up the supply air in winter and can cool and dehumidify the air in summer.
Other parameters which are going to be investigated will be the illuminance level and the acoustics in the indoor environment.
The purpose of this chapter is to show the test room first steps (design and partial realization). As a matter of fact this part of the work took much time and required lot of effort during the Ph.D activity, even though no useful results and possible publications could be exploited in this period. First the

concept design has been carried out, then the final detailed design has been produced for a tender which was quite long. Despite the small size of the test room, the amount of companies providing the different components and/or systems was quite huge, thus requiring lots of time and effort in the project management.
Among the companies, the Consortium Q-Rad (Italian consortium of radiant systems producers) was very helpful in collaborating and managing the different companies. Moreover the project is financed in part by TWINNING, a funding program supplied by the Department of Industrial Engineering.

6.2 DESIGN OF THE TEST ROOM

6.2.1 General description

The spaces available for the laboratory were two rooms at the 3rd floor of the headquarter V of the Department of Industrial Engineering at the University of Padova (Figure 6.1 and Figure 6.2). The external wall of the test room is East-Southeast oriented. There is no building in front of the test room which can shade the building or can inhibit the external view.

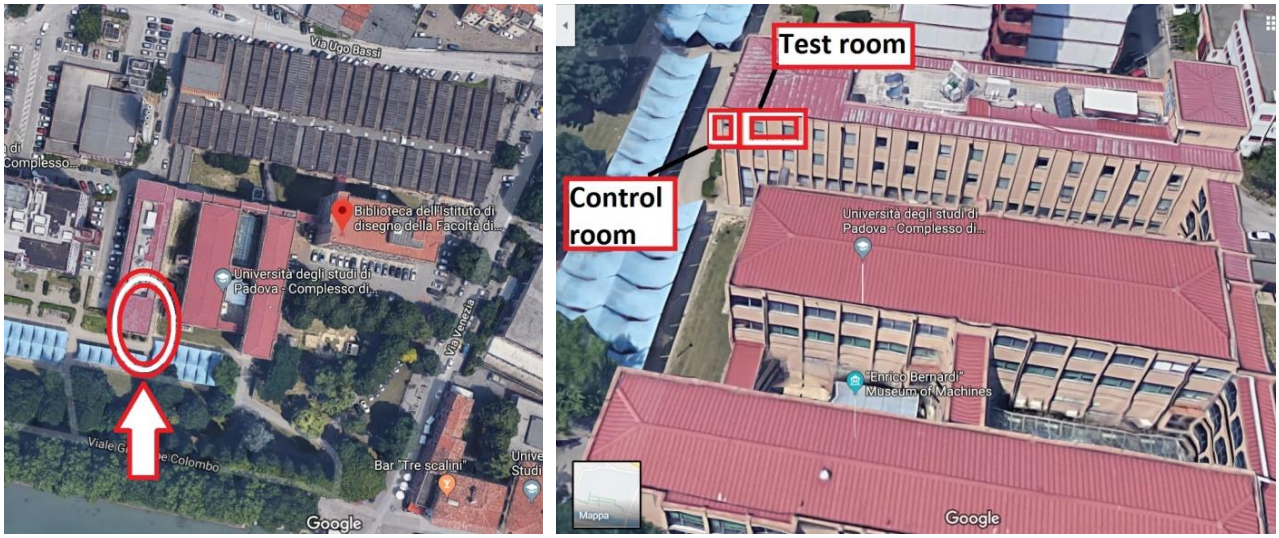

Figure 6.1 - Location of the building where the test chamber and the control room are.

The test room, of about 18 m^2 and 3 m height, is to be equipped with radiant systems on all its surfaces. Dry radiant systems have been chosen for the ceiling and the walls (excluded the area of the windows), while for the floor a radiant system with quartzite and resin screed has been preferred, in order to have a finished surface without the need of a covering. The water loop of each surface is independently controlled thus enabling to reproduce a real room with one or more cold or warm external surfaces and at the same time a heating or cooling surface. The room is also provided with fresh air with controlled flow rate, supply temperature and relative humidity.
The other room (named control room) is used to house the technical equipment, which consists mainly in:

- 2 primary loops, one for heating and one for cooling;
- 6 secondary loops (one for each surface) with 6 mixing and pumping units;
- 3 inertial tanks (heating loop, cooling loop and chiller loop);

- 1 air handling unit and related air ducts;
- pumps and valves for each circuit;
- control system.

The water of the heating loop is heated in the tank by electrical resistances, while cooling is provided by a chiller placed on the roof of the building. Glycol antifreeze is used in the chiller loop, which is separated from the cooling loop by means of a plate heat exchanger.

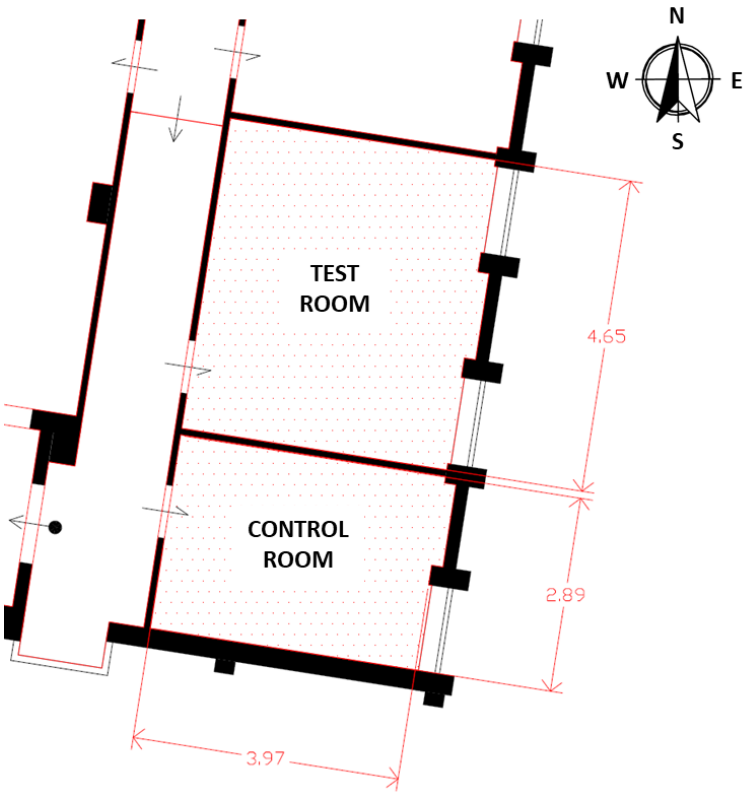

Figure 6.2 - Planimetry of the test room and the adjoining control room.

New windows have been installed on the external dry-wall to avoid problems during the tests, since the pre-existing windows presented low thermal and acoustical performances. The old windows remained on the external side of the wall and the new ones have been installed on the internal side. Between the two windows new Venetian blinds will be installed, ready to be electrically driven and eventually controlled on the basis of the light illuminance inside the room.

The project of the test room has been realized thanks to the collaboration with 18 companies which donated most of the materials needed for the construction (Table 6.1).

Table 6.1 - Materials donated by companies.

Companies	Materials provided
6	radiant panels of the walls,ceiling and floor, manifolds, connections and pipes
1	quartzite and resin screed of the floor
1	pipes and connections for the circuits in the control room and for the chiller loop
1	manifolds for the heating and cooling primary loops
1	mixing units, pumps, valves, control system
1	chiller
1	heat exchanger for the chiller loop
1	water treatment products
1	air handling unit
1	air ducts, silencers, plenum, shutters, linear slot diffusers, grilles
1	windows
1	Venetian blinds
1	mineral wool, structural frames, gypsum boards, finishing materials

6.2.2 Radiant surfaces

The design of the radiant surfaces has been be the most critical and challenging phase of the entire project. Dry systems were chosen (except for the floor), and in the case of the external wall the presence of the windows made particularly difficult to find panels with a size which fits the available space. Moreover, it was not possible to choose the same manufacturer for the modules of all the walls since the material was donated. This implicated to deal with 6 different systems which had different pipe diameters (the pipes inside this kind of panels are not standardised), different connectors, different dimensions of the panels, different layout of the structure behind the panels and different laying rules. In this section the layout of the panels and of the hydronic connections of each surface of the room is presented.

Table 6.2 - Main technical data of the floor radiant system.

Insulation panels	11 mm minimum thickness + 16 mm clew 1420 x 890 mm 0.034 W $m^{-1} K^{-1}$
Screed	19 mm maximum thickness (3 mm above the clew) 1.1 W $m^{-1} K^{-1}$
Pipe diameter	external 10.5 mm, internal 8.0 mm
Loops	5 loops, for 212 m of pipes with a spacing of 9 cm
Thermally active surface	17.2 m^2

As regards the floor, a radiant system with quartzite and resin screed has been chosen. Its main technical data are listed in Table 6.2. The distinctive trait of this system is the very low thickness of the screed above the clew, which is only 3 mm.
Since the dry walls must be installed after the floor, a reduced available surface has been considered for the position of the pipes. The resulting thermally active surface is 17.2 m^2 with 5 loops. The manifold has been placed in the control room because in the test room there was no space available on the walls. The layout of the floor radiant system can be seen in Figure 6.3.

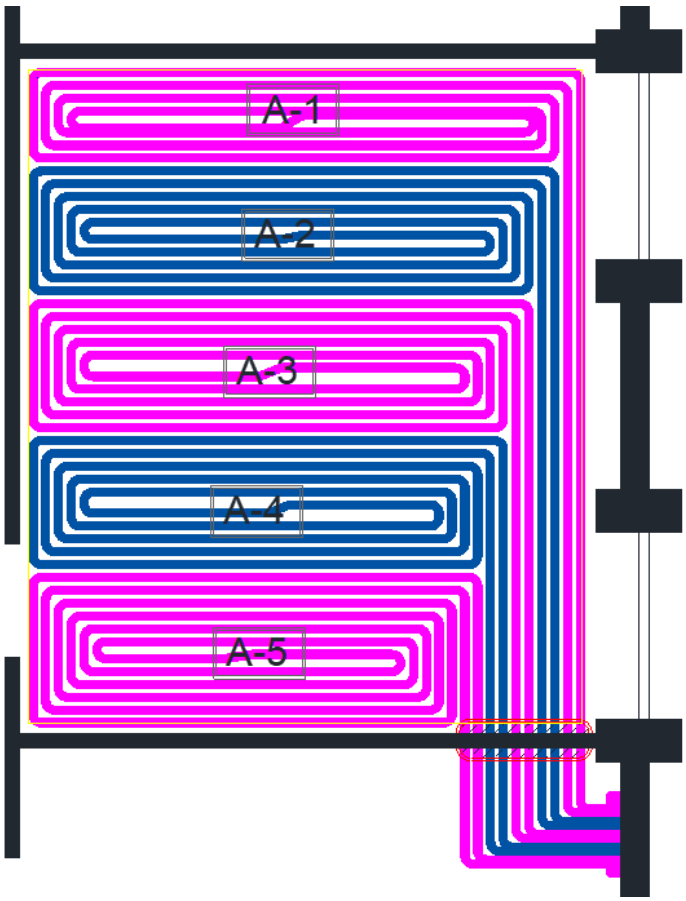

Figure 6.3 - Layout of the radiant floor system.

As regards the ceiling, a system made of plasterboard panels coupled with insulation and aluminum plate diffusers has been chosen. The main technical data are listed in Table 6.3.
The panels are to be screwed on a structure of metal profiles hang to the ceiling and can be drilled in some marked position for placing spot lights with a diameter of maximum 10 cm. The position of the panels has been studied to allow the positioning of 2 linear slot diffusers near the North wall. The resulting layout of the ceiling radiant system can be seen in Figure 6.4.
The thermally active surface is about 13 m^2, i.e. the 75% of the surface of the ceiling (considering the surface of the new room). The panels are supplied by two loops and the related manifold is placed on the ceiling of the control room.

Table 6.3 - Main technical data of the ceiling radiant system.

Panel stratigraphy	12.5 mm plasterboard (0.25 W m^{-1} K^{-1}) 0.04 mm aluminum plate diffuser (200 W m^{-1} K^{-1}) 40 mm EPS (0.033 W m^{-1} K^{-1})
Panel pipe diameter	external 8 mm, internal 6 mm
Distribution pipe diameter	external 20 mm, internal 16 mm
Loops	2 loops supplying 5 and 4 panels
Panel dimensions	6 panels 600 x 2400 mm 3 panels 1200 x 1200 mm
Thermally active surface	12.96 m^2

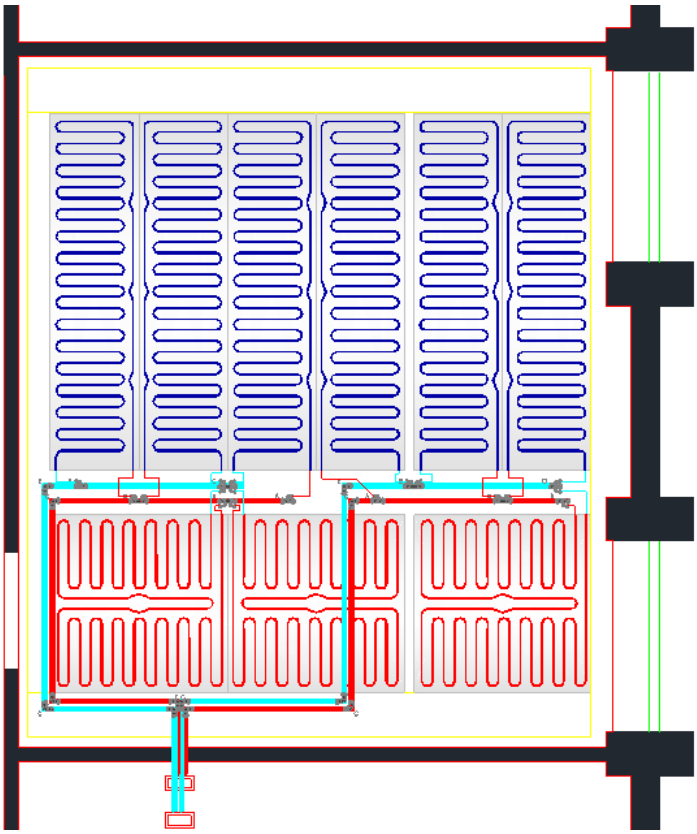

Figure 6.4 - Layout of the radiant panels of the ceiling and hydronic connections.

Dry radiant panels have been used also for the walls of the test room. The stratigraphy and dimensions of the panels and the dimensions of the pipes inside the panels are listed in Table 6.4. The positions of the panels on each wall, which can be seen in Figure 6.5, has been defined taking into account the space needed by the exhaust air grilles and by the new electrical system (light switches, wall sockets, data network access points, etc). The layout of the hydronic connections is also shown: for each wall an independent circuit has been realized using pipes with an external diameter of 20 mm which connect the radiant panels according to the Tichelmann system. The connections have been realized from the upper side of the modules, except for the modules of the external wall, which have been connected from the lower side, with the pipes placed in the recess

behind the dry wall. As already seen in Table 6.4, the panels of the South and West walls are not pre-insulated, thus mineral wool insulation (5 cm thick) has been placed behind them. Mineral wool has been also used to fill the recess behind the external dry wall, between the vapor barrier on the rear part of the radiant panels and the vapor barrier placed on the internal side of the concrete wall.

Table 6.4 - Main technical data of the radiant panels installed on the walls.

Surface	Panel dimensions [mm]	Number of panels	Active surface [m^2]	Pipe diameter ext / int [mm]	Stratigraphy of the panel
North wall	1200 x 2000	3	7.20	10 / 7.4	15 mm plasterboard 35 mm EPS with graphite
East wall	600 x 2000 1000 x 1200	3 2	6.00	8 / 6	15 mm plasterboard 30 mm EPS
South wall	625 x 2000	6	7.50	9.9 / 7.7	15 mm plasterboard
West wall	625 x 2000	4	5.00	10.1 / 7.9	15 mm plasterboard

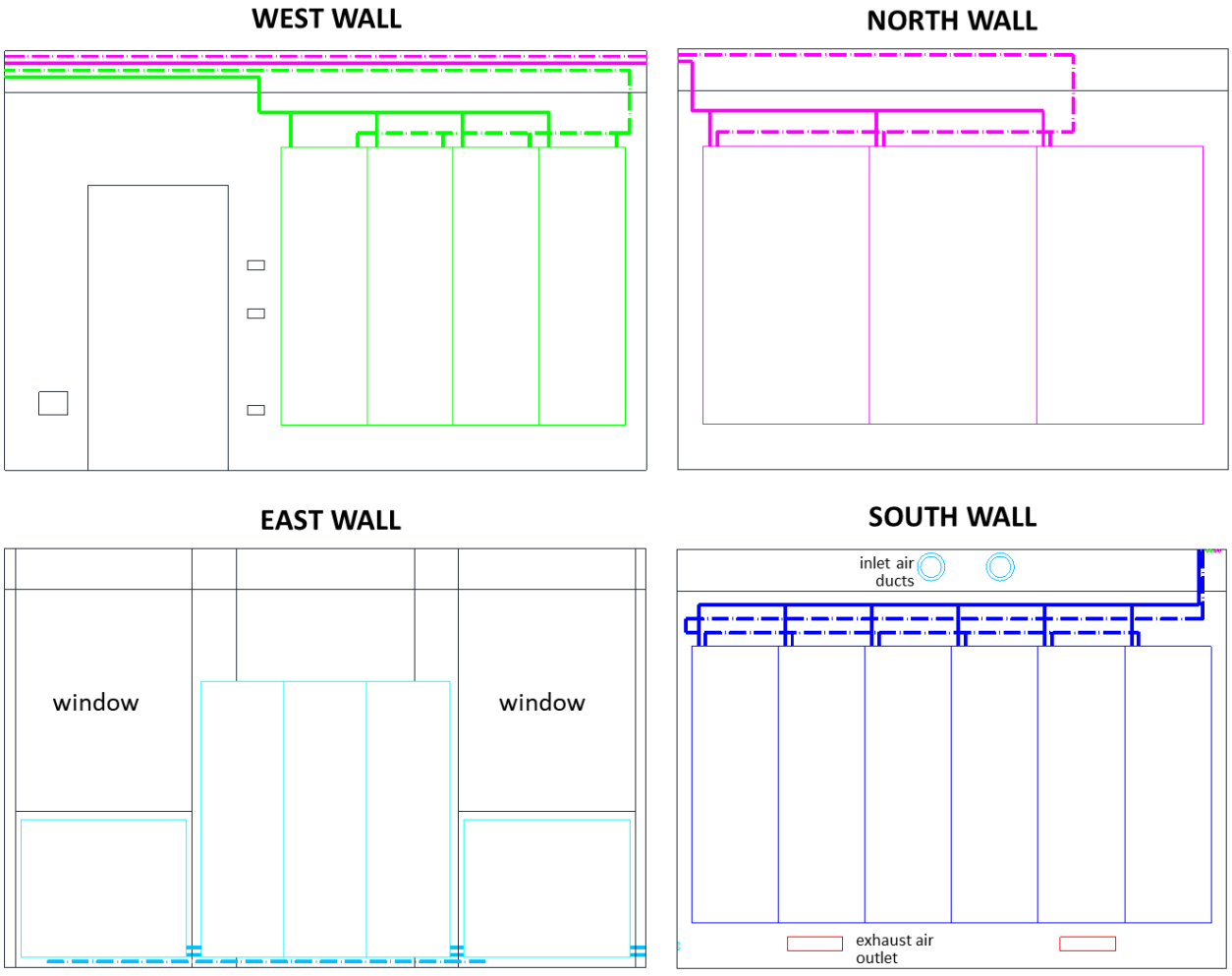

Figure 6.5 - Layout and hydronic connections of the radiant panels on the walls.

Usual design conditions of the radiant systems cannot be defined in a test room like this, since there is no heating or cooling load to be supplied. As a matter of fact, many combinations of temperature for the radiant surfaces are possible, with some of the surfaces heated and some cooled at the same time and other surfaces at neutral temperature. Hence the boundary conditions have to be set for checking all possible tests which can be performed for heating and cooling, looking at minimum and maximum allowable temperature which in case can be exceeded.
Herein the results of the calculation of the mass flow rate of each radiant surface is shown only for the extreme conditions of operation. For winter investigations, a maximum surface temperature of 40 °C has been considered, except the floor surface which was considered at 29 °C. For summer investigations, a minimum surface temperature of 16 °C has been considered.
The mass flow rate can be calculated as:

$$\dot{m}_w = \frac{q_u S_p}{c_w \Delta T_w}\left(1 + \frac{R_i}{R_e} + \frac{T_i - T_e}{q_u R_e}\right) \quad (6.1)$$

where S_p is the radiant surface, T_i is the indoor temperature, T_e is the temperature of the space behind the radiant surface, R_i is the thermal resistance of the layers between the pipe and the indoor temperature and R_e is the thermal resistance of the layers between the pipe and the temperature of the adjacent space, as described in EN 1264-3 [108]. In the calculation of R_i and R_e also the heat transfer resistance on the surface must be computed, according to Table 6.5.
The thermal power P_w is then calculated as:

$$P_w = S_p(q_u + q_l) = \dot{m}_w c_w \Delta T_w \quad (6.2)$$

The calculated mass flow rate and thermal power in the above defined reference conditions can be seen in Table 6.6 and Table 6.7.

Table 6.5 - Heat transfer resistances on a heated or cooled radiant surface ($R_{\alpha,i}$) and on the rear surface of the same building structure ($R_{\alpha,e}$).

	Heated surface		Cooled surface	
	$R_{\alpha,i}$	$R_{\alpha,e}$	$R_{\alpha,i}$	$R_{\alpha,e}$
Floor	0.093	0.170	0.154	0.100
Ceiling	0.154	0.100	0.093	0.170
Internal wall	0.125	0.130	0.125	0.130
External wall	0.125	0.040	0.125	0.040

Table 6.6 - Mass flow rate and thermal power evaluation for heated surfaces in winter.

		Floor	Ceiling	North wall	East wall	South wall	West wall
ΔT_w	[°C]	5	5	5	5	5	5
T_i	[°C]	20	20	20	20	20	20
T_e	[°C]	20	-5	20	-5	20	20
T_s	[°C]	29	40	40	40	40	40
q_u	[W m^{-2}]	97	130	160	160	160	160
R_i	[m^2 K W^{-1}]	0.101	0.204	0.149	0.149	0.135	0.135
R_e	[m^2 K W^{-1}]	1.008	1.690	1.587	3.612	1.663	1.663
	[kg h^{-1}]	327	357	217	179	223	149
P_w	[W]	1903	2080	1260	1041	1297	865

Table 6.7 - Mass flow rate and thermal power evaluation for cooled surfaces in summer.

		Floor	Ceiling	North wall	East wall	South wall	West wall
ΔT_w	[°C]	3	3	3	3	3	3
T_i	[°C]	26	26	26	26	26	26
T_e	[°C]	26	34	26	34	26	26
T_s	[°C]	16	16	16	16	16	16
q_u	[W m^{-2}]	65	108	80	80	80	80
R_i	[m^2 K W^{-1}]	0.162	0.143	0.149	0.149	0.135	0.135
R_e	[m^2 K W^{-1}]	0.938	1.760	1.587	3.612	1.663	1.663
	[kg h^{-1}]	388	450	180	147	186	124
P_w	[W]	1356	1572	630	513	649	432

6.2.3 Hydronic system

As can be seen in Figure 6.6, the radiant panels of the 6 surfaces of the test room are supplied by means of 6 secondary loops, each equipped with its own mixing and pumping unit. Upstream 4 ball valves allow to manually commute between heating and cooling. The 2 primary loops are provided with modular manifolds made of reinforced polyamide and equipped with micrometric flow regulator and flow-rate meter for each circuit. Not only the radiant panels, but also the air handling unit is supplied by the manifolds.

The heating loop has a tank of 200 litres with 4.5 kW of electric heaters. The electrical resistance has been chosen to allow a short time of pre-heating before the start of the tests. The time needed to warm up the water in the tank from the initial temperature T_{in} of 20 °C (air temperature inside the control room in winter) to different final temperatures T_{fin} is shown in Table 6.8, calculated according to the following equation:

$$t = \frac{c_w V \left(T_{fin} - T_{in}\right)}{P_{el}} \qquad (6.3)$$

Table 6.8 - Evaluation of the time needed to heat the water in the hot tank.

P_{el} [kW]	V [l]	T_{fin} [°C]	T_{in} [°C]	t [h]
1.5				5.4
3.0	200	55	20	2.7
4.5				1.8
1.5				4.7
3.0	200	50	20	2.3
4.5				1.6
1.5				3.9
3.0	200	45	20	1.9
4.5				1.3

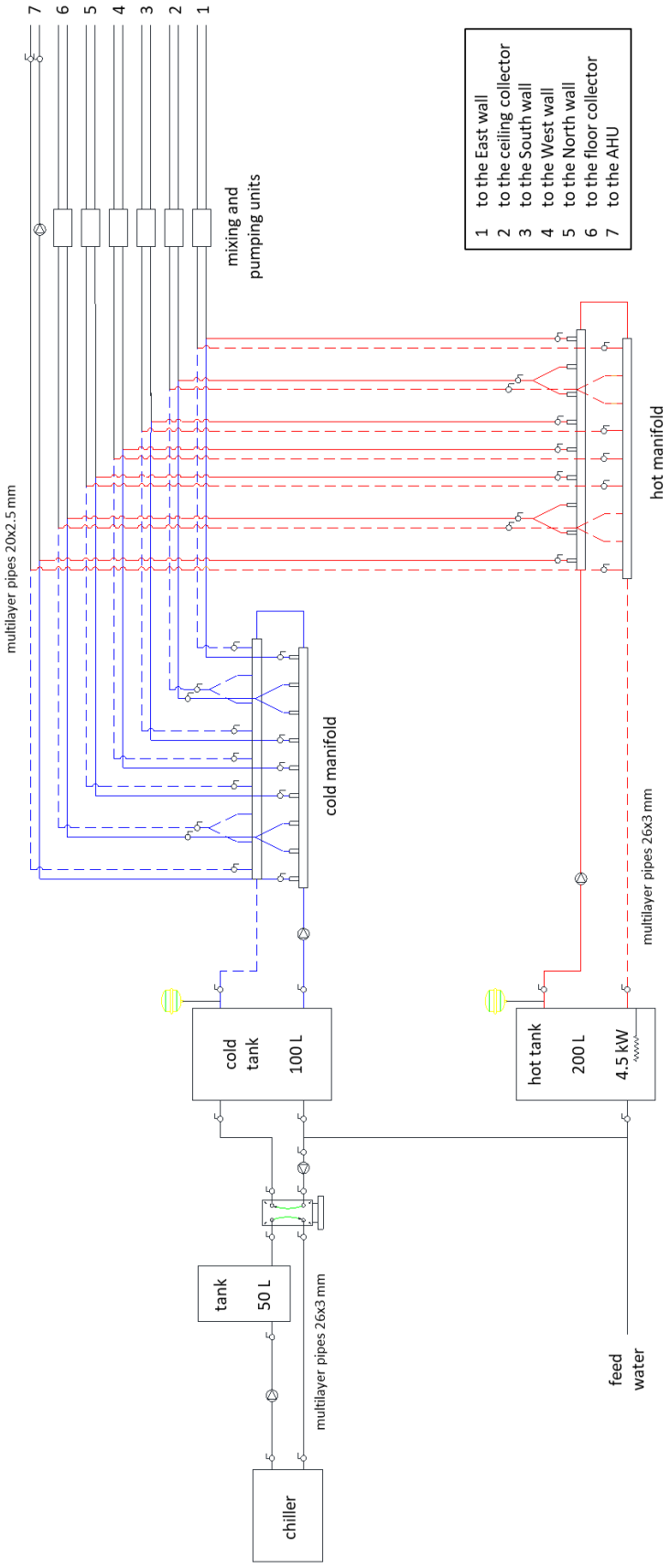

Figure 6.6 - The hydronic system of the test room.

The cooling loop has a tank of 100 litres and is de-coupled from the chiller loop by means of a plate heat exchanger. The chiller loop is 80 m long and has an inertial tank of 50 litres, for a total volume of 90 litres. This loop is treated with a dosage of 30% of an inhibited antifreeze, formulated to help control corrosion and to provide frost protection down to -15 °C.
The primary and secondary circuits, included the hot and the cold tanks, have a volume of 375 litres and must be treated with a dosage of 1% of inhibitor, which provides protection against limescale and corrosion, and a dosage of 0.3% of sanitizer and biocide, which prevents the development of bacteria and fungi and their associated problems.
Expansion vessels, safety valves, air purge valves and filters complete the system, even if not shown in Figure 6.6 - The hydronic system of the test room.Figure 6.6.
More than 20 cockpits for thermometer probes (Pt 500 will be used) will be installed for properly monitoring the temperatures of the radiant circuits and in other important points of the hydronic system.

6.2.4 Aeraulic system

The test room is provided with fresh air with controlled flow rate, supply temperature and relative humidity. The following operation modalities are possible for the chosen air handling unit:

- fresh air ventilation;
- winter integration;
- dehumidification and/or summer integration;
- free cooling or free heating.

It uses the outside air only, it is equipped with a high-efficiency counter-current heat exchanger (about 90%) for heat recovery from exhaust air and with a by-pass connection for free-cooling, controlled by an NTC probe placed in the outdoor air intake duct. It ensures summer dehumidification and can also integrate heating and cooling, operating as a heat pump. It consists of three separate modules, two fan units and one recovery/handling unit, which can be installed close together or in different positions, depending on the space availability.

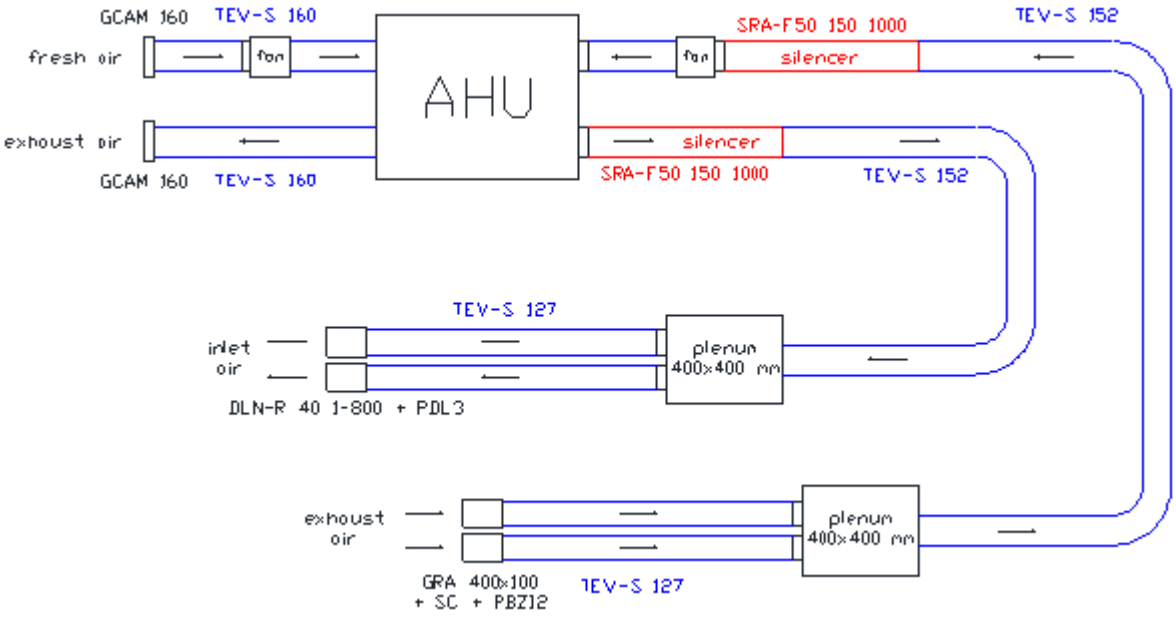

Figure 6.7 - The aeraulic system of the test room.

The selected air handling unit can provide an air flow rate from 80 to 200 m3h-1 to the test room, ensuring an air change from 1.7 h-1 to 4.2 h-1. It is independently controlled by a TH controller user terminal but can also be controlled by an external device.

The components of the aeraulic system can be seen in Figure 6.7. Silencers are installed between the AHU and the test room to reduce noise transmission. The distribution of air is done through flexible insulated air ducts with diameters of 160 mm and 125 mm and distribution boxes. Two linear slot diffusers (800x100 mm) equipped with air shutters and placed on the ceiling are used for supply air, while two grilles (400x400 mm) are placed on the lower part of the opposite wall for exhaust air extraction. The dimensions of the diffusers and the grilles ensure low air velocity near the inlet and extraction areas in the test room. The layout of the aeraulic system is shown in Figure 6.8.

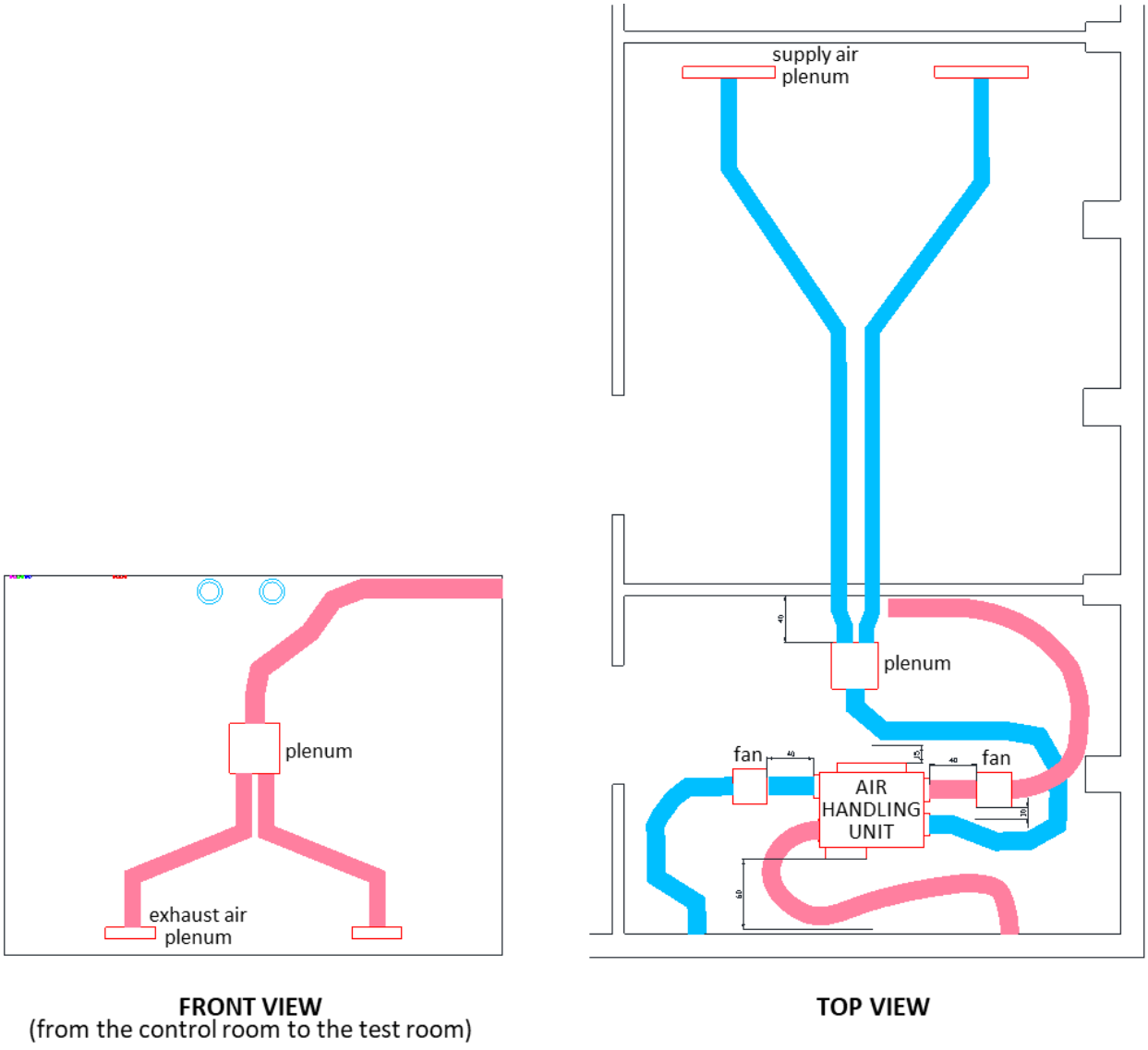

Figure 6.8 - Layout of the aeraulic system.

6.3 BUILDING UP OF THE TEST ROOM

The works for building up the test room started before the summer 2018 and will be completed in October 2018.
Two images of the room before starting the works can be seen in Figure 6.9. After the clear out of the room, the first work to do was the radiant floor system. As can be seen in Figure 6.10, the strip was laid over the entire wall perimeter after demolishing the plasterboard columns of the external wall. Then the insulation panels were laid and the pipes were placed according to the layout defined in the design phase. Particular attention was given to the crossing point between the test room and the control room, where the manifold of the floor circuits was placed. The quartzite and resin screed was then prepared and levelled, with a height of only 3 mm above the clew of the insulation panels. Immediately after the net and the first coat of resin were laid, and just after 24 hours of ripening the first finishing coat of resin was laid. A second finishing coat of resin was completed on the following days.

Figure 6.9 - The room before starting the works.

Figure 6.10 - Installation of the floor radiant system and making of the resin flooring.

Then the construction of the dry walls started, placing the metal profiles on the existing walls and screwing the panels on the profiles (Figure 6.11). At the same time the electric system of the room was arranged.

Figure 6.11 - Construction phase of the radiant dry walls.

Particular attention was given to the external wall. As can be seen in Figure 6.12, the hydronic connections were placed behind the panels because the space under the windows was limited. A vapor barrier was placed on the external existing concrete wall, then all the space behind the dry wall was filled with mineral wool insulation and another vapor barrier was placed immediately behind the radiant panels (Figure 6.13).
In Figure 6.14 the external wall after the installation of the new internal windows is shown.

Figure 6.12 - Details of the external wall: position of the hydronic connections, insulation of the recess under the windows and electrical set-up for the new Venetian blinds which will replace the old ones which are still present.

Figure 6.13 - Details of the external wall: insulation of the space behind the dry wall, with a vapor barrier placed on the existing external concrete wall and a vapor barrier immediately behind the radiant panels.

Figure 6.14 - The external wall after the installation of the new windows.

The space behind the radiant panels installed on the internal walls was also filled with mineral wool insulation, except the panels of the North wall which were pre-insulated.
In Figure 6.15 two views of the test room are shown, with the hydraulic connections of two walls completed. Then the drills for the air extraction under the panels of the South wall and for the supply air from the ceiling were done. The air ducts were hung on the ceiling, waiting for the installation of the profiles and radiant panels which will be placed just after the dry walls of the room will be completed. After the hydronic connection of the ceiling, the hydronic system for the production and supply of warm and cold water will be completed in the adjacent control room.

Figure 6.15 - Views of the room with the hydraulic connections of two walls completed.

6.4 FUTURE RESEARCH ACTIVITY

The first activity which will be carried out will be the starting up of the system and the evaluation of the time needed to reach steady state conditions as well as how these are maintained over the time. Measurements by infrared camera will be taken with many combinations of surface temperatures in order to check how the different surface temperatures affect indoor operative temperature. The set-up of the room will include measurements of air velocity, temperature and turbulence under different flow rates in order to avoid draft risk problems in the rooms.
At the same time a correlation between supply temperature of the water and surface temperature will be carried out. A suitable number of thermocouples will be installed in active and passive surfaces of each wall, as well as inner surface of windows. The view factor model already used for

the TUD test chamber [103] will be considered to calculate the view factors between the human body and the different surfaces in various positions inside the room. The measured mean radiant temperature with and without occupants will be compared to the one calculated through the measured surface temperature and the calculated view factors.
At the same time a model for the hydronic circuit will be developed in order to find the best strategies to control the temperatures of the warm and cold water in the two tanks, as well as the proper mixing temperatures to supply the water in all the circuits. Also the AHU operation will be tested and tuned as a function of the different external conditions (temperature and relative humidity).

Once tuned the control of the room, the work including panels of occupants will start. At first the test room will be used to evaluate, by means of questionnaires, psychological and productivity tests, the acceptability of defined factors of local thermal discomfort and their influence on human productivity. As regards thermal comfort, an argument which needs in-depth investigations is surely the radiant temperature asymmetry. In particular the analysis on comfort and productivity of people under heated ceiling deserves a prominent attention.
The idea is to study the radiant asymmetry of a room with warm ceiling and one or more cold walls or cold floor, along with the acceptability for people of a possible discomfort. For this purpose, a working space with 2-4 people should be reproduced in the test room. The possibility to plan the activities as complementary studies to the ones in TUD and/or other research centres will be taken into account.

For this purpose, a preliminary simplified analysis was done to evaluate the value of radiant temperature asymmetry which can be reached with assumed surface temperatures. As well known, in ISO 7730 the maximum radiant asymmetry to avoid discomfort for the occupants is set to 5 °C.
First of all the angle factors of all the surfaces from a point in the centre of the room at 0.6 m height were calculated according to [103]. In Table 5.1 the overall angle factors f are listed, along with the angle factors f_l and f_u of the lower and upper part of the room, i.e. the surfaces of the room below and above a plane at 0.6 m height.

Table 6.9 - Angle factors for the evaluation of the mean radiant temperature and the vertical radiant temperature asymmetry in the centre of the room at 0.6 m height

Surface of the room	f	f_l	f_u
North wall	0.1005	0.0530	0.1480
West wall	0.1356	0.0746	0.1966
South wall	0.1005	0.0530	0.1480
Windows on East wall	0.0302	-	0.0604
East wall (windows excluded)	0.1054	0.0746	0.1362
Ceiling	0.1555	-	0.3109
Floor	0.3723	0.7447	-

The mean radiant temperature T_{mr} can be calculated from the temperature of the surfaces T_s as:

$$T_{mr} = \sum f\, T_s \qquad (6.4)$$

The radiant temperature asymmetry ΔT_{pr} can be calculated as:

$$\Delta T_{pr} = T_{pr,u} - T_{pr,l} = \sum f_u T_{s,u} - \sum f_l\, T_{s,l} \qquad (6.5)$$

Surface temperature values are assumed for all the surfaces of the room except for the ceiling which has to provide the heating load depending on the other surface temperatures. The other walls and the floor have an imposed surface temperature, while for the windows the external outdoor air has been fixed, due to the fact that they are not active. Hence the heat exchanged from each surface temperature with indoor air can be calculated, using the heat transfer coefficients of Table 6.5; for the windows, the U-value (1.5 ° W m^{-2} K^{-1}) and the outdoor temperature are used. The thermal load which should be provided by the ceiling is then calculated from the heat balance. Thus the temperature of the ceiling is also known through the heat transfer coefficient of the heated ceiling. Knowing all the surface temperatures of the room, the mean radiant temperature and the radiant temperature asymmetry can be calculated using the Equations 6.4 and 6.5.
In the following tables some examples of mean radiant temperature and vertical radiant temperature asymmetry are shown, considering an indoor temperature of 20 °C, three values of surface temperature for the external wall $T_{s,ew}$ (12 °C, 15 °C and 18 °C) and three values of outdoor temperature T_e (0 °C, 5 °C and 10 °C).
In Table 6.10 a surface temperature of 20 °C was considered for the floor $T_{s,f}$ and for the internal walls $T_{s,iw}$. The surface temperature of the windows $T_{s,w}$ and of the ceiling $T_{s,c}$ are calculated. The resulting vertical radiant temperature asymmetry is low, about 2 °C in the worst conditions.
Lowering the surface temperature of the floor to 17 °C results in a vertical radiant temperature asymmetry about 0.5 °C higher (Table 6.11).
If also the internal walls are slightly cooled (to a surface temperature of 19 °C), the ceiling temperature needed to keep the indoor temperature at 20 °C is high and the resulting temperature asymmetry is significant, always higher than 5 °C (Table 6.12).

Table 6.10 - Example of mean radiant temperature and radiant temperature asymmetry with heated ceiling and cooled external wall.

$T_{s,ew}$ [°C]	$T_{s,f}$ [°C]	$T_{s,iw}$ [°C]	T_e [°C]	$T_{s,w}$ [°C]	$T_{s,c}$ [°C]	T_{mr} [°C]	$T_{pr,l}$ [°C]	$T_{pr,u}$ [°C]	ΔT_{pr} [°C]
			0.0	16.3	29.2	20.5		21.6	2.2
12.0	20.0	20.0	5.0	17.2	28.8	20.4	19.4	21.5	2.1
			10.0	18.1	28.4	20.4		21.4	2.0
			0.0	16.3	26.4	20.4		21.1	1.5
15.0	20.0	20.0	5.0	17.2	26.0	20.3	19.6	21.0	1.4
			10.0	18.1	25.6	20.3		20.9	1.3
			0.0	16.3	23.6	20.2		20.6	0.8
18.0	20.0	20.0	5.0	17.2	23.2	20.2	19.9	20.5	0.7
			10.0	18.1	22.8	20.2		20.5	0.6

Table 6.11 - Example of mean radiant temperature and radiant temperature asymmetry with heated ceiling and cooled external wall and floor.

$T_{s,ew}$ [°C]	$T_{s,f}$ [°C]	$T_{s,iw}$ [°C]	T_e [°C]	$T_{s,w}$ [°C]	$T_{s,c}$ [°C]	T_{mr} [°C]	$T_{pr,l}$ [°C]	$T_{pr,u}$ [°C]	ΔT_{pr} [°C]
			0.0	16.3	34.2	20.2		21.6	2.8
12.0	17.0	20.0	5.0	17.2	33.8	20.2	18.9	21.6	2.7
			10.0	18.1	33.4	20.2		21.5	2.6
			0.0	16.3	31.4	20.1		21.2	2.1
15.0	17.0	20.0	5.0	17.2	31.0	20.1	19.1	21.1	2.0
			10.0	18.1	30.6	20.0		21.0	1.9
			0.0	16.3	28.6	20.0		20.7	1.4
18.0	17.0	20.0	5.0	17.2	28.2	20.0	19.3	20.6	1.3
			10.0	18.1	27.8	19.9		20.5	1.2

Table 6.12 - Example of mean radiant temperature and radiant temperature asymmetry with heated ceiling and cold external wall, floor and internal walls.

$T_{s,ew}$ [°C]	$T_{s,f}$ [°C]	$T_{s,iw}$ [°C]	T_e [°C]	$T_{s,w}$ [°C]	$T_{s,c}$ [°C]	T_{mr} [°C]	$T_{pr,l}$ [°C]	$T_{pr,u}$ [°C]	ΔT_{pr} [°C]
			0.0	16.3	38.0	20.4		23.8	6.8
12.0	17.0	19.0	5.0	17.2	37.6	20.4	17.0	23.7	6.7
			10.0	18.1	37.1	20.3		23.6	6.6
			0.0	16.3	35.2	20.3		23.3	6.1
15.0	17.0	19.0	5.0	17.2	34.8	20.2	17.2	23.2	6.0
			10.0	18.1	34.3	20.2		23.2	6.0
			0.0	16.3	32.4	20.1		22.9	5.4
18.0	17.0	19.0	5.0	17.2	32.0	20.1	17.4	22.8	5.3
			10.0	18.1	31.5	20.1		22.7	5.3

Much more combinations of surface temperature can be studied, considering also the possibility to control the supply air of the ventilation system. The experimental investigations with test subjects will be performed considering realistic combination of the surface temperatures of a typical room in a building during the winter, e.g. two cold walls or the cold floor and one cold wall.

In the future other works are planned looking at integrated methods for multi-parameter analysis of global comfort & IEQ in office buildings.
As a matter of fact, the studies of the characterizing parameters and of the control methods for the optimization of comfort in building environments are currently mainly focused on the aspects related to thermal comfort and IEQ. Many other aspects and potential correlations, though not neglected, are not yet fully investigated and can be hence currently the subject of in-depth studies. It is the case of the acoustic and lighting environment, yet both are directly dependent on the energy management strategies of buildings. The noise level generated inside a building environment is mainly due to the operation and characteristics of the service equipment, mainly HVAC and mechanical ventilation systems. Natural and artificial lighting are increasingly connected to the managing the contribution of solar radiation through the transparent components of the building envelope. The purpose of the

research program is to deepen the interactions between different parameters on global comfort, especially for offices and commercial buildings. To do this, the development of specific methods for analysing the subjective response is expected from the current standardised procedures used for the analysis of comfort in thermally controlled environments. These methods will be developed taking into account the most recent advancements in dialogic psychology, for the analysis of the subjective response of users, and the assessment of productivity related to the daily variation of comfort indicators, following the implementation of energy saving strategies.

7 CONCLUSIONS

The premise of this work is the awareness that people spend most of their time in indoor environments and that the main task of buildings should be to provide a comfortable, healthy and productive environment for their occupants. At the same time low temperature heating and high temperature cooling systems allow to use in a favorabe way renewable energies. Therefore, energy and comfort aspects should be considered simultaneously when dealing with these kinds of emission systems, since the terminal units directly affect the indoor thermal environment.

In the present work theoretical analyses have been performed by means of steady state calculations and dynamic simulations properly taking into account the dynamic behaviour of building structures as well as the transient operation of water in the embedded pipes. From the experimental point of view, both field measurements in buildings and laboratory measurements in a test room have been carried out.

The emission efficiency of the most common residential radiant systems (a traditional wet floor system, a dry floor system and a ceiling system) were studied by means of dynamic simulations in buildings with different levels of insulation (no insulation, insulated building and well-insulated building). The work looked at the performance of these systems in heating conditions. Three types of insulated buildings (with internal, intermediate and external insulation) and four types of well-insulated buildings (masonry with external and internal insulation, timber structure and light structure) were analysed. Dynamic simulations with constant supply water temperature and with variable temperature according to outdoor temperature were compared with an ideal convective dynamic simulation. Results were analysed in terms of control and embedded efficiency of the radiant system, energy performance of the radiant system with a water to water heat pump at constant source temperature as well as thermal comfort.

Resuming the results, the work carried out shows that in general the better the quality of the envelope the better the overall performance of the radiant system. The seasonal emission efficiency evaluated by means of dynamic simulations of the radiant system and the building was found to be slightly higher than the one which can be calculated by means of steady-state calculations of the radiant system alone: 1.5% in the case of well-insulated buildings, 4% in insulated buildings and 6% in non-insulated buildings. The climatic control is confirmed to ensure, despite the much higher number of hours of operation, a lower overall energy consumption (auxiliaries included) when coupled to generation systems like heat pumps. Overheating effects are not especially due to radiant system, but they happen in any case also with ideal convective systems. As all emission systems, the radiant systems may lead to higher overheating effects, but the effect is evident in terms of higher amount of hours when the overheating happens rather than too high temperatures because of the radiant system operation. In general the radiant ceilings perform worse than radiant floor systems in heating conditions and there is no evidence that dry floor systems perform better than wet screed systems in all the types of buildings regardless the level of insulation.

As final remarks, it would be interesting to analyze the same building in cooling conditions, where the radiant ceiling could work better than the radiant floor system. Moreover the work which has been carried out here considers a unique room; a further interesting study would be to analyse different rooms, i.e. looking in detail on the distribution of the inner space and check the different possible control strategies.

Another activity was focused on the performance of a wet floor radiant system with a reduced thickness of the screed, which was studied in comparison to a traditional floor radiant system. The investigation was both experimental, by means of field measurements in two flats of a new building, and theoretical, by means of dynamic simulations of the two systems under the same boundary conditions. Despite the high number of measurement points and the choice of instruments and sensors with good accuracy level, the field measurements revealed to be quite complicated and, for some aspects, even misleading. During the period of continuous operation both the traditional floor heating system and the thin-screed floor system accurately followed the set-point for the air temperature. During the period of intermittent operation both the systems had problems to reach the higher set-point temperature because of their high inertia.
The available environmental data presented many critical points, denoting probable calibration and/or acquisition errors, but also the data from the energy meters could not be used for a fine tuning of simulations reproducing the period of field measurements. Simulations have been anyway compared to measurements to check the trends of internal temperatures.
Simulations under the same boundary conditions were then performed for the two systems. No significant difference was found in the thermal energy need of the two types of floor radiant heating systems. The thin-screed system presents a lower response time, but intermittent operation does not lead to a lower energy consumption. Moreover, if the supply water temperature is the same used during continuous operation, the set-point is hardly reached during short time-slots. To ensure comparable indoor conditions in the occupied time periods, the radiant system should be turned on earlier or the supply water temperature should be increased, with resulting higher energy consumption. From the analysis of the temperature inside the rooms, a negligible difference was found between air and operative temperature for both the radiant systems. A slightly lower risk of overheating was found for the thin-screed system, but the intensity of overheating is very low with both the systems.
The coupling of the emission system with the generation system is an interesting point to be further investigated, since the water temperature difference available from the generation system significantly influences the transient operation of the radiant system and the time needed to reach the indoor set-point. Also from the field measurements it was found that the generator can be quite critical for the proper operation of the radiant system.

During laboratory tests a more rigorous experimental approach can be followed than in field measurements, with better defined boundary and test conditions and generally a more accurate measurement equipment. An activity focused on comfort aspects was carried out in a test room. Thermal global and local sensations were assessed by means of questionnaires during 38 tests in which the surface temperatures of the upper and lower parts of the room were progressively increased and decreased, while inlet air temperature was kept constant. Air stratification and vertical radiant asymmetry were analysed in the two kinds of tests, along with air velocity.
No relevant asymmetry problem resulting in opposite sensations on head and feet at the same time was found in the analysis of the answers, while other factors played a significant role. The feet in contact with an increasingly cold surface and uncovered arms affected by an increasing air velocity were confirmed to be the more relevant source of discomfort. Significant differences were found in the answers of males and females, who were much more sensible from a local point of view, highlighting the importance of a differentiated analysis with a proper number of female test subjects. Despite the initial adaptation phase, the effects of the decreasing metabolic rate of the test subjects was also detected.

These experimental investigations were a very first step towards a better understanding of the complex matter of indoor thermal comfort in buildings with heated/cooled surfaces. Much more investigations are needed to fully understand all the effects on the test subjects and a multidisciplinary approach would be useful to solve some questionnaire-related interpretation matters. More realistic combination of surface temperatures should be analysed to understand the effects of a heated/cooled surface on the perceived thermal comfort and resulting productivity of people. In particular the maximum comfortable ceiling temperature is a crucial point to be investigated, since ceiling systems could be an easy and quite affordable solution in the renovation of existing buildings. For this purpose and for more comprehensive analyses on well-being of people, perception of the indoor environment and productivity, a novel test room equipped with radiant systems on all the surfaces and fresh air with controlled flow rate, supply temperature and relative humidity has been designed and is currently under construction. The test room first steps were shown in the thesis.

REFERENCES

[1] *Directive 2009/28/EC of the European Parliament and of the Council on the promotion of the use of energy from renewable sources and amending and subsequently repealing Directives 2001/77/EC and 2003/30/EC,* 2009.

[2] *Directive 2010/31/EU of the European Parliament and of the Council of 19 May 2010 on the energy performance of buildings (recast),* 2010.

[3] L. Carnieletto, O. B. Kazanci, M. De Carli and B. W. Olesen, "Why couple renewable energy sources with radiant systems: current trends, limitations and potential", in *Roomvent and Ventilation*, Espoo, 2018.

[4] K.-N. Rhee and K. W. Kim, "A 50 year review of basic and applied research in radiant heating and cooling systems for the built environment", *Building and Environment,* vol. 91, pp. 166-190, 2015.

[5] S. N. K. Bansal, "Characteristic parameters of a hypocaust construction", *Building and Environment,* vol. 34, pp. 305 - 318, 1999.

[6] R. Bean, B. W. Olesen and K. W. Kim, "Hystory of Radiant Heating and Cooling systems", *ASHRAE Journal,* pp. 40-47, 2010.

[7] K.-N. Rhee, B. W. Olesen and K. W. Kim, "Ten questions about radiant heating and cooling systems", *Building and Environment,* vol. 112, pp. 367 - 381, 2017.

[8] R. D. Watson, K. S. Chapman and D. Richard, "Radiant Heating and Cooling Handbook".

[9] B. Lin, Z. Wang, H. Sun, Y. Zhu and Q. Ouyang, "Evaluation and comparison of thermal comfort of convective and radiant heating terminals in office buildings", *Building and Environment,* vol. 106, pp. 91-102, 2016.

[10] T. Catalina, J. Virgone and F. Kuznik, "Evaluation of thermal comfort using combined CFD and experimentation study in a test room equipped with a cooling ceiling", *Building and Environment,* vol. 44, pp. 1740-1750, 2009.

[11] B. Olesen, "Radiant Floor Heating in Theory and Practice", *ASHRAE Journal,* pp. 19-24, 2002.

[12] B. Kilkis, "Exergy metrication of radiant panel heating and cooling with heat pumps", *Energy Conversion and Management,* vol. 63, pp. 218-224, 2012.

[13] R. A. Meierhans, "Slab cooling and earth coupling", *ASHRAE Transactions Symposia,* vol. 99, 1993.

[14] *ISO 11855. Building environment design - Design, dimensioning, installation and control of embedded radiant heating and cooling systems,* International Organization for Standardization, 2015.

[15] K. W. Kim and B. W. Olesen, "Radiant Heating and Cooling Systems, Part I", *ASHRAE Journal,* pp. 28-37, 2015.

[16] J. Babiak, B. Olesen and D. Petras, REHVA Guidebook No. 7: Low Temperature Heating and High Temperature Cooling, Brussels: REHVA, 2009.

[17] B. Ning, S. Schiavon and F. S. Bauman, "A novel classification scheme for design and control of radiant systembased on thermal response time", *Energy and Buildings,* vol. 137, pp. 38-45, 2017.

[18] F. Riva, Impianti di riscaldamento a pannelli radianti, L'installatore italiano, 1991.

[19] G. Yu, L. Xiong, D. Chengjun and H. Chen, "Simplified model and performance analysis for top insulated metal ceiling radiant cooling panels with serpentine tube arrangement", *Case Studies in Thermal Engineering,* vol. 11, pp. 35-42, 2018.

[20] ASHRAE System and Equipment Handbook, chapter 6, ASHRAE, 1996.

[21] "Brundtland Report, Our Common Future", World Commission on Environment and Development, 1987.

[22] *United Nations Framework Convention on Climate Change,* Rio de Janeiro, 1994.

[23] B. Kilkis, "Exergy metrication of radiant panel heating and cooling with heat pumps", *Energy Conversion and Management,* vol. 63, pp. 218-224, 2002.

[24] Y. Jiang, X. Liu, L. Zhang and T. Zhang, "High Temperature Cooling and Low Temperature Heating in Buildings of EBC Annex 59", *Energy Procedia,* vol. 78, pp. 2433-2438, 2015.

[25] M. Bojić, D. Cvetković, V. Marjanović, M. Blagojević and Z. Djordjević, "Performances of low temperature radiant heating systems", *Energy and Buildings,* vol. 61, pp. 233-238, 2013.

[26] M. Bojić, D. Cvetković, M. Miletić, J. Malešević and H. Boyer, "Energy, cost, and CO2 emission comparison between radiant wall panel systems and radiator systems", *Energy and Buildings,* vol. 54, pp. 496 - 592, 2012.

[27] E. Olsen and Q. Chen, "Energy consumption and comfort analysis for different low-energy cooling systems in a mild climate", *Energy and Buildings,* vol. 35, pp. 560-571, 2003.

[28] B. Olesen, E. Mortensen, J. Thorshauge and B. Berg-Munch, "Thermal comfort in a room heated by different methods", *ASHRAE Trans.,* vol. 86, pp. 34-48, 1980.

[29] P. Mustakallio, Z. Bolashikov, K. Kostov, A. Melikov and R. Kosonen, "Thermal environment in simulated offices with convective and radiant cooling systems under cooling (summer) mode of operation", *Building and Environment,* vol. 100, pp. 82-91, 2016.

[30] L. Schellen, M. Loomans, M. De Wit, B. Olesen and W.D. Van Marken Lichtenbelt, "Effects of different cooling principles on thermal sensation and physiological responses", *Energy and Buildings,* vol. 62, pp. 116-125, 2013.

[31] L. Schellen, M. Loomans, M. De Wit, B. Olesen and W.D. Van Marken Lichtenbelt, "The influence of local effects on thermal sensation under non-uniform environmental conditions - gender differences in thermophysiology, thermal comfort and productivity during convective and radiant cooling", *Physiological Behaviour,* vol. 107, pp. 252-261, 2012.

[32] G. Sastry and P. Rumsey, "VAV vs. Radiant: side-by-side comparison", *ASHRAE Journal,* vol. 56, pp. 16-24, 2014.

[33] C. Karmann, S. Schiavon and F. Bauman, "Thermal comfort in buildings using radiant vs. all-air systems: A critical literature review", *Building and Environment,* vol. 111, pp. 123-131, 2017.

[34] "International Energy Outlook", *U.S. Energy Information Administration,* vol. 484, 2016.

[35] O. B. Kazanci, M. Skrupskelis, P. Sevela, G. K. Pavlov and B. W. Olesen, "Sustainable heating, cooling and ventilation of a plus-energy house via photovoltaic/thermal panels", *Energy and Buildings,* vol. 83, pp. 122-129, 2014.

[36] S. J. Self, B. V. Reddy and M. A. Rosen, "Geothermal heat pump systems: Status review and comparison with other heating options", *Applied Energy,* vol. 101, pp. 341-348, 2013.

[37] C. Sebarchievici and I. Sarbu, Ground-Source Heat Pumps, 1st edition., 2015.

[38] F. Ascione, "Energy conservation and renewable technologies for buildings to face the impact of the climate change and minimize the use of cooling", *Solar Energy,* vol. 154, pp. 34-100, 2017.

[39] M. De Carli, A. Galgaro, M. Pasqualetto and A. Zarrella, "Energetic and economic aspects of a heating and cooling district in a mild climate based on closed loop ground source heat pump", *Applied Thermal Engineering,* vol. 71, pp. 895-904, 2014.

[40] O. B. Kazanci, M. Skrupskelis, P. Sevela, G. K. Pavlov and B. W. Olesen, "Sustainable heating, cooling and ventilation of a plus-energy house via photovoltaic/thermal panels", *Energy and Buildings,* vol. 83, p. 122–129, 2014.

[41] M. Bojić, D. Cvetković and L. Bojić, "Decreasing energy use and influence to environment by radiant panel heating using different energy sources", *Applied Energy,* vol. 138, pp. 404-413, 2015.

[42] J. Lizana, R. Chacartegui, A. Barrios-Padura and J. M. Valverde, "Advances in thermal energy storage materials and their applications towards zero energy buildings: A critical review", *Applied Energy,* vol. 203, pp. 219-239, 2017.

[43] G. K. Pavlov and B. W. Olesen, "Building Thermal Energy Storage, PhD Thesis", *Technical University of Denmark, Department of Civil Engineering,* pp. 308-310, 2014.

[44] G. K. Pavlov, B. W. Olesen, M. Skrupskelis, O. B. Kazanci, B. W. Olesen, M. Skrupskelis and O. B. Kazanci, "Ground source heat pump combined with thermo-active building system with incorporated PCM for low-energy residential house", in *Proceedings of Innostock 2012 12th International Conference on Energy Storage*, 2012.

[45] O. B. Kazanci, M. Shukuya and B. W. Olesen, "Exergy performance of different space heating systems: A theoretical study", *Building and Envieronment,* vol. 99, pp. 119-129, 2016.

[46] O. B. Kazanci, "Low Temperature Heating and High Temprature Cooling in buildings", DTU, Department of Civil Engineering, 2016.

[47] A. Boerstra, P. Op't Veld and H. Eijdems, "The health, safety and comfort advantages of low temperature heating systems: a literature review", in *Healthy Buildings*, Helsinki, 6th-10th August 2000.

[48] *ISO 7730. Ergonomics of the thermal environment - Analytical determination and interpretation of thermal comfort using calculation of the PMV and PPD indices and local thermal comfort criteria,* International Organization for Standardization, 2006.

[49] F. Causone, F. P. Corgnati, E. Fabrizio and M. Filippi, Radiant systems solutions, Technical guidelines, UPONOR, 2009.

[50] *EN 15251. Indoor environmental input parameters for design and assessment of energy performance of buildings- addressing indoor air quality, thermal environment, lighting and acoustics,* European Committee for Standardization, 2007.

[51] *ASHRAE 55. Thermal environmental conditions for human occupancy,* ASHRAE, 2017.

[52] *EN 1264. Water based surface embedded heating and cooling systems,* European Committee for Standardization, 2009.

[53] *ISO 18566. Building environment design - Design, test methods and control of hydronic radiant heating and cooling panel systems Vocabulary, symbols, technical specifications and requirements,* International Organization for Standardization: 2017.

[54] *EN 14037. Suspended radiant panels for heating and cooling supplied with water at temperature lower than 120°C,* European Committee for Standardization, 2016.

[55] *EN 14240. Building ventilation - Cold ceilings - Testing and evaluation (rating),* European Committee for Standardization, 2005.

[56] *UNI-TS 11300-2. Energy performance of buildings - Part 2: Determination of primary energy needs and yields for winter air conditioning, domestic hot water production, ventilation and lighting in non-residential buildings,* UNI, 2014.

[57] *EN 15316. Energy performance of buildings - Method for calculation of system energy requirements and system efficiencies - Part 2: Space emission systems (heating and cooling),* CEN, 2017.

[58] R. W. Shoemaker, "Le chauffage par rayonnement", *Editions Eyrolles,* 1954.

[59] B. Olesen, "Possibilities and Limitations of Radiant Floor cooling", *ASHRAE Transactions,* vol. 103, 1997.

[60] M. Bojic and D. Loveday, "The influence on building thermal behavior of the insulation/masonry distribution in a three-layered construction", *Energy and Buildings,* vol. 26, pp. 153-157, 1997.

[61] A. Gagliano, F. Patania, F. Nocera and C. Signorello, "Assessment of the dynamic thermal performance of massive buildings", *Energy and Buildings,* vol. 72, pp. 361-370, 2014.

[62] C. Balaras, "The role of thermal mass on the cooling load of buildings. An overview of computational methods", *Energy and Buildings,* vol. 24, pp. 1-10, 1996.

[63] N. Aste, A. Angelotti and M. Buzzetti, "The influence of the external walls thermal inertia on the energy performance of well insulated buildings", *Energy and Buildings,* vol. 41, pp. 1181-1187, 2009.

[64] F. Stazia, C. Bonfiglia, E. Tomassonia, C. Di Perna and P. Munafò, "The effect of high thermal insulation on high thermal mass:Is the dynamic behaviour of traditional envelopes in Mediterranean climates still possible?", *Energy and Buildings,* vol. 88, pp. 367-383, 2015.

[65] N. Aste, F. Leonforte, M. Manfren and M. Mazzon, "Thermal inertia and energy efficiency - Parametric simulation assessment on a calibrated case study", *Applied Energy,* vol. 145, pp. 111-123, 2015.

[66] S. Verbekea and A. Audenaerta, "Thermal inertia in buildings: A review of impacts across climate and building use", *Renewable and Sustainable Energy Reviews,* vol. 82, pp. 2300-2318, 2018.

[67] ASHRAE Handbook - HVAC Systems and Equipment, Atlanta: ASHRAE, 2012.

[68] M. Koschenz and V. Dorer, "Interaction of an air system with concrete core conditioning", *Energy and Buildings,* vol. 30, pp. 139-145, 1999.

[69] S. Sattari and B. Farhanieh, "A parametric study on radiant floor heating system performance", *Renewable Energy,* vol. 31, pp. 1617-1626, 2006.

[70] J. Seo, J. Jeon, J. Lee and S. Kim, "Thermal performance analysis according to wood flooring structure for energy conservation in radiant floor heating systems", *Energy and Buildings,* vol. 43, pp. 2039-2042, 2011.

[71] J. Seo, Y. Park, J. Kim, S. Kim, S. Kim and J. Kim, "Comparison of thermal transfer characteristics of wood flooring according to the installation method", *Energy and Buildings,* vol. 70, pp. 422-426, 2014.

[72] X. Wu, J. Zhao, B. Olesen, L. Fang and F. Wang, "A new simplified model to calculate surface temperature and heat transfer of radiant floor heating and cooling systems", *Energy and buildings,* vol. 105, p. 285–293, 2015.

[73] D. Zhang, N. Cai and Z. Wang, "Experimental and numerical analysis of lightweight radiant floor heating system", *Energy and Buildings,* vol. 61, pp. 260-266, 2013.

[74] K. Zhao, X.-H. Liu and Y. Jiang, "Dynamic performance of water-based radiant floors during start-up and high-intensity solar radiation", *Solar Energy,* vol. 101, pp. 232-244, 2014.

[75] L. Qiu and Q. Li, "Analyses on two paving types of floor heating", in *Proceedings of the 2011 International Conference on Computer Distributed Control and Intelligent Environmental Monitoring*, Changsha, China, 19–20 February 2011.

[76] S. Thomas, P. Franck and P. Andre, "Model validation of a dynamic embedded water base surface heat emitting system for buildings", *Building simulation,* vol. 4, pp. 41-48, 2011.

[77] T. Weber, G. Jóhannesson, M. Koschenz, B. Lehmann and T. Baumgartner, "Validation of a FEM-program (frequency-domain) and a simplified RC-model (time-domain) for thermally activated building component systems (TABS) using measurement data", *Energy and Buildings,* vol. 37, pp. 707-724, 2005.

[78] M. De Carli, M. Scarpa, R. Tomasi and A. Zarrella, "DIGITHON: A numerical model for the thermal balance of rooms equipped with radiant systems", *Building and Environment,* vol. 57, pp. 126-144, 2012.

[79] M. De Carli and M. Tonon, "Effect of modelling solar radiation on the cooling performance of radiant floors", *Solar Energy,* vol. 85, p. 689–712, 2011.

[80] L. G. Berglund and A. P. Gagge, "Human response to thermal conditions maintained in an office by radiant ceiling, baseboard, forced air and floor heating systems", *ASHRAE Transactions,* vol. 91, pp. 488 - 502, 1985.

[81] R. W. Külpmann, "Thermal comfort and air quality in rooms with cooled ceilings - results of scientific investigations", *ASHRAE Transactions,* vol. 99, pp. 488 - 502, 1993.

[82] D. R. Fisher and C. O. Pedersen, "Convective heat transfer in building energy and load calculation", *ASHRAE Transactions,* vol. 103, 1997.

[83] M. De Carli and R. Tomasi, "A critical review on heat exchange coefficients between heated and cooled horizontal surfaces and room", in *Proceedings of 11th Roomvent Conference*, Korea, 2009.

[84] E. Z. A. Schlunder, "Fluid Mechanics and Heat Transfer", in *Heat exchanger design handbook*, New York, Begell House Publishers, 1983.

[85] D. G. Stephenson and G. P. Mitalas, "Cooling load calculation by thermal response factor method", *ASHRAE Transactions,* vol. 73, 1967.

[86] T. Kusuda, "Thermal response factors for multi-layer structures of various heat conduction systems", in *ASHRAE semi-annual Meeting*, Chicago, IL, 1969.

[87] T. Blomberg, *HEAT2 – A PC-program for heat transfer in two dimensions. Manual with brief theory and examples,* Sweden: Lund Group for Computational Building Physics, 1999.

[88] *EN 12831-1:2017. Energy performance of buildings. Method for calculation of the design heat load. Space heating load,* European Committee for Standardization, 2017.

[89] B. W. Olesen, F. Bonnefoi, E. Michel and M. De Carli, "Heat exchange coefficient between floor surface and space by floor cooling - theory or a question of definition", in *ASHRAE Transactions: Symposia, vol. DA-00-8-2*, 2000.

[90] B. W. Olesen, "New European standards for design, dimensioning and testing embedded radiant heating and cooling systems", in *Proceedings of CLIMA 2007 WellBeing Indoors*, Helsinki, 2007.

[91] L. Mazzarella, "Dati climatici G. De Giorgio", in *Proceedings of Giornata di studio Giovanni De Giorgio*, Milano, 1997.

[92] *EN 15316. Heating systems in buildings - Method for calculation of system energy requirements and system efficiencies — Part. 2-1: Space heating emission systems,* Brussels: CEN, 2007.

[93] *EN 15316. Energy performance of buildings - Method for calculation of system energy requirements and system efficiencies - Part 2: Space emission systems (heating and cooling),* Brussels: CEN, 2017.

[94] B. Ning, S. Schiavon and F. Bauman, "A novel classification scheme for design and control of radiant system based on thermal response time", *Energy and Buildings,* vol. 137, pp. 38-45, 2017.

[95] P. Fanger, L. Banhidi, B. Olesen and G. Langkinle, "Comfort limits for heated ceilings", *ASHRAE Transactions,* vol. 86, no. 2, pp. 141-156, 1980.

[96] P. Fanger, B. Ipsen, G. Langkilde, B. Olesen, N. Christensen and S. Tanabe, "Comfort limits for asymmetric thermal radiation", *Energy and Buildings,* vol. 8, 1985.

[97] F. A. Chrenko, "Heated ceilings and comfort", *Journal of the institute of Heating and Ventilating Engineers,* vol. 20, pp. 375-396, 1953.

[98] P. Mc Nall and R. Biddison, "Thermal and comfort sensations of sedentary persons exposed to asymmetric radiant fields", *ASHRAE Transactions,* vol. 76, no. 1, 1970.

[99] I. Griffiths and D. McIntyre, "Subjective response to overheat thermal radiation", *Human factors,* vol. 16, no. 3, pp. 415-422, 1974.

[100] B. Glück, "Zulässige Strahlungstemperatur-Asymmetrie", *Gesundheits Ingenieur,* vol. 115, no. 6, pp. 285-344, 1994.

[101] J. Seifert, B. Oschatz, A. Buchheim, L. Schinke, M. Beyer, S. Paulick and B. Mailach, "Instationäre, gekoppelte, energetische und wärmephysiologische Bewertung von Regelungsstrategien für HLK-Systeme", Technische Universität Dresden, Institut für Technische Gebäudeausrüstung Dresden, Dresden, 2016.

[102] J. Seifert, L. Schinke, M. Beyer and A. Buchheim, "The New Climate Room for transient investigations of thermal comfort", *REHVA Journal,* vol. 54, no. 1, February 2017.

[103] F. Bonavita, P. Brunello and R. Zecchin, "Metodo di calcolo dei fattori di forma tra corpo umano e superfici interne in un ambiente", *CDA,* no. 2, pp. 217-225, (I) 1989.

[104] *ISO 7726. Ergonomics of the thermal environment - Instruments for measuring physical quantities,* International Organization for Standardization, 2001.

[105] L. Fontana, "Experimental study on the globe thermometer behaviour in conditions of asymmetry of the radiant temperature", *Applied Thermal Engineering,* vol. 30, pp. 732-740, 2010.

[106] F. D'Ambrosio Alfano, M. Dell'Isola, B. Palella, G. Riccio and A. Russi, "On the measurement of the mean radiant temperature and its influence on the indoor thermal environment assessment", *Building and Environment,* vol. 63, pp. 79-88, 2013.

[107] J. Kolarik, J. Toftum, B. W. Olesen and A. Shitzer, "Occupant Responses and Office Work Performance in Environments with Moderately Drifting Operative Temperatures (RP-1269)", *HVAC&R Research,* vol. 15, no. 5, pp. 931-960, 2009.

[108] *EN 1264-3. Water based surface embedded heating and cooling systems - Part 3: Dimensioning,* European Committee for Standardization, 2009.

APPENDIX

Table A.1 - Stratigraphy and thermal properties of the structures of the not insulated building (N).

	Layer	s [m]	λ [W m^{-1} K^{-1}]	ρ [kg m^{-3}]	c [J kg^{-1} K^{-1}]	R [m^2 K W^{-1}]	U [W m^{-2} K^{-1}]
External wall	Liminar inner layer	-	-	-	-	0.125	1.333
	Plaster	0.015	0.900	1800	1000	0.017	
	Hollow brick	0.120	0.660	1100	840	0.182	
	Hollow brick	0.250	0.676	1516	840	0.370	
	Plaster	0.015	0.900	1800	1000	0.017	
	Liminar outer layer	-	-	-	-	0.040	
Internal wall	Liminar inner layer	-	-	-	-	0.125	2.069
	Plaster	0.015	0.900	1800	1000	0.017	
	Hollow brick	0.080	0.400	775	840	0.200	
	Plaster	0.015	0.900	1800	1000	0.017	
	Liminar outer layer	-	-	-	-	0.125	
Floor	Liminar inner layer	-	-	-	-	0.125	1.444
	Ceramic tiles	0.010	1.000	2300	840	0.010	
	Screed	0.060	0.700	1600	880	0.086	
	Concrete	0.040	1.480	2200	1000	0.027	
	Structural Slab	0.200	0.660	1100	840	0.303	
	Plaster	0.015	0.900	1800	1000	0.017	
	Liminar outer layer	-	-	-	-	0.125	

Table A.2 - Stratigraphy and thermal properties of the structures of the insulated buildings (IM, IE and II).

	Layer	s [m]	λ [W m^{-1} K^{-1}]	ρ [kg m^{-3}]	c [J kg^{-1} K^{-1}]	R [m^2 K W^{-1}]	U [W m^{-2} K^{-1}]
External wall with insulation in the middle	Liminar inner layer	-	-	-	-	0.125	0.566
	Plaster	0.015	0.900	1800	1000	0.017	
	Hollow brick	0.080	0.400	775	840	0.200	
	EPS	0.040	0.040	30	1450	1.000	
	Hollow brick	0.250	0.676	1516	840	0.370	
	Plaster	0.015	0.900	1800	1000	0.017	
	Liminar outer layer	-	-	-	-	0.040	
External wall with insulation on the external surface	Liminar inner layer	-	-	-	-	0.125	0.484
	Plaster	0.015	0.900	1800	1000	0.017	
	Hollow brick	0.250	0.676	1516	840	0.370	
	EPS	0.060	0.040	30	1450	1.500	
	Plaster	0.004	0.300	1300	840	0.013	
	Liminar outer layer	-	-	-	-	0.040	
External wall with insulation on the inner surface	Liminar inner layer	-	-	-	-	0.125	0.474
	Plasterboard	0.012	0.210	700	1000	0.057	
	EPS	0.060	0.040	30	1450	1.500	
	Hollow brick	0.250	0.676	1516	840	0.370	
	Plaster	0.015	0.900	1800	1000	0.017	
	Liminar outer layer	-	-	-	-	0.040	
Internal wall	Liminar inner layer	-	-	-	-	0.125	2.069
	laster	0.015	0.900	1800	1000	0.017	
	Hollow brick	0.080	0.400	775	840	0.200	
	Plaster	0.015	0.900	1800	1000	0.017	
	Liminar outer layer	-	-	-	-	0.125	
Floor	Liminar inner layer	-	-	-	-	0.125	0.955
	Ceramic tiles	0.010	1.000	2300	840	0.010	
	Screed	0.050	0.900	1800	880	0.056	
	Light concrete	0.050	0.130	250	1000	0.385	
	Concrete	0.040	1.480	2200	1000	0.027	
	Structural slab	0.200	0.660	1100	840	0.303	
	Plaster	0.015	0.900	1800	1000	0.017	
	Liminar outer layer	-	-	-	-	0.125	

Table A.3 - Stratigraphy and thermal properties of the structures of the well-insulated masonry buildings (WIE and WII).

	Layer	s [m]	λ [W m^{-1} K^{-1}]	ρ [kg m^{-3}]	c [J kg^{-1} K^{-1}]	R [m^2 K W^{-1}]	U [W m^{-2} K^{-1}]
External wall with insulation on the external surface	Liminar inner layer	-	-	-	-	0.125	0.215
	Plaster	0.015	0.900	1800	1000	0.017	
	Light bricks	0.250	0.430	870	1000	0.581	
	EPS with graphite	0.120	0.031	20	1450	3.871	
	Plaster	0.004	0.300	1300	840	0.013	
	Liminar outer layer	-	-	-	-	0.040	
External wall with insulation on the inner surface	Liminar inner layer	-	-	-	-	0.125	0.224
	Plasterboard	0.012	0.210	700	1000	0.057	
	EPS with graphite	0.120	0.031	20	1450	3.871	
	Bricks	0.280	0.778	1800	840	0.360	
	Plaster	0.015	0.900	1800	1000	0.017	
	Liminar outer layer	-	-	-	-	0.040	
Internal wall	Liminar inner layer	-	-	-	-	0.125	2.069
	Plaster	0.015	0.900	1800	1000	0.017	
	Hollow brick	0.080	0.400	775	840	0.200	
	Plaster	0.015	0.900	1800	1000	0.017	
	Liminar outer layer	-	-	-	-	0.125	
Floor	Liminar inner layer	-	-	-	-	0.125	0.719
	Ceramic tiles	0.010	1.000	2300	840	0.010	
	Screed	0.030	0.900	1800	880	0.033	
	EPS	0.030	0.040	30	1450	0.750	
	Concrete	0.040	1.480	2200	1000	0.027	
	Structural slab	0.200	0.660	1100	840	0.303	
	Plaster	0.015	0.900	1800	1000	0.017	
	Liminar outer layer	-	-	-	-	0.125	

Table A.4 - Stratigraphy and thermal properties of the structures of the well-insulated light-weight buildings (WIX and WIL).

	Layer	s [m]	λ [W m^{-1} K^{-1}]	ρ [kg m^{-3}]	c [J kg^{-1} K^{-1}]	R [m^2 K W^{-1}]	U [W m^{-2} K^{-1}]
Wood external wall	Liminar inner layer	-	-	-	-	0.125	0.150
	Plasterboard	0.0125	0.210	700	1000	0.060	
	Wood fiber	0.100	0.039	150	2100	2.564	
	Cross laminated timber	0.100	0.130	500	1600	0.769	
	Wood fiber	0.120	0.039	150	2100	3.077	
	Plaster	0.015	0.900	1800	1000	0.017	
	Liminar outer layer	-	-	-	-	0.040	
Light external wall	Liminar inner layer	-	-	-	-	0.125	0.190
	Plasterboard	0.015	0.210	700	1000	0.071	
	EPS	0.200	0.040	30	1450	5.000	
	Plaster	0.015	0.900	1800	1000	0.017	
	Liminar outer layer	-	-	-	-	0.040	
Internal wall	Liminar inner layer	-	-	-	-	0.125	0.377
	Plasterboard	0.0125	0.210	700	1000	0.060	
	Mineral wool	0.080	0.035	40	1030	2.286	
	Plasterboard	0.0125	0.210	700	1000	0.060	
	Liminar outer layer	-	-	-	-	0.125	
Floor	Liminar inner layer	-	-	-	-	0.125	0.199
	Ceramic tiles	0.010	1.000	2300	840	0.010	
	Concrete	0.060	1.000	1800	880	0.060	
	EPS	0.030	0.039	30	1250	0.769	
	Wood fiber	0.040	0.039	150	2100	1.026	
	Light concrete	0.100	0.130	250	1000	0.769	
	Cross laminated timber	0.160	0.130	500	1600	1.231	
	Mineral fiber	0.030	0.035	40	1030	0.857	
	Plasterboard	0.0125	0.210	700	1000	0.060	
	Liminar outer layer	-	-	-	-	0.125	

Table A.5 - Stratigraphy and thermal properties of the radiant floor with wet screed (FW).

Layer	s [m]	λ [W m^{-1} K^{-1}]	ρ [kg m^{-3}]	c [J kg^{-1} K^{-1}]	R [m^2 K W^{-1}]	U [W m^{-2} K^{-1}]
Ceramic tiles	0.010	1.000	2300	840	0.010	1.10
Screed	0.060	1.000	1800	880	0.060	
Pipes 17 x 2 mm, 15 cm pitch	-	0.360	951	2300	-	
Insulation	0.025	0.033	30	1250	0.750	

Table A.6 - Stratigraphy and thermal properties of the radiant floor with dry screed and aluminum diffusers (FD).

Layer	s [m]	λ [W m^{-1} K^{-1}]	ρ [kg m^{-3}]	c [J kg^{-1} K^{-1}]	R [m^2 K W^{-1}]	U [W m^{-2} K^{-1}]
Ceramic tiles	0.010	1.000	2300	840	0.010	1.10
Dry screed	0.009	0.170	950	1030	0.053	
Pipes 14 x 2 mm, 10 cm pitch	-	0.360	951	2300	-	
Conducting device	0.001	237	2710	896.9	$4.2 \cdot 10^{-6}$	
Insulation	0.025	0.033	30	1250	0.750	

Table A.7 - Stratigraphy and thermal properties of the radiant ceiling with plasterboard coupled to insulation panels (C).

Layer	s [m]	λ [W m^{-1} K^{-1}]	ρ [kg m^{-3}]	c [J kg^{-1} K^{-1}]	R [m^2 K W^{-1}]	U [W m^{-2} K^{-1}]
Plasterboard	0.0125	0.210	700	1000	0.060	0.89
Pipes 10 x 1 mm, 6 cm pitch	-	0.360	951	2300	-	
Insulation	0.030	0.033	35	1450	0.91	